Metabolomics and proteomics identify the toxic form and the associated cellular binding targets of the anti-proliferative drug AICAR

Delphine C Douillet, Benoit Pinson, Johanna Ceschin, Hans C Hürlimann, Christelle Saint-Marc, Damien Laporte, Stéphane Claverol, Manfred Konrad, Marc Bonneu, Bertrand Daignan-Fornier

Metabolomics and proteomics identify the toxic form and the associated cellular binding targets of the anti-proliferative drug AICAR

Received for publication, July 19, 2018, and in revised form, November 9, 2018 Published, Papers in Press, November 26, 2018, DOI 10.1074/jbc.RA118.004964

Delphine C. Douillet[‡§1,2], Benoît Pinson[‡§1], Johanna Ceschin[‡§], Hans C. Hürlimann[‡§3], Christelle Saint-Marc[‡§], Damien Laporte[‡§], Stéphane Claverol[¶], Manfred Konrad[‖4], Marc Bonneu[¶], and Bertrand Daignan-Fornier[‡§5]

From the [‡]Université de Bordeaux, IBGC UMR 5095, F-33077 Bordeaux, France, the [§]Centre National de la Recherche Scientifique, IBGC UMR 5095, F-33077 Bordeaux, France, the [¶]University of Bordeaux, Bordeaux INP, Plateforme Proteome, F-33076 Bordeaux, France, and the [‖]Max-Planck-Institute for Biophysical Chemistry, D-37077 Goettingen, Germany

Edited by Patrick Sung

5-Aminoimidazole-4-carboxamide 1-β-D-ribofuranoside (AICAR, or acadesine) is a precursor of the monophosphate derivative 5-amino-4-imidazole carboxamide ribonucleoside 5′-phosphate (ZMP), an intermediate in *de novo* purine biosynthesis. AICAR proved to have promising anti-proliferative properties, although the molecular basis of its toxicity is poorly understood. To exert cytotoxicity, AICAR needs to be metabolized, but the AICAR-derived toxic metabolite was not identified. Here, we show that ZMP is the major toxic derivative of AICAR in yeast and establish that its metabolization to succinyl-ZMP, ZDP, or ZTP (di- and triphosphate derivatives of AICAR) strongly reduced its toxicity. Affinity chromatography identified 74 ZMP-binding proteins, including 41 that were found neither as AMP nor as AICAR or succinyl-ZMP binders. Overexpression of karyopherin-β Kap123, one of the ZMP-specific binders, partially rescued AICAR toxicity. Quantitative proteomic analyses revealed 57 proteins significantly less abundant on nuclei-enriched fractions from AICAR-fed cells, this effect being compensated by overexpression of *KAP123* for 15 of them. These results reveal nuclear protein trafficking as a function affected by AICAR.

AICAR[6] is a natural metabolite that can be taken up by nucleoside transporters in human cells (1) and has multiple promising pharmacological properties (2). Indeed, AICAR has proved *in vivo* anti-tumor effects in xenograft models (3–5). It is currently under clinical trial phase I/II to treat patients with chronic lymphocytic leukemia and has shown good safety and tolerability properties, although some side effects have been reported (6). Most of the described AICAR effects require its metabolic conversion to the monophosphate form ZMP by adenosine kinase (2). As an intermediate of the purine *de novo* pathway, ZMP is naturally present in cells at low concentration (7). ZMP and its precursor SZMP are important regulatory molecules that promote interactions between specific transcription factors and thereby directly couple the flux in the purine *de novo* pathway to transcription of the genes encoding the corresponding enzymes (8, 9). In addition, ZMP co-regulates purine synthesis to phosphate utilization through its interaction with common transcription factors (10). Strikingly, the regulatory role of ZMP is conserved in bacteria, although the riboswitch mechanism involved is totally different (11). Although under physiological conditions ZMP is present in the micromolar range (7), upon feeding of the riboside precursor AICAR, ZMP concentration can increase to milli molar levels (1), and, as a result, AICAR displayed cytotoxicity in yeast and mammalian cells (2), although the exact mechanisms involved are not known. The best documented pharmacological effect of ZMP is activation of the low-energy sensor AMP-activated protein kinase (AMPK) (12, 13). This well-characterized effect was attributed to the AMP-mimetic properties of ZMP (14) because of the structural similarity of these nucleotides (see Fig. 1*A*). However, the anti-proliferative effects of AICAR were shown to be largely AMPK-independent (1, 15), thus implying that other critical ZMP targets exist in the cell that have not yet been identified.

Characterization of yeast mutants hypersensitive to AICAR revealed its uptake by the nicotinamide riboside transporter Nrt1 (see Fig. 1*B*) (1) and gave the first clues on the molecular basis of AICAR toxicity. Indeed, this approach established AICAR transport, ATP homeostasis, histone methylation, and ubiquitin metabolism as critical mechanisms underlying AICAR sensitivity (1, 16–18). Importantly, some of these mechanisms are conserved from yeast to human cells (16, 17). However, in these chemogenetic studies based on synthetic lethality, neither the toxic derivative of AICAR nor its protein target(s) were identified. Aiming to

This work was supported by a Ligue contre le Cancer Dordogne 2016–2017 grant (to B. D.-F.). The authors declare that they have no conflicts of interest with the contents of this article.

This article contains Tables S1–S8 and Figs. S1–S9.

The mass spectrometry proteomics data have been deposited to the Proteome Xchange Consortium via the PRIDE partner repository with the dataset identifiers PXD007780 and PXD007779.

[1] Both authors contributed equally to this work.

[2] Present address: Northwestern University Feinberg School of Medicine, 320 East Superior St., Chicago, IL 60611.

[3] Present address: Martin-Luther Universität, Genetik, Molekulargenetik, Weinbergweg 10, D-06120 Halle, Germany.

[4] Supported by the Max Planck Institute.

[5] To whom correspondence should be addressed: Institut de Biochimie et Génétique Cellulaires, CNRS UMR 5095, 1 Rue C. Saint-Saëns, CS 61390 F-33077 Bordeaux, France. Tel.: 33-556-999-001; Fax: 33-556-999-059; E-mail: b.daignan-fornier@ibgc.cnrs.fr.

[6] The abbreviations used are: AICAR, 5-aminoimidazole-4-carboxamide 1-β-D-ribofuranoside; ZMP, 5-amino-4-imidazole carboxamide ribonucleoside monophosphate; SZMP, succinyl-ZMP; ZDP, 5-amino-4-imidazole carboxamide ribonucleoside diphosphate; ZTP, 5-amino-4-imidazole carboxamide ribonucleoside triphosphate; AMPK, AMP-activated protein kinase; SAICAR, succinyl-AICAR; GO, Gene Ontology.

unveil the identity of the toxic derivative, our previous work established that intracellular AICAR and its succinyl-derivative SAICAR, which are the riboside forms of ZMP and SZMP, respectively, were not toxic for yeast cells (7). This situation is reminiscent of what happens in mammalian cells, in which the vast majority of AICAR effects are abolished by adenosine kinase inhibitors that block ZMP synthesis (19). Thus, for both yeast and mammalian cells, it was concluded that AICAR riboside had to be metabolically converted to the monophosphate form to become pharmacologically active and cytotoxic. Understanding how small molecules promote cytotoxicity is a complex task because small molecules are frequently metabolized to derivatives that may affect more than one biological process through interaction with multiple targets. This led us to ask two essential questions. First, is it ZMP itself and/or derived metabolites that are the toxic species? Second, which proteins are affected by the toxic metabolite?

In this work, we addressed these questions by combining yeast genetics, metabolic profiling, and proteomics to substantiate the assumption that ZMP itself is the toxic compound for yeast cells. Based on this result, we detected multiple ZMP-binding proteins and identified nuclear trafficking as one of the key functions affected by AICAR.

Results

AICAR treatment results in accumulation of ZMP, SZMP, and ZTP

Effects of AICAR feeding on yeast cells were evaluated by metabolic profiling of an *ade16 ade17 ade8 his1* strain that is unable to metabolize ZMP to IMP (20) (Fig. 1*B*). As previously reported (1), in this genetic background, AICAR treatment caused massive ZMP accumulation (Fig. 1*C*). In addition, metabolic profile analysis revealed that AICAR treatment resulted in accumulation of SZMP, as well as of SAICAR, its riboside form (Fig. 1*C*). This is because in yeast, ZMP can be converted back to SZMP by adenylosuccinate lyase (Adsl), encoded by the *ADE13* gene (21) (Fig. 1*B*). In turn, SZMP is dephosphorylated to SAICAR, which is nontoxic even at very high concentrations in yeast (7). We also observed that AICAR feeding led to accumulation of the triphosphate form, ZTP, whereas the diphosphate form ZDP was not detected (Fig. 1*C*). Finally, as expected, AICAR itself accumulated in yeast cells (Fig. 1*C*), but intracellular accumulation of this compound was previously demonstrated to be nontoxic (7).

Thus, AICAR treatment resulted in accumulation of ZMP, SZMP, and ZTP that could potentially affect cellular functions and result in toxicity. We thus used yeast genetics to identify the toxic derivative(s) of AICAR.

SZMP synthesis is not required for AICAR toxicity

We first asked whether SZMP could contribute to AICAR toxicity. The *ade13* knockout mutation blocking SZMP synthesis from ZMP (Fig. 1*B*) was introduced in an *ade16 ade17 ade8 his1* strain, and the resulting quintuple mutant strain was found to be highly sensitive to AICAR (Fig. 2*A*). As expected, the *ade13* mutation abolished SZMP accumulation, whereas intracellular ZMP was higher than in the control strain (Fig. 2, *B* and *C*). We conclude that AICAR toxicity was not due to SZMP synthesis from ZMP but correlated with intracellular ZMP accumulation. These conclusions were strongly supported by analysis of a fumarase knockout mutant *fum1*, which accumulates fumarate (Fig. 2*D*) and thereby favors the reverse reaction from ZMP to SZMP by adenylosuccinate lyase Adsl (Ade13) (Fig. 1*B*), leading to increased SZMP and decreased ZMP levels (Fig. 2, *E* and *F*). In the corresponding mutant strain (*fum1 ade16 ade17 ade8 his1*), AICAR toxicity was abolished (Fig. 2*G*). From these results, we conclude that, in yeast, SZMP is not the metabolite that causes AICAR toxicity, but synthesis of SZMP rather contributes to its detoxification.

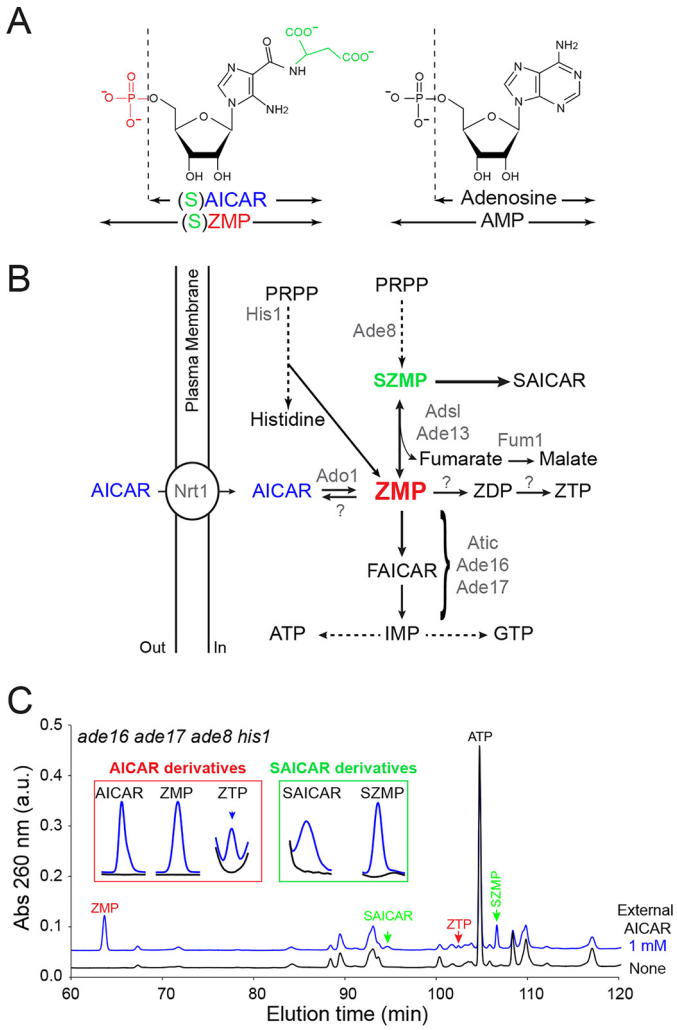

Figure 1. AICAR feeding of yeast cells results in accumulation of several AICAR-derived metabolites. *A*, chemical structure of ZMP and AMP derivatives. *B*, *Adsl*, adenylosuccinate lyase; *Atic*, AICAR transformylase IMP-cyclohydrolase; *FAICAR*, 5-formamido-4-imidazole carboxamide ribonucleoside 5′-phosphate; *PRPP*, 5-phosphoribosyl-1-pyrophosphate. Only the enzymes mentioned in the text are listed (in *gray*). *Question marks* correspond to enzymatic activities catalyzed by unidentified proteins prior to this work. *C*, accumulation of AICAR derivatives in yeast (*ade8 ade16 ade17 his1*; Y2950) fed (*blue lines*) or not (*black lines*) for 24 h with extracellular AICAR. Similar patterns were found in three independent metabolic extractions. *Insets* correspond to enlargement of chromatogram sections where AICAR and SAICAR derivatives were eluted.

ZDP and ZTP are not toxic for yeast cells

To get a deeper insight into the mechanisms leading to AICAR toxicity, we performed an unbiased search for genes that suppress AICAR toxicity when overexpressed. A yeast

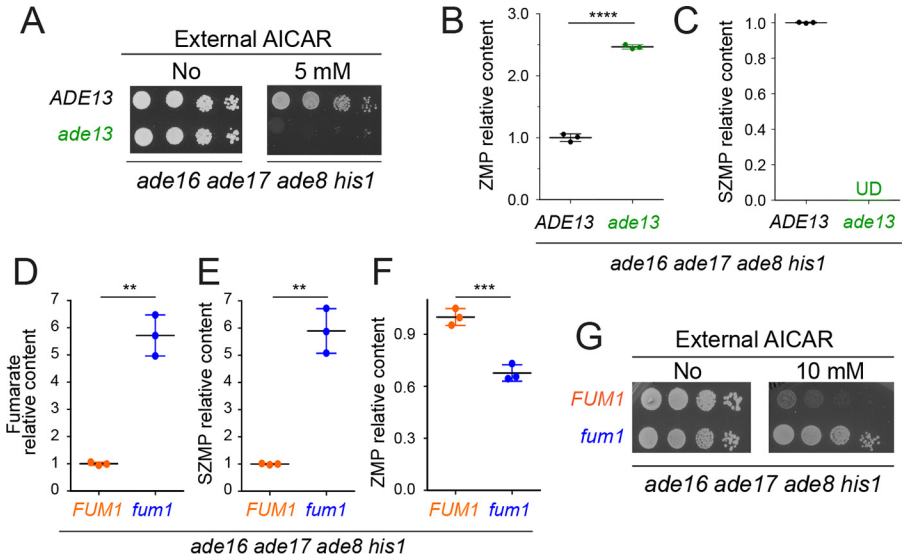

Figure 2. SZMP is not required for AICAR toxicity but rather contributes to its detoxification in yeast. *A–C*, deletion of the *ADE13* gene leads to increased ZMP accumulation and AICAR toxicity. *A*, yeast strains (Y2950 and Y10422) were grown overnight, serially diluted (1/10), and spotted on SDcasaWAU medium containing or lacking AICAR. The plates were imaged after 48 h of incubation at 30 °C. *B* and *C*, ZMP (*B*) and SZMP (*C*) relative content was determined on metabolic extracts from three independent cell cultures of each strain (Y2950 and Y10422) grown in SDcasaWAU medium and treated with AICAR (0.5 mM) for 24 h. Relative contents were set at 1 for the *ADE13* control strain. *D–G*, favoring SZMP synthesis from ZMP lowers AICAR toxicity. *D–F*, metabolic analyses were done on three independent extractions from cells (Y2950 and Y3655) grown in SDcasaWAU medium and treated with AICAR (0.5 mM, 24 h). Relative content was set at 1 for the *FUM1* control strain (Y2950). *G*, AICAR resistance was increased in a *FUM1*-deleted strain (Y3655) grown for 48 h in SDcasaWAU medium at 30 °C. *B–F*, *errors bars* and statistics correspond to standard deviation and Welch's unpaired *t* tests. **, $p < 0.01$; ***, $p < 0.001$; ****, $p < 0.0001$; *UD*, undetectable.

genomic library carried on a multicopy vector was used to search for gene dosage suppressors of AICAR sensitivity in a yeast strain that can accumulate ZMP and derivatives when the riboside is provided (see "Experimental procedures" for details). The suppressor plasmids all carried an overlapping DNA region of chromosome XI containing four genes: two genes of unknown function (*YKL023C-A* and *YKL023W*), *PAN3* encoding a subunit of the Pan2p-Pan3p poly(A)-RNase complex, and *URA6*, an essential gene encoding UMP kinase, which was reported to have significant AMP kinase activity (22). Of note, *URA6* was previously identified as a suppressor of AICAR sensitivity hypomorphic allele of *UBA1* but was not further characterized (18). Because ZMP is structurally close to AMP (Fig. 1*A*), we hypothesized that Ura6 could phosphorylate ZMP and thereby improve growth upon AICAR feeding. Indeed, overexpression of *URA6* alone was sufficient to confer robust resistance to AICAR similarly to the initial suppressor plasmid (Fig. 3*A*). Metabolic profiling on yeast cells grown in the presence of AICAR revealed that overexpression of *URA6* resulted in accumulation of ZDP and ZTP, both of which are hardly detectable in the control strain (Fig. 3, *B* and *C*). Noticeably, in the AICAR-resistant strain overexpressing *URA6*, ZMP was lower (Fig. 3*D*), whereas both ZDP and ZTP levels were higher than in the AICAR-sensitive control strain (Fig. 3, *B* and *C*). We conclude that ZMP, rather than its di- or triphosphate derivatives, is the toxic metabolite derived from AICAR. Accordingly, AICAR feeding had no effect on mutation rates in yeast (Fig. S1*A*) even under conditions (*URA6* overexpression) resulting in high ZTP levels (Fig. S1*B*). Similarly, AICAR feeding did not affect other aspects of DNA metabolism such as mitotic recombination rate (Fig. S2) or telomere length (Fig. S3). Together, these results establish that AICAR toxicity is not associated with ZTP synthesis.

Notably, recombinant yeast Ura6 purified from *Escherichia coli* (Fig. 3*E*) could synthesize ZDP, but not ZTP, from ZMP *in vitro* (Fig. 3, *F–H*), as expected for a nucleoside monophosphate kinase. However, both ZTP and ZDP were found as reaction products when the reaction was run with total extracts from *URA6*-expressing bacteria (Fig. 3, *G* and *H*). Altogether, these results show that Ura6 can synthesize ZDP from ZMP and that another enzyme(s) can further phosphorylate it to ZTP in both yeast and bacteria. We established that yeast NDP-kinase Ynk1 was not required because *ynk1* knockout had no effect on ZTP production (Fig. S4). Of note, purified yeast adenylate kinase Adk1, which was not found in the gene-dosage suppressor screening had no detectable ZMP-kinase activity *in vitro*.

Thus, our genetic and biochemical experiments in yeast demonstrate that ZMP, rather than SZMP, ZDP, or ZTP, is the toxic molecule derived from AICAR. The question arising then was: why is ZMP toxic?

Proteome-wide identification of ZMP binders

To identify potential effectors of ZMP toxicity, we isolated yeast proteins that interact with ZMP by an affinity chromatography approach (for details, see "Experimental procedures" and Ref. 10). Whole-cell protein extracts from six independent cultures were loaded on a ZMP-Sepharose resin. The eluted proteins (herein called ZMP binders) were identified by MS. A total of 74 proteins, representing ~1.1% of the yeast proteome, were identified by at least two different peptides in at least four of six experiments (Fig. 4*A* and Table S1). Among them was the enzyme adenylosuccinate lyase (Ade13), a known ZMP binder (10), synthesizing ZMP from SZMP. However, identification of ZMP binders by this approach was not exhaustive because other ZMP-metaboliz-

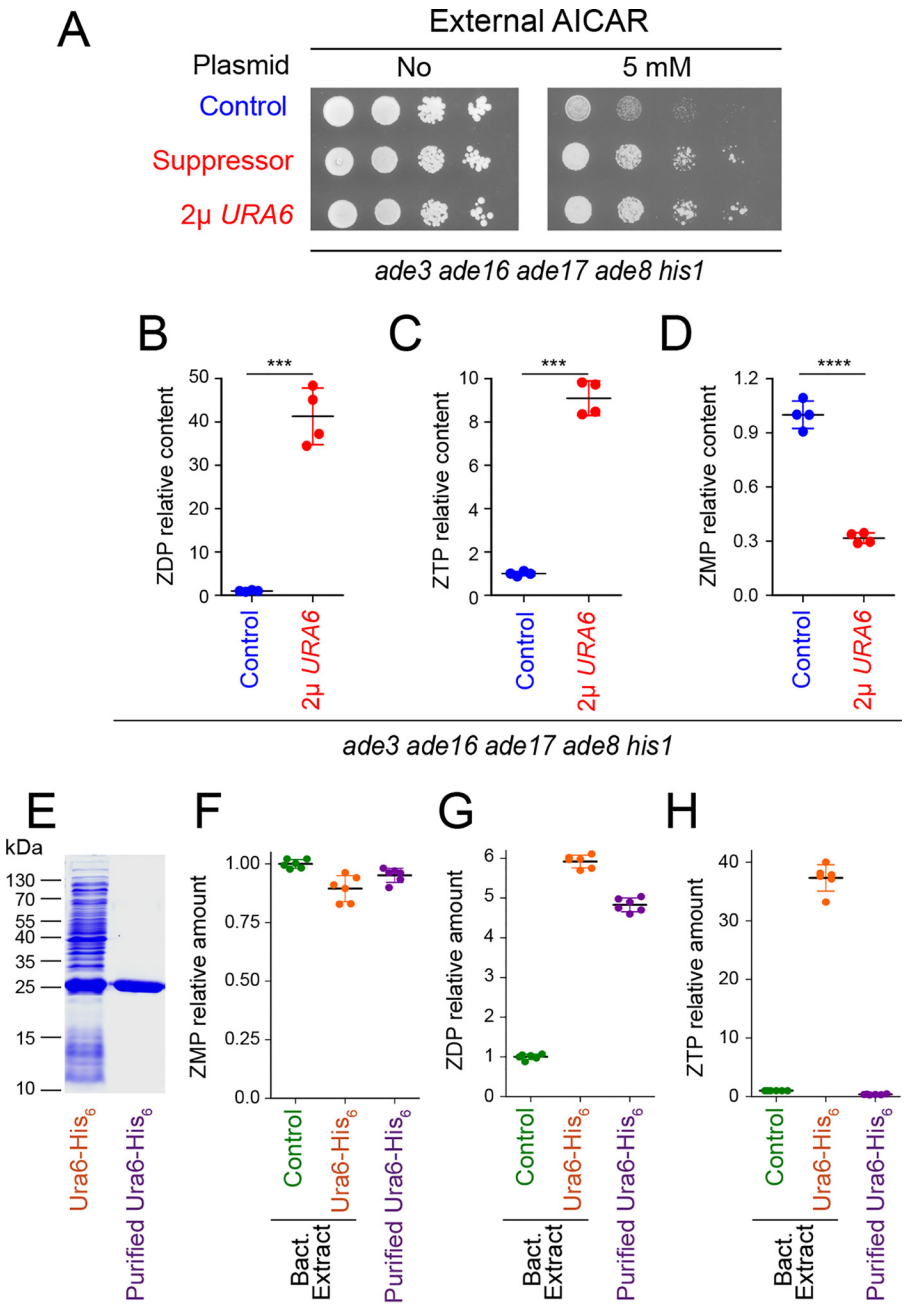

Figure 3. The UMP kinase Ura6 promotes ZMP phosphorylation in yeast. *A*, overexpression of the *URA6* gene strongly reduces ZMP toxicity. The *ade3 ade16 ade17 ade8 his1* strain (Y8908) was transformed with either the suppressor plasmid isolated during the genetic screen (suppressor, P4979), a plasmid overexpressing *URA6* gene (P4919), or the cognate empty vector as control (control; YEplac195). Transformants were grown overnight, serially diluted, and spotted on SDCasaWA medium containing, or lacking, AICAR. The plates were imaged after 2 days at 30 °C. *B–D*, effect of *URA6* overexpression (p4919) on relative content of AICAR derivatives in the *ade3 ade8 ade16 ade17 his1* strain (Y8908). Quantifications of metabolites were obtained from four independent extractions for each condition on strains grown in SDcasaWA medium for 24 h in the presence of 0.5 mM AICAR. Standard deviations are presented. Statistics correspond to Welch's *t* tests. ***, $p < 0.001$; ****, $p < 0.0001$. *E–H*, purified Ura6 (*E*) catalyzes ZDP, but not ZTP, synthesis *in vitro*. *F–H*, ZMP, ZDP, and ZTP were measured after a 15-min incubation at 30 °C with ZMP (1 mM) and ATP (2 mM) and His_6–Ura6 either in total protein bacterial (*Bact.*) extracts or purified (*E*). Metabolite amounts were set at 1 for the amounts measured with bacterial extracts containing the empty vector (control). *Errors* correspond to standard deviation obtained from six independent measurements.

ing enzymes (Ade16, Ade17, or Ura6) or previously identified binders (Pho2 or Pho4 (10)) were not found. Most interestingly, the ubiquitin-activating enzyme Uba1 was found as a ZMP binder, suggesting that it could be a direct target for ZMP and account for reported chemo-genetic effects of AICAR on the ubiquitin pathway (18). Analysis of the biological processes (Gene Ontology (GO) terms), associated with the proteins retained on the ZMP resin, showed a strong enrichment in purine nucleotide binding, unfolded protein binding, and translation factor activity (Fig. 4*B*). The best score was for "purine nucleotide binding" (p value 2.7×10^{-9}), thus validating the affinity chromatography approach because ZMP is a precursor of purine nucleotides.

To evaluate the specificity of ZMP-binding proteins, a similar approach was applied to closely related molecules, namely AMP, SZMP, and AICAR. A list of proteins retained on AMP,

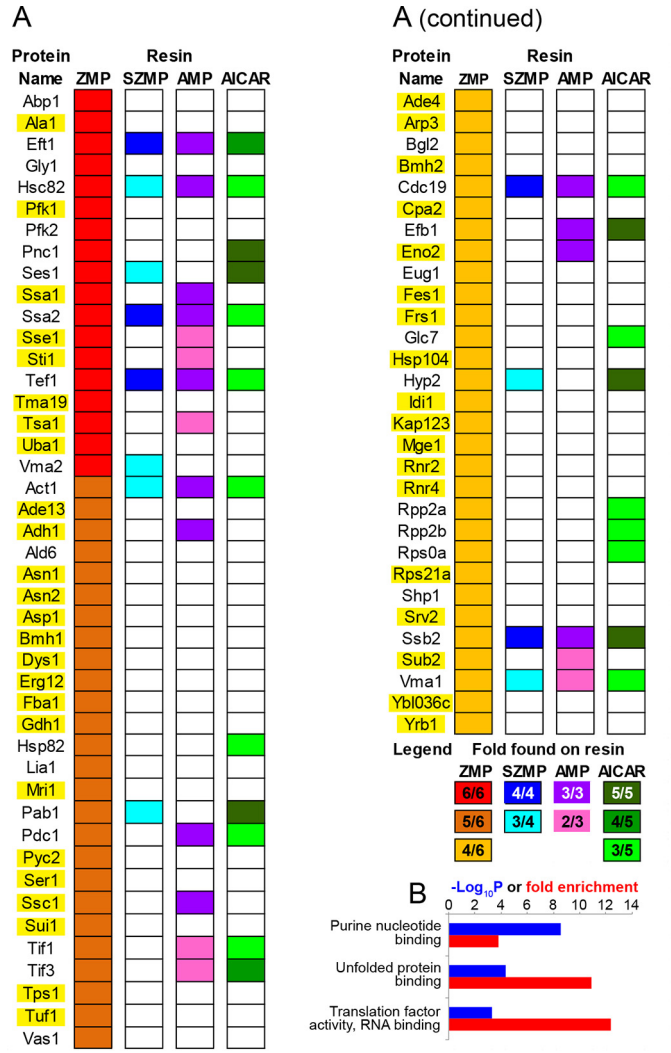

Figure 4. Proteome-wide identification of yeast ZMP binders by affinity chromatography. *A*, list of ZMP binders found at least four times in six affinity-chromatography experiments performed with independent samples. Proteins also found on other affinity resins are indicated. Complete lists are shown in Table S1. Genes highlighted in *yellow* were overexpressed, and their effects on AICAR sensitivity are shown in Fig. S7. *B*, biological process GO terms enrichment analysis for the 74 ZMP binders (http://www.geneontology.org/; please note that the JBC is not responsible for the long-term archiving and maintenance of this site or any other third party hosted site) (34, 35).

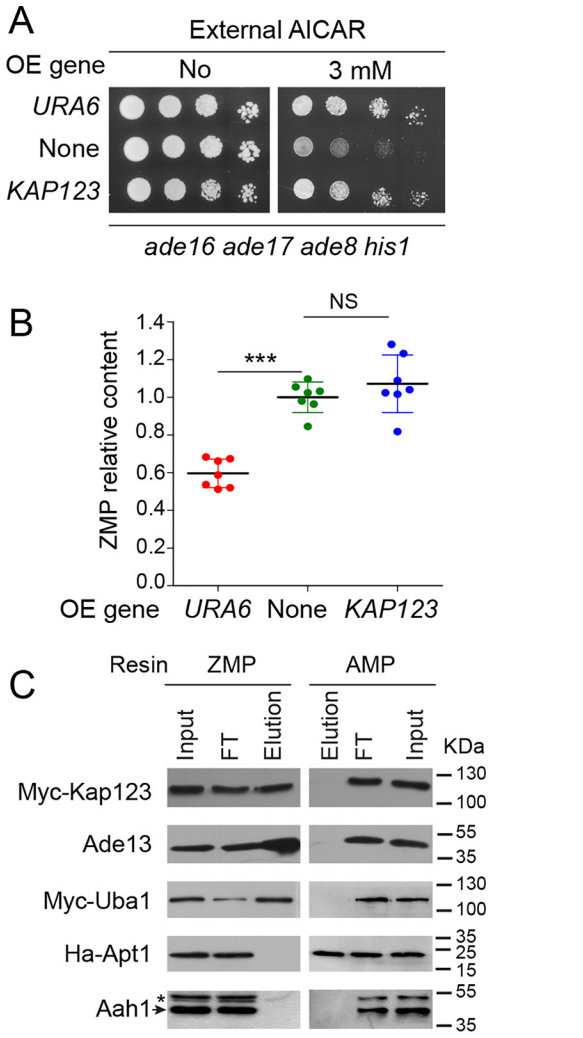

Figure 5. Overexpression of *KAP123* enhances AICAR resistance without changing ZMP intracellular content. *A*, cells (*ade8 ade16 ade17 his1*; Y2950) were transformed with plasmids allowing overexpression (*OE*) of either *URA6* (p4919) or *KAP123* (p4983) or with the empty vector (YepLac195, none). Transformants were serially diluted and spotted on SDcasaWA medium. The plates were imaged after 2 days at 37 °C. *B*, ZMP relative content was determined on seven independent transformants from Fig. 5*A* and exponentially grown in SDcasaWA medium for 24 h in the presence of AICAR (3 mM). *Errors bars* and statistics correspond to standard deviation and Welch's *t* test. *NS*, nonsignificant; ***, $p < 0.001$. *C*, specific binding of Myc-tagged Kap123 and Uba1 proteins to the ZMP-affinity resin was confirmed by Western blotting. *FT*, flow through. Elution corresponds to the fraction eluted with the cognate specific nucleotide (5 mM) on each affinity resin.

SZMP, and AICAR resins is presented in Table S1, revealing enrichment for specific functions. The best scores for SZMP and AICAR corresponded to "structural constituent of the ribosome," whereas for AMP it was "nucleotide binding" (Fig. S5). Among the 74 ZMP binders, 30 bound at least another compound tested (Fig. 4*A*). Interestingly, only eight proteins were found exclusively on ZMP and AMP columns, a binding pattern that would be expected for proteins echoing the AMP-mimetic effects of ZMP described for AMPK. Of note, the γ subunit of yeast AMPK (Snf4) was not retained on the columns as expected because yeast AMPK was found to be activated by ADP rather than AMP (23). Accordingly, a *snf4* mutant did not show altered AICAR sensitivity (Fig. S6). Among the 74 ZMP binders, 44 were exclusive ZMP binders, strongly suggesting that ZMP effects are most likely not restricted to AMP mimicry.

Overexpression of ZMP binders reveals nuclear trafficking as a function affected by AICAR

We reasoned that the most likely effectors of ZMP toxicity *in vivo* are proteins that bind ZMP (and also possibly AMP) but not the nontoxic derivatives SZMP and AICAR. The genes encoding 44 such yeast proteins (highlighted in *yellow* in Fig. 4*A*) were overexpressed from multicopy plasmids, and their ability to affect resistance to AICAR in yeast cells was evaluated. These 44 proteins comprised 36 of the 44 exclusive ZMP binders, and all the 8 AMP/ZMP exclusive binders. Overexpression of most of these genes, including *UBA1*, had no or little effect (Fig. S7), but overexpression of *KAP123* clearly improved the ability to grow in the presence of AICAR, as *URA6* did (Fig. 5*A*). However, in contrast to *URA6*, overexpression of *KAP123* did

not lower intracellular ZMP (Fig. 5*B*), as expected for a ZMP target.

We then confirmed the binding to ZMP of Kap123 (but also Uba1; see "Proteome-wide identification of ZMP binders"), using epitope-tagged versions of the proteins. Indeed, both Kap123 and Uba1 proteins were retained on the ZMP resin, but not on the AMP resin, as revealed by Western blotting analysis (Fig. 5*C*). In this experiment, Ade13 (adenylosuccinate lyase) and Apt1 (adenine phosphoribosyltransferase), for which ZMP and AMP are the corresponding reaction products, were used as positive controls for the ZMP and AMP resin, respectively (Fig. 5*C*). Aah1 (adenine deaminase) was used as a negative control for both resins (Fig. 5*C*).

Because Kap123 is an importin mediating the nuclear trafficking of several cargoes, including ribosomal proteins (24), we hypothesized that ZMP could affect nuclear transport. We first monitored nuclear localization of the Rpl25–NLS–GFP fusion (ribosomal 60S subunit protein L25 fused to green fluorescent protein via a nuclear localization signal), which is fully dependent on Kap123 (24). We found that it was not affected by AICAR (Fig. S8), indicating that AICAR does not primarily act through inhibition of Kap123, although overexpression of Kap123 can clearly bypass defects associated with AICAR treatment. The effect of AICAR on nuclear trafficking was then directly and globally assayed by comparing protein composition of nuclei-enriched extracts from yeast treated or not treated with AICAR by label-free quantitative analysis. Strikingly, 57 proteins were significantly less abundant (at least 2-fold) in the nuclei-enriched fraction following AICAR treatment (Fig. 6*A* and Table S2). Among these 57 proteins, 17 (highlighted in *yellow* in Table S2) were also detected in whole cell protein extracts by quantitative MS, and in all cases their abundance was not significantly changed in response to AICAR. We conclude that AICAR affects their nuclear localization rather than their overall abundance. GO-term analysis revealed that, among these 57 proteins, nuclear components and nuclear functions such as chromatin assembly and organization, rRNA metabolism, or transcription, were most significantly over-represented (Table S3).

A parallel analysis, performed on yeast cells grown in the presence of AICAR and overexpressing or not *KAP123*, revealed 92 proteins that were significantly more abundant in the nuclei-enriched fraction when *KAP123* was overexpressed (Table S4). Among those, proteins involved in chromatin and transcription-related processes were very significantly over-represented (Table S5). Most conspicuously, 15 proteins, less abundant in the nuclei-enriched fraction following AICAR treatment, were "restored" when *KAP123* was overexpressed (Fig. 6*B*). This overlap is statistically highly significant (hypergeometric distribution: $p = 2.16 \times 10^{-5}$), pointing to a strong functional connection between AICAR feeding and *KAP123* overexpression. Again, proteins involved in chromatin organization and transcription were overrepresented among these 15 proteins (Fig. 6*C*). This result shows that *KAP123* overexpression can compensate for some of the effects that AICAR exerts on nuclear traffic and could in this way contribute to the suppression of AICAR-induced phenotypic effects. Taken together, these results reveal nuclear trafficking as a critical cellular function that is altered by AICAR and point to Kap123 as an important, although nonexclusive, effector protein.

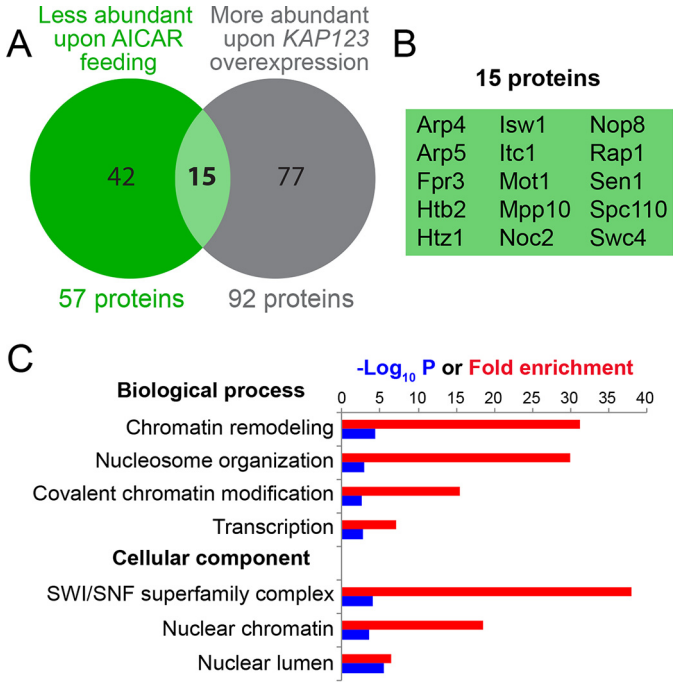

Figure 6. Nuclear protein content is altered by AICAR treatment in yeast. *A*, Venn diagram representation for proteins less abundant in the nuclei-enriched fraction after AICAR treatment (*green circle*) and proteins more abundant in nuclei-enriched fraction of cells overexpressing *KAP123* in the presence of AICAR (*gray circle*). The entire lists of proteins that significantly changed in both conditions are presented in Tables S3 and S4. *B*, list of the 15 common proteins in the Venn diagram presented in Fig. 6*A*. *C*, GO term analysis (http://www.geneontology.org/; please note that the JBC is not responsible for the long-term archiving and maintenance of this site or any other third party hosted site) (34, 35)[8] for the 15 proteins listed in Fig. 6*B*.

Specificity of KAP123 and URA6 as dosage suppressors

In previous work, we identified several mutants that showed high sensitivity to AICAR because of increased uptake and accumulation (*thi3*, *pdc2*, and *thi80* mutant strains) (1); impaired purine metabolism (*aah1*, *ade13*, and *hpt1*) (17); or interference with cell cycle progression (*bre1*, *rad6*, *set1*, and *swd1*) (16). Representative mutants among those were assayed to establish whether they could be phenotypically suppressed by *URA6* or *KAP123* overexpression. In fact, *URA6* overexpression efficiently suppressed AICAR sensitivity of the *set1* and *thi3* mutants (Fig. 7, *A* and *B*) and had a weaker but reproducible effect on the *aah1* mutant (Fig. 7*C*). By contrast, overexpression of *KAP123* only rescued AICAR sensitivity of the *set1* mutant (Fig. 7*A*) and not that of other mutants such as *thi3* or *aah1* (Fig. 7, *B* and *C*), indicating that increased sensitivity of the various mutants has distinct causes. Consistent with our previous findings (16), other mutants in the *set1* pathway (*bre1*, *swd1*, and *swd3*) were also suppressed by *KAP123* overexpression (Fig. S9). Overall, these results point to a central role for nuclear trafficking in AICAR sensitivity of yeast mutants affecting cell-cycle progression.

Discussion

The purine biosynthesis metabolic intermediate ZMP is naturally present in eukaryotic cells at low concentration. It can

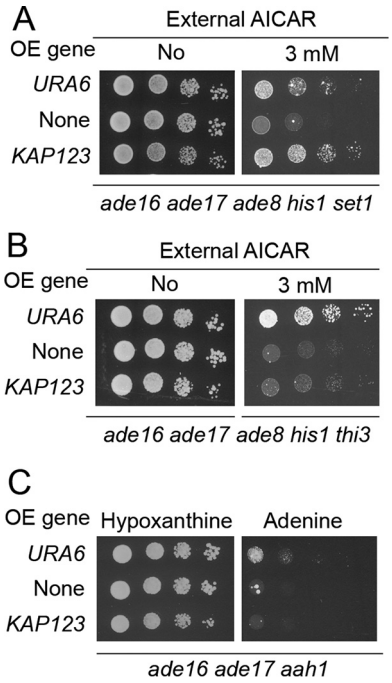

Figure 7. AICAR toxicity is alleviated by *KAP123* overexpression specifically in the AICAR-sensitive *set1* mutant affected in cell cycle progression. *A–C*, effect of *URA6* and *KAP123* overexpression on growth of AICAR-sensitive strains affected in cell-cycle progression (*A*), in AICAR uptake (*B*), and in purine metabolism (*C*). Mutant strains (Y9168, Y7321, and Y10846) were transformed with the empty plasmid (YepLac195, none) or with plasmids allowing overexpression (*OE*) of either *URA6* (p4919) or *KAP123* (p4983). Transformants were serially diluted and spotted on SDcasaWA medium ± AICAR (*A* and *B*) or SDcasaW medium supplemented with either hypoxanthine or adenine (*C*). The plates were imaged after 3 days at 37 °C.

accumulate when its riboside precursor AICAR is provided to the cell, but also in several metabolic diseases. Indeed, ZMP as well as ZDP and ZTP were found at very high concentrations (ZTP reaching even higher levels than ATP) in red blood cells of an AICAR transformylase IMP-cyclohydrolase–deficient patient lacking the enzyme that catalyzes the last two steps of the purine biosynthesis pathway (25) and was the best marker for hypoxanthine-guanine phospho-ribosyl-transferase deficiency in a large cohort of Lesch–Nyhan syndrome patients (26). The precise role of ZMP in the etiology of these diseases is unclear but should be addressed in connection with the fact that treating eukaryotic cells with AICAR at high concentration is toxic. In many studies, it was shown that the riboside precursor of ZMP had no biological effects, suggesting that ZMP itself, or a derivative, is the active compound. In our study, taking advantage of the power of yeast genetics, we established that AICAR toxicity tightly correlates with ZMP accumulation; lowering ZMP accumulation by stimulating its conversion to SZMP, ZDP, or ZTP derivatives decreased toxicity of the prodrug AICAR. Thus, increasing the levels of intracellular ZTP did not enhance toxicity of AICAR but rather decreased it. This suggests that AICAR toxicity is not due to massive incorporation of AICAR-nucleotides into nucleic acids. Accordingly, we found no effect of AICAR on mutation or recombination rate, as well as telomere length. These results are consistent with those obtained in previous work showing that yeast mutants displaying increased AICAR uptake became hypersensitive to this compound and that the sensitivity was associated with a 10-fold increase of the monophosphate (ZMP) concentration (1), whereas the di- and triphosphate forms (ZDP and ZTP) were hardly detectable.[7] Altogether, these results reveal ZMP as the toxic compound in yeast cells treated with the prodrug AICAR.

Affinity chromatography allowed us to identify a spectrum of AMP- and ZMP-binding proteins from yeast, thus providing a new resource of nucleotide-binding proteins. Only 20 of the 81 AMP binders and 74 ZMP binders were retained on both AMP and ZMP resins, indicating that not all AMP binders are able to efficiently bind ZMP despite its well-established AMP-mimetic role best exemplified as an effector molecule acting on mammalian AMP-activated kinase (14). Symmetrically, most ZMP binders were not identified as AMP binders. Why do these proteins bind ZMP? It is possible that some of the identified proteins physiologically bind ZMP, as Ade13 does? It could also be that ZMP binding imitates physiological interaction of these proteins with another nucleotide. In any case, our results strongly suggest that some of the AICAR effects are not due to AMP-mimetic interactions of ZMP with target proteins. Thus, our data support the view that the toxic effects of ZMP are not due to its AMP-mimetic properties.

Overexpression of *KAP123*, which has been identified as an "exclusive ZMP binder," significantly improved AICAR resistance, and this effect was enhanced in *bre1*, *set1*, *swd1*, and *swd3* AICAR-sensitive mutants affecting histone methylation. Kap123 is a karyopherin-β involved in the nuclear entry of multiple proteins including ribosomal proteins and histones (24, 27). Strikingly, Srm1, the guanyl-nucleotide exchange factor for yeast Ran Gsp1p, was among the 57 proteins for which nuclear localization was impaired by AICAR. This protein, homologous to human RCC1, is critical for nuclear trafficking, and its mislocalization upon AICAR treatment could, in a cascading effect, contribute to mislocalization of several other proteins. Thus, these results point to AICAR affecting nuclear trafficking in a way that is at least partly Kap123-dependent.

Suppression of *bre1*, *set1*, and *swd1* by Kap123 overexpression confirmed that nuclear trafficking contributes to the chemo-genetic effect of AICAR in several histone modification mutants, as proposed previously (16). It should be stressed that *KAP123* overexpression only partially suppressed AICAR sensitivity and was not a suppressor of all AICAR-sensitive mutants (Fig. 7), implying that some AICAR effects most probably involve targets other than Kap123. Indeed, we had previously identified the ubiquitin pathway as an important target for ZMP toxicity (18), and remarkably, unfolded protein binding was the second enriched GO term among the ZMP binders (Fig. 4). In this work, Uba1, the ubiquitin-activating enzyme at the apex of the ubiquitin pathway, was identified as a ZMP binder, suggesting that it could be a direct target of ZMP. However, overexpression of *UBA1* alone was not sufficient to increase the ability of yeast cells to cope with AICAR (Fig. S7), revealing a rather complex situation, as previously highlighted by our genetic analyses (18). Even at the level of nuclear trafficking, our finding of a partial overlap between *KAP123* over-

[7] J. Ceschin, B. Daignan-Fornier, and B. Pinson, unpublished results.

expression and AICAR effect on nuclear protein content suggests a complex interplay between ZMP and the nuclear trafficking machinery involving additional players. One such candidate is Yrb1, a Ran GTPase-binding protein involved in nuclear protein trafficking that was identified as one of the ZMP-specific binders in this work. However, overexpression of *YRB1* had no major effect on growth in the presence of AICAR (Fig. S7).

This study illustrates that a molecule with anti-proliferative properties interacts with multiple proteins and, even on a single process such as nuclear trafficking, most probably acts through more than one effector. The polypharmacology paradigm proposed 10 years ago (28) underlines how combined effects of a drug on multiple targets can bypass phenotypic robustness while limiting toxicity. Importantly, acadesine (AICAR) was well-tolerated in clinical trials (6) and was found pharmacologically active in several animal-model studies (3–5, 15, 29). Understanding the diverse molecular bases of AICAR effects will give clues to its beneficial and adverse effects and could permit synthetic-lethality predictions, smart development of derived compounds, and drug repurposing (30).

Experimental procedures

Yeast media, yeast strains, and plasmids

SD is a synthetic minimal medium containing 0.5% ammonium sulfate, 0.17% yeast nitrogen base (BD-Difco, Franklin Lakes, NJ), 2% glucose. SDcasaW is SD medium supplemented with 0.2% casamino acids (catalog no. 233520; BD-Difco) and tryptophan (0.2 mM). When indicated, adenine (0.3 mM), hypoxanthine (0.3 mM), and/or uracil (0.3 mM) were added in SDcasaW medium, resulting in media termed SDcasaWA (+ adenine), SDcasaWHypox (+ hypoxanthine), SDcasaWU (+ uracil), and SDcasaWAU (+ adenine + uracil). Yeast strains are listed in Table S6 and belong to, or are derived from, a set of knockout mutant strains isogenic to BY4742 purchased from Euroscarf (Frankfurt, Germany). Multimutant strains were obtained by crossing, sporulation, and micromanipulation of meiosis progeny. The plasmids used in this study are described in Table S7. Cloning details for the unpublished plasmids are available upon request.

Yeast growth test

Yeast cells were resuspended in sterile water to 2×10^7 cells/ml and subjected to 1/10 serial dilutions. Drops (5 μl) of each dilution were spotted on freshly prepared plates and were incubated at indicated temperature for 48–72 h.

Isolation of multicopy suppressors of AICAR toxicity

To obtain multicopy suppressors of AICAR toxicity, an *ade3 ade16 ade17 ade8 his1 strain* (Y8908) was used because in such a strain both *ade3* and *ade16 ade17* mutations block AICAR transformylase IMP-cyclohydrolase activity and therefore neither *ADE3*, *ADE16*, nor *ADE17* can be selected as a suppressor. This strain was transformed with a multicopy plasmid library (PFL44L backbone, generous gift from F. Lacroute), and transformants were selected on SDcasaWA medium after 48 h of incubation at 30 °C. The colonies were then transferred by replica plating on the same medium containing 5 mM AICAR and grown for 48 h at 37 °C. This screening temperature was chosen because in previous work we noticed that addition of AICAR was much more toxic for yeast cells at 37 °C than at 30 °C (1). Multicopy plasmids were extracted from six clones able to grow in the presence of AICAR and were sequenced. These plasmids contained a DNA fragment from the same region of chromosome 11. The plasmid (p4979) containing the 4.6-kbp fragment with chromosome coordinates 390,252–394,835 bp was further studied (see "Results").

Metabolite extraction from yeast cells and separation by LC

Extraction of metabolites was performed in an ethanol with 10 mM HEPES, pH 7.2 (3/1), solution for 3 min at 80 °C for yeast as described (1). The extracts were then evaporated using a rotary evaporator (8 min, 65 °C), and the dried residues were resuspended in MilliQ water. Insoluble particles were removed by centrifugation (21,000 × g, 4 °C; 1 h). Metabolites were then separated on an ICS3000 chromatography station (Dionex, Sunnyvale, CA) using a carbopac PA1 column (250 × 2 mm; catalog no. 057178; Thermo Fisher Scientific) with a 0.25 ml/min flow rate. Elution of metabolites was achieved with a sodium acetate gradient in 50 mM NaOH as follows: elution was started at 50 mM sodium acetate for 2 min, rising up to 75 mM in 8 min, then to 100 mM in 25 min, and finally to 350 mM in 30 min, followed by a step at 350 mM for 5 min, rising to 500 mM in 10 min, and being kept at this sodium acetate concentration for 5 min, and finally raised to 800 mM within 10 min followed by a step at this concentration for 20 min. The resin was then equilibrated at 50 mM sodium acetate for 15 min before injection of a new sample. The peaks were identified by their retention time and their UV spectrum signature (Diode Array Detector Ultimate 3000 RS; Dionex), and when necessary by co-injection with standards. For each strain analyzed, normalization to cellular volume was done with a Multisizer 4 (Beckman Coulter). Peak quantifications were done at the following wavelengths: 230 nm for fumarate, 260 nm for ATP, and 269 nm for AICAR, SAICAR, ZMP, and SZMP. All metabolite extractions were performed on at least three to six independent yeast cell cultures.

Affinity chromatography

ZMP-binding proteins were identified by affinity chromatography using the ZMP-Sepharose resin described previously (10). Protein extracts were prepared from the BY4742 WT strain as described (10), except that elution of the ZMP binders was performed with ZMP (5 mM; catalog no. A611705; Toronto Research Chemicals) in buffer A (Na_2HPO_4/HCl, pH 7.2, 10 mM NaCl). Elution fractions were concentrated on a Nanosep 10K Omega filter, and protein concentration was measured. The ZMP binders were then identified using MS according to the procedure described in protein identification by LC-MS/MS and database search and results processing sections. A stringent cutoff was then applied, retaining only proteins identified with at least two peptides, and found at least four times in six independent experiments (Table S1). The ability of proteins to bind AMP, SZMP, or AICAR was also assayed using either a commercial AMP-agarose resin (catalog no. A1271; Merck) or

SZMP- and AICAR-resins prepared as described for the ZMP resin (10). In each case, elution of interacting proteins was performed with 5 mM of the corresponding metabolite (AMP (catalog no. A1752; Merck), SZMP (lab collection, (8)), or AICAR (catalog no. A611700; Toronto Research Chemicals)) dissolved in buffer A.

Immunoblot

Western blots were hybridized with the following antibodies: anti-Myc (1/5,000; catalog no. MMS-150R; Covance), anti-Ade13 (1/15,000 (8)), anti-HA (1/10,000, catalog no. H9658; Sigma–Aldrich), and anti-Aah1 (1/10,000 (31)).

Protein identification by LC-MS/MS

Concentrated proteins from each affinity-chromatography elution fractions were solubilized in Laemmli sample buffer and subjected to SDS-PAGE to evaluate concentration and for cleaning purposes. After entering the resolving gel, separation was stopped. Following colloidal blue staining, the bands were cut out from the SDS-PAGE gel and subsequently cut into 1 × 1 mm gel pieces. Gel pieces were destained in 25 mmol/liter ammonium bicarbonate 50% (w/v), rinsed twice in ultrapure water, and shrunk in acetonitrile for 10 min. After acetonitrile removal, gel pieces were dried at room temperature, covered with trypsin solution (10 ng/μl in 40 mM NH_4HCO_3 and 10% acetonitrile), rehydrated at 4 °C for 10 min, and finally incubated overnight at 37 °C. Gel pieces were then incubated for 15 min in 40 mM NH_4HCO_3 and 10% acetonitrile at room temperature on a rotary shaker. The supernatant was collected, and an extraction solution (H_2O, acetonitrile, HCOOH (47.5/47.5/5)) was added to the gel slices for 15 min. This extraction step was repeated twice. Supernatants were pooled and concentrated with a vacuum centrifuge to a final volume of 25 μl. Digests were finally acidified by addition of 1.5 μl of formic acid (5%, v/v) and stored at −20 °C. The peptide mixture was analyzed on an Ultimate 3000 nano-LC system (Dionex) coupled to either a LTQ, a LTQ-Orbitrap XL, or a Q-Exactive mass spectrometer (ThermoFinnigan, San Jose, CA). In all cases, 10 μl of peptide digests were loaded onto a C18 PepMap™ trap column (300-μm; 5-mm LC Packings) at a 30 μl/min flow rate. Peptides were eluted from the trap column and then loaded onto an analytical C18 Pep-Map column (75 mm × 15 cm; LC Packings) for 105 min with a 5–40% linear gradient of 80% acetonitrile with 0.1% formic acid in 5% acetonitrile with 0.1% formic acid at a 200 nl/min flow rate. The mass spectrometer operated in positive ion mode at a 1.8–2-kV needle voltage. Mass spectrometry acquisition parameters are given in Table S8.

Nuclei-enriched fractions preparation and label-free quantitative data analysis

Yeast cells (*ade16 ade17 ade8 his1*; Y8480) were transformed by the plasmid allowing *KAP123* overexpression or by the cognate empty vector serving as negative control. Transformants exponentially grown in SDcasaWA were treated with 0 or 1 mM AICAR for 2 h. The cells were collected and used to prepare total protein extracts and in parallel to perform nuclei enrichment with a commercial kit (Abnova catalog no. KA3951). For each condition, the experiments were done in triplicate with samples obtained from independent cultures. LC-MS/MS data were acquired on a Q-Exactive mass spectrometer as described above and were subsequently imported in Progenesis LC-MS 4.0 (Non Linear Dynamics). Data processing included the following steps: (i) features detection, (ii) features alignment across the LC-MS/MS runs, (iii) volume integration for 2–6 charge-state ions, (iv) normalization on feature median ratio, (v) import of sequence information, (vi) analysis of variance test at peptide level and filtering for features ($p < 0.05$), (vii) calculation of protein abundance (sum of the volume of corresponding peptides), and (viii) analysis of variance test at protein level and filtering for features ($p < 0.05$). Proteins were grouped according to the parsimony principle so as to establish the minimal protein list covering all detected peptides. Noticeably, only nonconflicting features and unique peptides were considered for calculation at protein level. Quantitative data were considered for proteins quantified by a minimum of two peptides.

Database search and processing of proteomic results

The data were searched by SEQUEST through Proteome Discoverer 1.4 (Thermo Fisher Scientific Inc.) against the *Saccharomyces cerevisiae* Reference Proteome Set (Uniprot 2015-05; 6636 entries). Spectra from peptides higher than 5,000 Da or lower than 350 Da were rejected. The search parameters were as follows: mass accuracy of the monoisotopic peptide precursor and peptide fragments were as described in Table S8. Only *b*- and *y*-ions were considered for mass calculation. Oxidation of methionine (+16 Da) was considered as variable modification. Two missed trypsin cleavages were allowed. Peptide validation was performed using Percolator algorithm (32), and only "high confidence" peptides were retained corresponding to a 1% false positive rate at peptide level. Data for the affinity-chromatography and label-free quantitative proteomics were deposited and are available in PRIDE at the following links: identification of the *S. cerevisiae* ZMP binders (project accession number PXD007780) and effect of acadesine and overexpression of the karyopherin Kap123 on nuclear abundance of yeast proteins (project accession number PXD007779).

His_6–Ura6 protein expression and purification

The His_6–Ura6 protein was expressed in BL21 C41(DE3)-pLysS bacteria (33) by transformation of the *URA6-HIS6* plasmid (p5334). Transformants were grown overnight in LB medium + ampicillin, diluted in 500 ml of the same medium to $A_{600\,nm} = 0.005$ and grown for 4 h at 30 °C before isopropyl β-D-1-thiogalactopyranoside addition (2 mM). The cells were harvested by centrifugation (5,000 × *g* for 10 min at 4 °C) after 2 h 30 min at 30 °C, and the cell pellet was washed with 50 mM Tris-HCl, pH 7, 0.15 M KCl and frozen at −80 °C. The pellet was resuspended in 50 mM Tris-HCl, pH 7, 0.1 M KCl, 1 mM EDTA, 1 mM DTT containing a tablet of protease/phosphatase inhibitor (buffer B). The cells were disrupted by four cycles of 1 min sonication on ice, and the suspension was clarified by centrifugation (21,000 × *g*) for 30 min at 4 °C. The supernatant was dialyzed twice against buffer B without EDTA (buffer C) containing 10 mM imidazole and then loaded onto 1.5 ml of nickel–nitrilotriacetic acid resin (Qiagen). The resin was washed with 15 volumes of Buffer C containing 50 mM imidazole, and puri-

fied His_6–Ura6 protein was then eluted with 250 mM imidazole in buffer C. The purified His_6–Ura6 protein was concentrated (0.7 ml at 10 mg/ml), aliquoted and frozen at −80 °C.

Ura6 enzymatic activity

Ura6 enzymatic activity was measured on both total protein extracts from bacteria (containing the His_6–Ura6 expressing plasmid (p5334) or the empty vector (pET15b; catalog no. 69661-3; Merck–Novagen)) and on the purified protein. In each case, measurements were carried out using initial rate conditions that were stable for at least 30 min at 30 °C. Enzymatic measurements were performed in 100 mM Tris-HCl, pH 7.5 buffer containing 100 mM KCl, 5 mM $MgCl_2$, 2 mM ATP, and 1 mM ZMP. The reactions were started by addition of either the purified protein (at 1 μg/ml in enzymatic assay) or the total protein extracts from bacteria expressing or not His_6–Ura6 (each at final concentration of 100 μg/ml in enzymatic assays). All enzymatic reactions were stopped by boiling (3 min at 80 °C) a 100-μl aliquot of the reaction mix in 900 μl of ethanol, 10 mM HEPES, pH 7 (4/1 v/v). Quantification of the reaction product(s) was done by LC under conditions described for intracellular metabolites determination. ZDP and ZTP standard solutions used for quantification were purchased from Jena Biosciences (catalog nos. NU-1167 and NU-1166, respectively).

Quantification and statistical analysis

All tests for significance were according to Welch's unpaired *t* tests, assuming bilateral distribution and unequal variances, by comparison with the relevant control as specified in legends of the figures and supplemental figures Experiments were in each case performed on at least three biologically independent samples ($n \geq 3$), as detailed in each figure legend. Significance was defined by *p* values and indicated as *, $p < 0.05$; **, $p < 0.01$; ***, $p < 0.001$; ****, $p < 0.0001$; *NS*, nonsignificant ($p > 0.05$).

Author contributions—D. C. D., B. P., J. C., H. C. H., C. S.-M., D. L., M. K., M. B., and B. D.-F. conceptualization; D. C. D., B. P., J. C., H. C. H., C. S.-M., D. L., S. C., M. B., and B. D.-F. data curation; D. C. D., B. P., J. C., C. S.-M., S. C., M. B., and B. D.-F. formal analysis; D. C. D., B. P., J. C., C. S.-M., and B. D.-F. supervision; D. C. D., B. P., J. C., C. S.-M., and B. D.-F. funding acquisition; D. C. D., B. P., J. C., C. S.-M., and B. D.-F. validation; D. C. D., B. P., J. C., H. C. H., C. S.-M., D. L., S. C., and B. D.-F. investigation; D. C. D., B. P., J. C., H. C. H., C. S.-M., D. L., S. C., and B. D.-F. methodology; D. C. D., B. P., J. C., C. S.-M., M. K., and B. D.-F. writing-original draft; D. C. D., B. P., J. C., C. S.-M., M. K., and B. D.-F. writing-review and editing; M. K. resources.

Acknowledgment—We thank Ioanna Lemnian for help with hypergeometric distribution.

References

1. Ceschin, J., Saint-Marc, C., Laporte, J., Labriet, A., Philippe, C., Moenner, M., Daignan-Fornier, B., and Pinson, B. (2014) Identification of yeast and human 5-aminoimidazole-4-carboxamide-1-β-D-ribofuranoside (AICAR) transporters. *J. Biol. Chem.* **289,** 16844–16854 CrossRef Medline
2. Daignan-Fornier, B., and Pinson, B. (2012) 5-Aminoimidazole-4-carboxamide-1-β-D-ribofuranosyl 5′-monophosphate (AICAR), a highly conserved purine intermediate with multiple effects. *Metabolites* **2,** 292–302 CrossRef Medline
3. Guo, D., Hildebrandt, I. J., Prins, R. M., Soto, H., Mazzotta, M. M., Dang, J., Czernin, J., Shyy, J. Y., Watson, A. D., Phelps, M., Radu, C. G., Cloughesy, T. F., and Mischel, P. S. (2009) The AMPK agonist AICAR inhibits the growth of EGFRvIII-expressing glioblastomas by inhibiting lipogenesis. *Proc. Natl. Acad. Sci. U.S.A.* **106,** 12932–12937 CrossRef Medline
4. Rattan, R., Giri, S., Singh, A. K., and Singh, I. (2005) 5-Aminoimidazole-4-carboxamide-1-β-D-ribofuranoside inhibits cancer cell proliferation *in vitro* and *in vivo* via AMP-activated protein kinase. *J. Biol. Chem.* **280,** 39582–39593 CrossRef Medline
5. Robert, G., Ben Sahra, I., Puissant, A., Colosetti, P., Belhacene, N., Gounon, P., Hofman, P., Bost, F., Cassuto, J. P., and Auberger, P. (2009) Acadesine kills chronic myelogenous leukemia (CML) cells through PKC-dependent induction of autophagic cell death. *PLoS One* **4,** e7889 CrossRef Medline
6. Van Den Neste, E., Cazin, B., Janssens, A., González-Barca, E., Terol, M. J., Levy, V., Pérez de Oteyza, J., Zachee, P., Saunders, A., de Frias, M., and Campàs, C. (2013) Acadesine for patients with relapsed/refractory chronic lymphocytic leukemia (CLL): a multicenter phase I/II study. *Cancer Chemother. Pharmacol.* **71,** 581–591 CrossRef Medline
7. Hürlimann, H. C., Laloo, B., Simon-Kayser, B., Saint-Marc, C., Coulpier, F., Lemoine, S., Daignan-Fornier, B., and Pinson, B. (2011) Physiological and toxic effects of purine intermediate 5-amino-4-imidazolecarboxamide ribonucleotide (AICAR) in yeast. *J. Biol. Chem.* **286,** 30994–31002 CrossRef Medline
8. Rébora, K., Desmoucelles, C., Borne, F., Pinson, B., and Daignan-Fornier, B. (2001) Yeast AMP pathway genes respond to adenine through regulated synthesis of a metabolic intermediate. *Mol. Cell Biol.* **21,** 7901–7912 CrossRef Medline
9. Rébora, K., Laloo, B., and Daignan-Fornier, B. (2005) Revisiting purine-histidine cross-pathway regulation in *Saccharomyces cerevisiae*: a central role for a small molecule. *Genetics* **170,** 61–70 CrossRef Medline
10. Pinson, B., Vaur, S., Sagot, I., Coulpier, F., Lemoine, S., and Daignan-Fornier, B. (2009) Metabolic intermediates selectively stimulate transcription factor interaction and modulate phosphate and purine pathways. *Genes Dev.* **23,** 1399–1407 CrossRef Medline
11. Kim, P. B., Nelson, J. W., and Breaker, R. R. (2015) An ancient riboswitch class in bacteria regulates purine biosynthesis and one-carbon metabolism. *Mol. Cell* **57,** 317–328 CrossRef Medline
12. Sullivan, J. E., Brocklehurst, K. J., Marley, A. E., Carey, F., Carling, D., and Beri, R. K. (1994) Inhibition of lipolysis and lipogenesis in isolated rat adipocytes with AICAR, a cell-permeable activator of AMP-activated protein kinase. *FEBS Lett.* **353,** 33–36 CrossRef Medline
13. Sullivan, J. E., Carey, F., Carling, D., and Beri, R. K. (1994) Characterisation of 5′-AMP-activated protein kinase in human liver using specific peptide substrates and the effects of 5′-AMP analogues on enzyme activity. *Biochem. Biophys. Res. Commun.* **200,** 1551–1556 CrossRef Medline
14. Day, P., Sharff, A., Parra, L., Cleasby, A., Williams, M., Hörer, S., Nar, H., Redemann, N., Tickle, I., and Yon, J. (2007) Structure of a CBS-domain pair from the regulatory γ1 subunit of human AMPK in complex with AMP and ZMP. *Acta Crystallogr. D Biol. Crystallogr.* **63,** 587–596 CrossRef Medline
15. Liu, X., Chhipa, R. R., Pooya, S., Wortman, M., Yachyshin, S., Chow, L. M., Kumar, A., Zhou, X., Sun, Y., Quinn, B., McPherson, C., Warnick, R. E., Kendler, A., Giri, S., Poels, J., *et al.* (2014) Discrete mechanisms of mTOR and cell cycle regulation by AMPK agonists independent of AMPK. *Proc. Natl. Acad. Sci. U.S.A.* **111,** E435–E444 CrossRef Medline
16. Albrecht, D., Ceschin, J., Dompierre, J., Gueniot, F., Pinson, B., and Daignan-Fornier, B. (2016) Chemo-genetic interactions between histone modification and the antiproliferation drug AICAR are conserved in yeast and humans. *Genetics* **204,** 1447–1460 CrossRef Medline
17. Ceschin, J., Hürlimann, H. C., Saint-Marc, C., Albrecht, D., Violo, T., Moenner, M., Daignan-Fornier, B., and Pinson, B. (2015) Disruption of nucleotide homeostasis by the antiproliferative drug 5-aminoimidazole-4-carboxamide-1-β-D-ribofuranoside monophosphate (AICAR). *J. Biol. Chem.* **290,** 23947–23959 CrossRef Medline

18. Albrecht, D., Hürlimann, H. C., Ceschin, J., Saint-Marc, C., Pinson, B., and Daignan-Fornier, B. (2018) Multiple chemo-genetic interactions between a toxic metabolite and the ubiquitin pathway in yeast. *Curr. Genet.* **64,** 1275–1286 CrossRef Medline
19. Nakamaru, K., Matsumoto, K., Taguchi, T., Suefuji, M., Murata, Y., Igata, M., Kawashima, J., Kondo, T., Motoshima, H., Tsuruzoe, K., Miyamura, N., Toyonaga, T., and Araki, E. (2005) AICAR, an activator of AMP-activated protein kinase, down-regulates the insulin receptor expression in HepG2 cells. *Biochem. Biophys. Res. Commun.* **328,** 449–454 CrossRef Medline
20. Tibbetts, A. S., and Appling, D. R. (1997) *Saccharomyces cerevisiae* expresses two genes encoding isozymes of 5-aminoimidazole-4-carboxamide ribonucleotide transformylase. *Arch. Biochem. Biophys.* **340,** 195–200 CrossRef Medline
21. Guetsova, M. L., Lecoq, K., and Daignan-Fornier, B. (1997) The isolation and characterization of *Saccharomyces cerevisiae* mutants that constitutively express purine biosynthetic genes. *Genetics* **147,** 383–397 Medline
22. Schricker, R., Magdolen, V., Kaniak, A., Wolf, K., and Bandlow, W. (1992) The adenylate kinase family in yeast: identification of URA6 as a multicopy suppressor of deficiency in major AMP kinase. *Gene* **122,** 111–118 CrossRef Medline
23. Mayer, F. V., Heath, R., Underwood, E., Sanders, M. J., Carmena, D., McCartney, R. R., Leiper, F. C., Xiao, B., Jing, C., Walker, P. A., Haire, L. F., Ogrodowicz, R., Martin, S. R., Schmidt, M. C., Gamblin, S. J., *et al.* (2011) ADP regulates SNF1, the *Saccharomyces cerevisiae* homolog of AMP-activated protein kinase. *Cell Metab.* **14,** 707–714 CrossRef Medline
24. Schlenstedt, G., Smirnova, E., Deane, R., Solsbacher, J., Kutay, U., Görlich, D., Ponstingl, H., and Bischoff, F. R. (1997) Yrb4p, a yeast ran-GTP-binding protein involved in import of ribosomal protein L25 into the nucleus. *EMBO J.* **16,** 6237–6249 CrossRef Medline
25. Marie, S., Heron, B., Bitoun, P., Timmerman, T., Van Den Berghe, G., and Vincent, M. F. (2004) AICA-ribosiduria: a novel, neurologically devastating inborn error of purine biosynthesis caused by mutation of ATIC. *Am. J. Hum. Genet.* **74,** 1276–1281 CrossRef Medline
26. Ceballos-Picot, I., Le Dantec, A., Brassier, A., Jaïs, J. P., Ledroit, M., Cahu, J., Ea, H. K., Daignan-Fornier, B., and Pinson, B. (2015) New biomarkers for early diagnosis of Lesch-Nyhan disease revealed by metabolic analysis on a large cohort of patients. *Orphanet J. Rare Dis.* **10,** 7 CrossRef Medline
27. Mosammaparast, N., Guo, Y., Shabanowitz, J., Hunt, D. F., and Pemberton, L. F. (2002) Pathways mediating the nuclear import of histones H3 and H4 in yeast. *J. Biol. Chem.* **277,** 862–868 CrossRef Medline
28. Hopkins, A. L. (2008) Network pharmacology: the next paradigm in drug discovery. *Nat. Chem. Biol.* **4,** 682–690 CrossRef Medline
29. Tang, Y. C., Williams, B. R., Siegel, J. J., and Amon, A. (2011) Identification of aneuploidy-selective antiproliferation compounds. *Cell* **144,** 499–512 CrossRef Medline
30. Medina-Franco, J. L., Giulianotti, M. A., Welmaker, G. S., and Houghten, R. A. (2013) Shifting from the single to the multitarget paradigm in drug discovery. *Drug Disc. Today* **18,** 495–501 CrossRef
31. Escusa, S., Camblong, J., Galan, J. M., Pinson, B., and Daignan-Fornier, B. (2006) Proteasome- and SCF-dependent degradation of yeast adenine deaminase upon transition from proliferation to quiescence requires a new F-box protein named Saf1p. *Mol. Microbiol.* **60,** 1014–1025 CrossRef Medline
32. Käll, L., Canterbury, J. D., Weston, J., Noble, W. S., and MacCoss, M. J. (2007) Semi-supervised learning for peptide identification from shotgun proteomics datasets. *Nat. Methods* **4,** 923–925 CrossRef Medline
33. Dumon-Seignovert, L., Cariot, G., and Vuillard, L. (2004) The toxicity of recombinant proteins in *Escherichia coli*: a comparison of overexpression in BL21(DE3), C41(DE3), and C43(DE3). *Protein Expr. Purif.* **37,** 203–206 CrossRef Medline
34. Ashburner, M., Ball, C. A., Blake, J. A., Botstein, D., Butler, H., Cherry, J. M., Davis, A. P., Dolinski, K., Dwight, S. S., Eppig, J. T., Harris, M. A., Hill, D. P., Issel-Tarver, L., Kasarskis, A., Lewis, S., *et al.* (2000) Gene ontology: tool for the unification of biology. The Gene Ontology Consortium. *Nat. Genet.* **25,** 25–29 CrossRef Medline
35. The Gene Ontology Consortium (2017) Expansion of the Gene Ontology knowledgebase and resources. *Nucleic Acids Res.* **45,** D331–D338 CrossRef Medline

Metabolomics and proteomics identify the toxic form and the associated cellular binding targets of the anti-proliferative drug AICAR

Delphine C. Douillet, Benoît Pinson, Johanna Ceschin, Hans C. Hürlimann, Christelle Saint-Marc, Damien Laporte, Stéphane Claverol, Manfred Konrad, Marc Bonneu and Bertrand Daignan-Fornier

J. Biol. Chem. 2019, 294:805-815.
doi: 10.1074/jbc.RA118.004964 originally published online November 26, 2018

Supporting information

Targeted-metabolomics and proteomics identify the toxic form and the associated binders of the anti-proliferative drug AICAR

Delphine C. Douillet[1,2 # §], Benoît Pinson[1,2 #], Johanna Ceschin[1,2], Hans C. Hürlimann[1,2 &], Christelle Saint-Marc[1,2], Damien Laporte[1,2], Stéphane Claverol[3], Manfred Konrad[4], Marc Bonneu[3] and Bertrand Daignan-Fornier[1,2*]

From [1] Université de Bordeaux IBGC UMR 5095 1, rue Camille Saint-Saëns F-33077 Bordeaux France
[2] Centre National de la Recherche Scientifique IBGC UMR 5095 1, rue Camille Saint-Saëns F-33077 Bordeaux France
[3] University of Bordeaux, Bordeaux INP, Plateforme Proteome, Bordeaux, France.
[4] Max-Planck-Institute for Biophysical Chemistry. Am Fassberg 11, D-37077 Goettingen, Germany

Running title: *AICAR monophosphate toxicity*

[#] Equal contribution
[§] Present address: Northwestern University Feinberg School of Medicine. 320 East Superior Street, Chicago, IL 60611 USA
[&] Present address: Martin-Luther Universität, Genetik, Molekulargenetik, Weinbergweg 10, D-06120 Halle, Germany

* To whom correspondence should be addressed: Bertrand Daignan-Fornier: Institut de Biochimie et Génétique Cellulaires, CNRS UMR 5095 1 rue C. Saint-Saëns CS 61390 F-33077 Bordeaux France. Tel: +33-556-999-001; Fax: +33-556-999-059; E-mail: b.daignan-fornier@ibgc.cnrs.fr

Supplemental Figures

Supplemental Tables

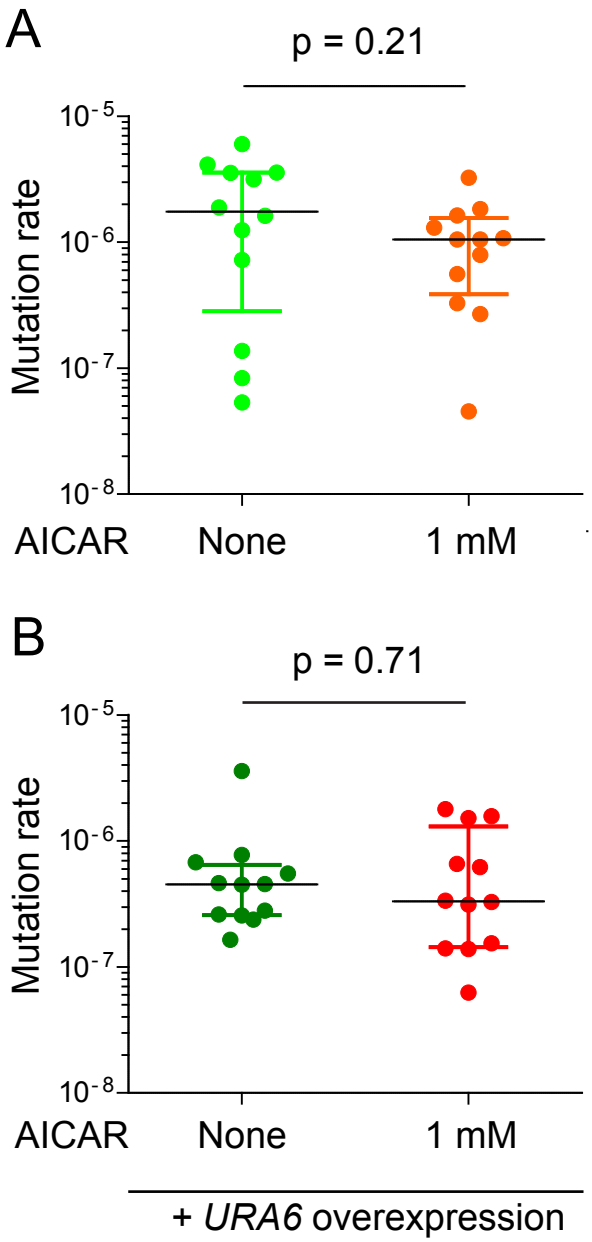

Figure S1. The mutation rate is not affected by AICAR feeding in yeast.
Quadruple mutant cells (*ade16 ade17 ade8 his1*, Y6986) were transformed (*B*) or not (*A*) with the plasmid allowing *URA6* overexpression (p4919). In each condition, twelve independent cell cultures were inoculated at low cell density (100 cells/ml) in a non-selective medium (SD casaWA) containing or not (none) AICAR (1 mM) and were grown for 72 h at 30°C to reach a cell density of about 8.10^7 cells/ml. Dilutions of each culture were plated on SD medium supplemented with uracil, adenine, histidine and containing or not canavanin (0.35 mM), a toxic analog of arginine. The mutation rate was determined from the number of canavanin-resistant clones by the method described by Hall *et al* (Hall,B.M., Ma, C.X., Liang, P., and Singh, K.K. (2009). Fluctuation AnaLysis CalculatOR: a Web tool for the determination of mutation rate using Luria–Delbrück fluctuation analysis. Bioinformatics 5, 1564–1565). Black and colored bars respectively correspond to the median and the interquartile range.

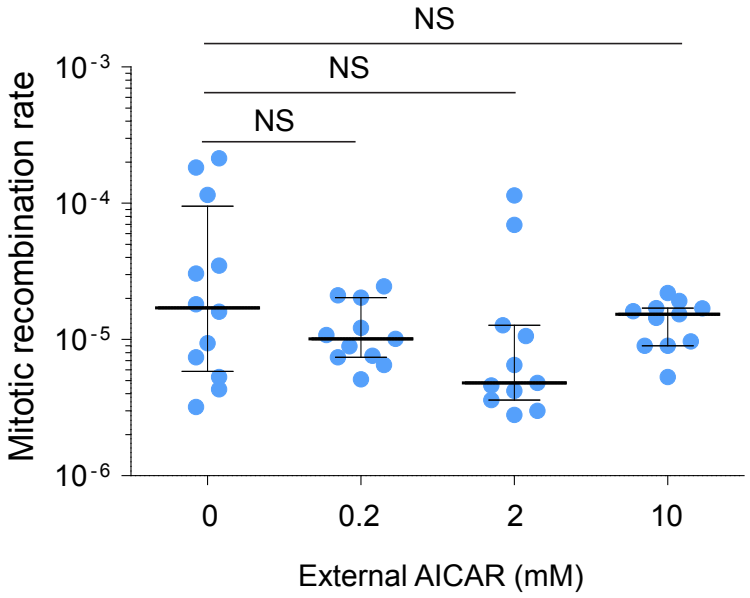

Figure S2. The mitotic recombination rate is not significantly modified by AICAR-feeding in yeast.
The pRS316-TINV plasmid carrying two inverted and partial *LEU2* sequences was used to estimate the effect of AICAR feeding on mitotic recombination rate of an *ade16 ade17 ade8 his1* strain (Y8480), as described (González-Barrera S, García-Rubio M and Aguilera A. Genetics. (2002) 162(2):603-14). Mitotic recombination rate were measured on twelve independent cultures for each condition and statistical analysis was performed using a Mann-Whitney test. NS: non-significant $p>0.05$. Bars correspond to the median and the interquartile range.

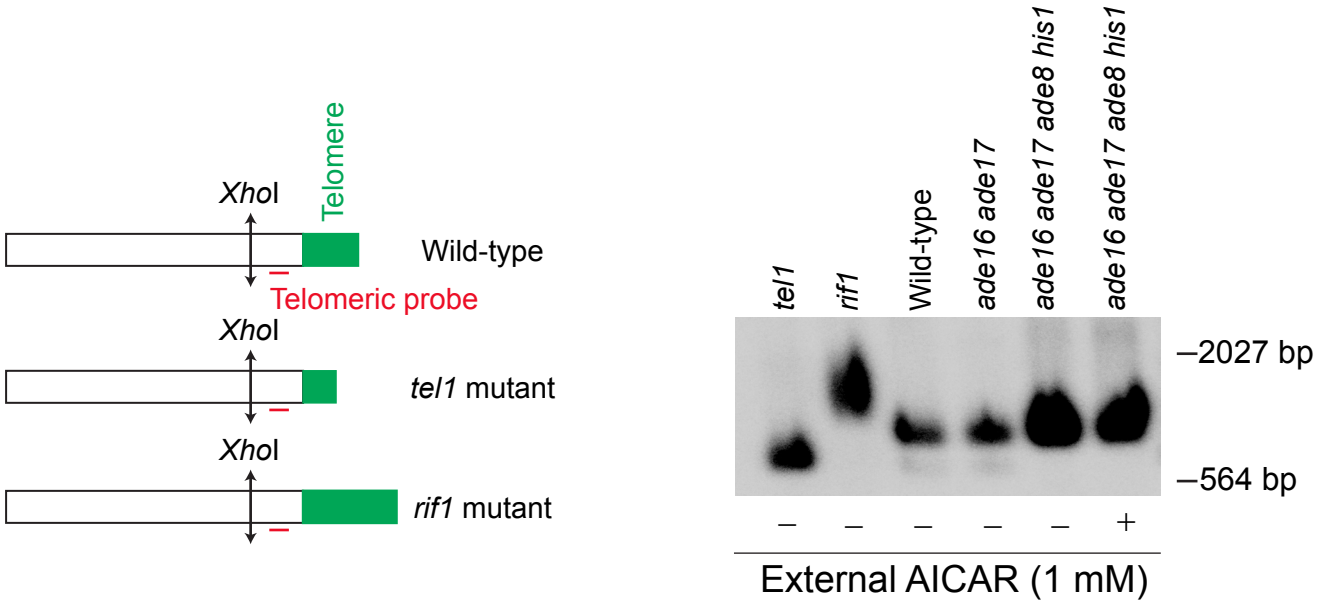

Figure S3. Yeast telomere length is not altered by ZMP accumulation.
Telomere length was estimated by Southern blotting after *Xho*I digestion of genomic DNA extracted from yeast cells accumulating ZMP by two different means, either endogenously from the purine pathway (*ade16 ade17*; Y1162) or exogenously by AICAR feeding (+; 1 mM) of the *ade8 ade16 ade17 his1* strain (Y2950). The radiolabeled telomeric probe was obtained by PCR on genomic DNA with oligonucleotides 5'CAGTTTAGCAGGCATCATCG3' and 5' -CGAGAACTTCAA-CGTTTGCC-3'. Mutants already shown to have a reduced (*tel1*) or an increased (*rif1*) telomere length were used as controls.

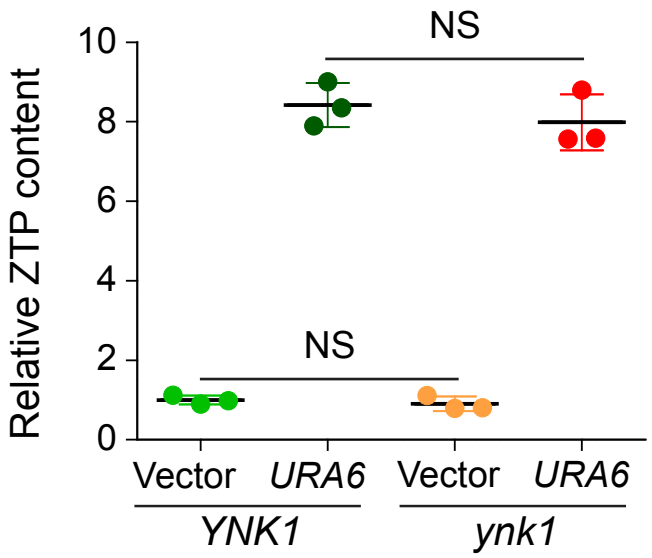

Figure S4. ZTP production is not affected in a strain lacking the NDP-kinase gene *YNK1*.
ZTP intracellular relative content was determined by High Performance Ion Chromatography on *ade16 ade17* AICAR-accumulating cells either *ynk1* (Y9715; orange and red dots) or *YNK1* (Y1162; light and dark green dots). Cells were transformed with a plasmid allowing *URA6* overexpression (p4919) or with the control empty vector. Metabolite extractions were done on transformants exponentially grown for 24 h in SDcasaWA medium. Analyses were done on three independent metabolite extractions and standard deviation is presented. Statistics correspond to a Welch's t-test: NS: Non-significant $p>0.05$. Black lines correspond to the mean. Relative ZTP content was set at 1 for the content measured in *the ade16 ade17 YNK1* strain containing the empty vector (light green dots).

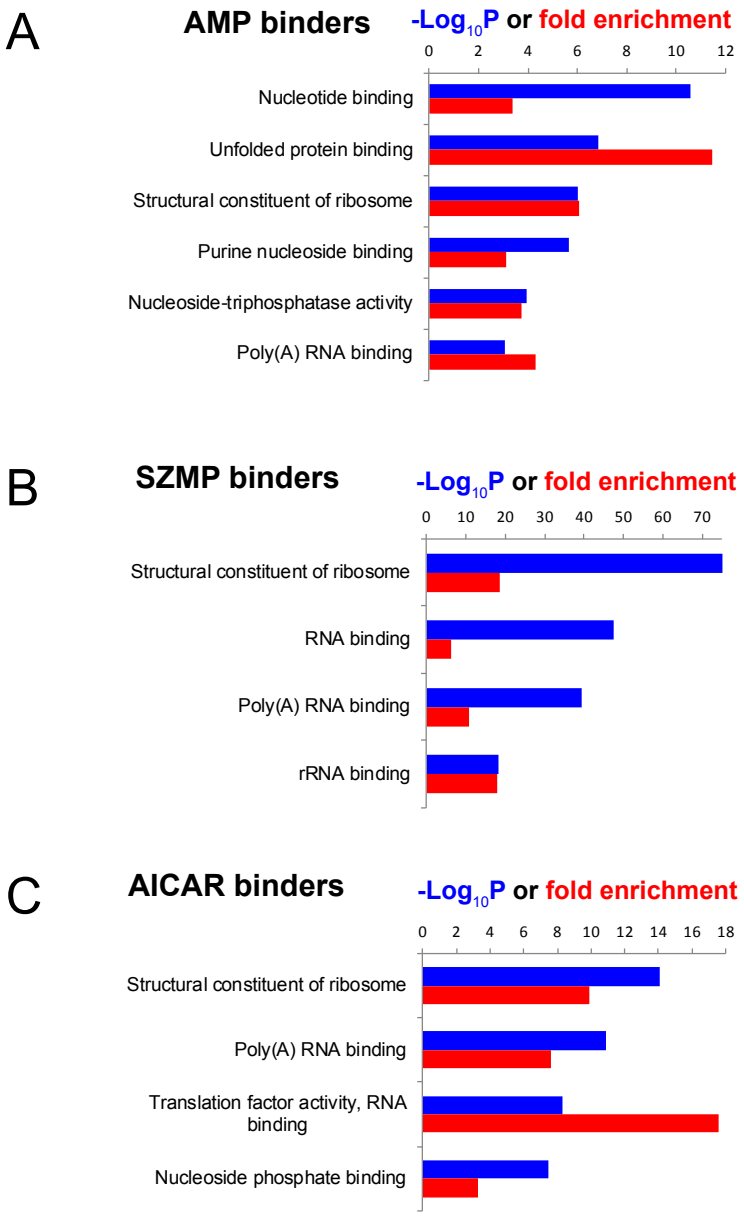

Figure S5. Biological Process GO-term enrichment analyses for the AMP- (*A*), SZMP- (*B*) and AICAR-binders (*C*) identified by affinity chromatography. The complete list of proteins identified in each case is presented in Table S1 part B-D. GO-term analyses were performed using the Gene Ontology Consortium web site (http://www.geneontology.org/).

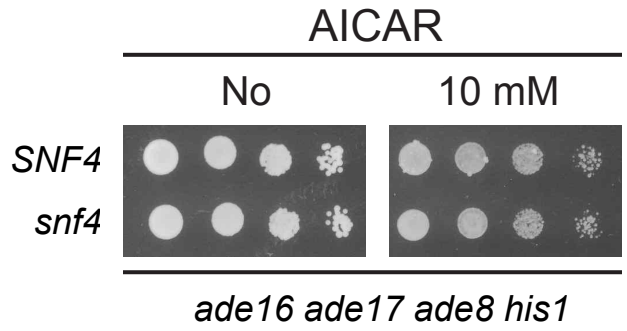

Figure S6. AICAR sensitivity is not altered by deletion of *SNF4*, the yeast gene for AMPK gamma subunit.
Yeast cells (Y8480 (*SNF4*) and Y10867 (*snf4*)) were serially diluted and spotted on SDcasaWA medium containing, or lacking, AICAR. Plates were imaged after 2 days at 30°C.

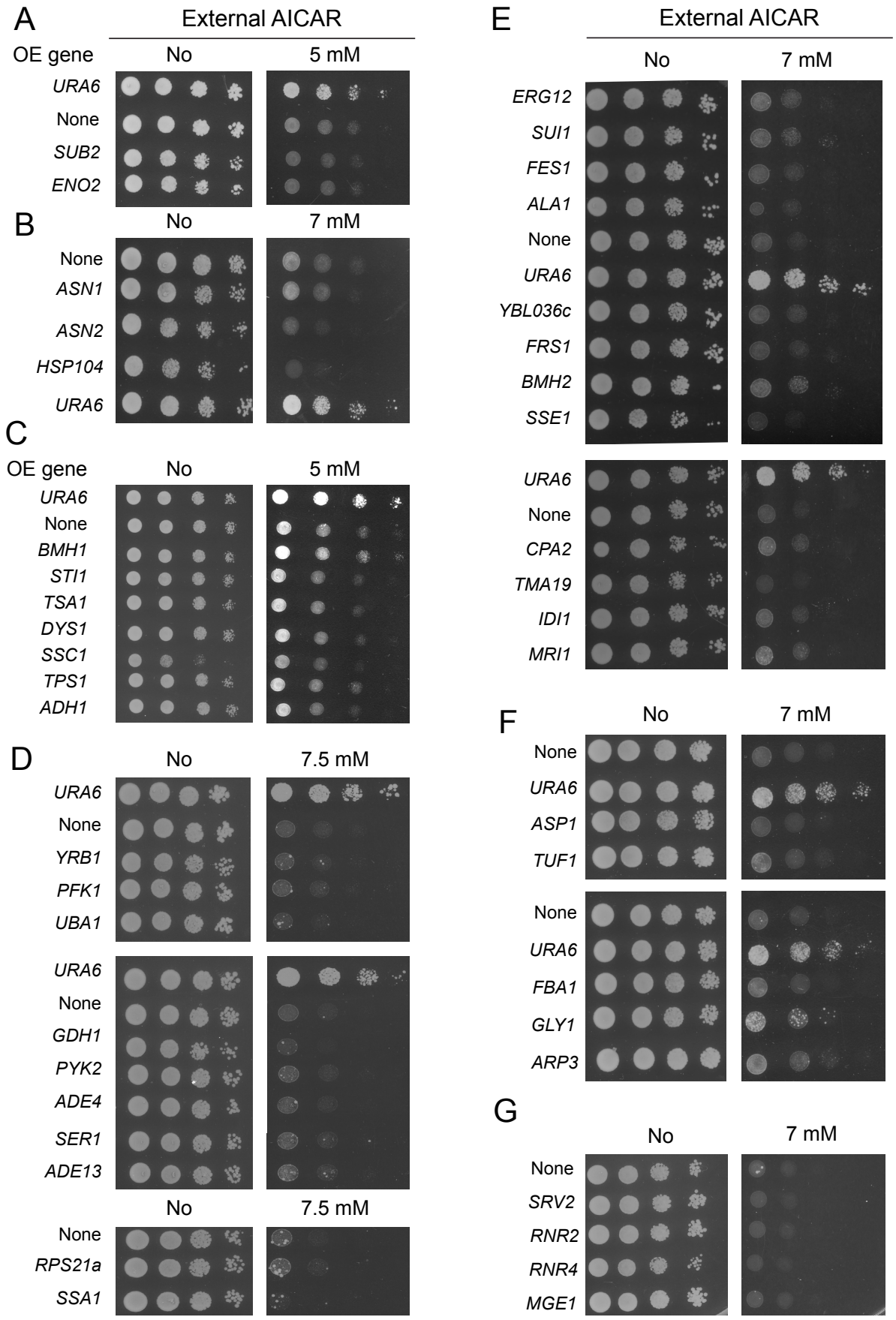

Figure S7. Effect of ZMP-binder gene overexpression on AICAR sensitivity.
Cells (*ade16 ade17 ade8 his1* (Y2950; *A-B*) or *ade3 ade16 ade17 ade8 his1* (Y8908; *C*)) were transformed with plasmids allowing overexpression of selected ZMP binder genes (boxed in yellow in Fig. 4) or by the cognate empty vector (None). Transformants were serially diluted and spotted on SC-Leu (*A-B*) or SDcasaWA medium (*C-G*) containing or not AICAR. Plates were imaged after 2 days at 30°C (A-B) or 37°C (C-G).

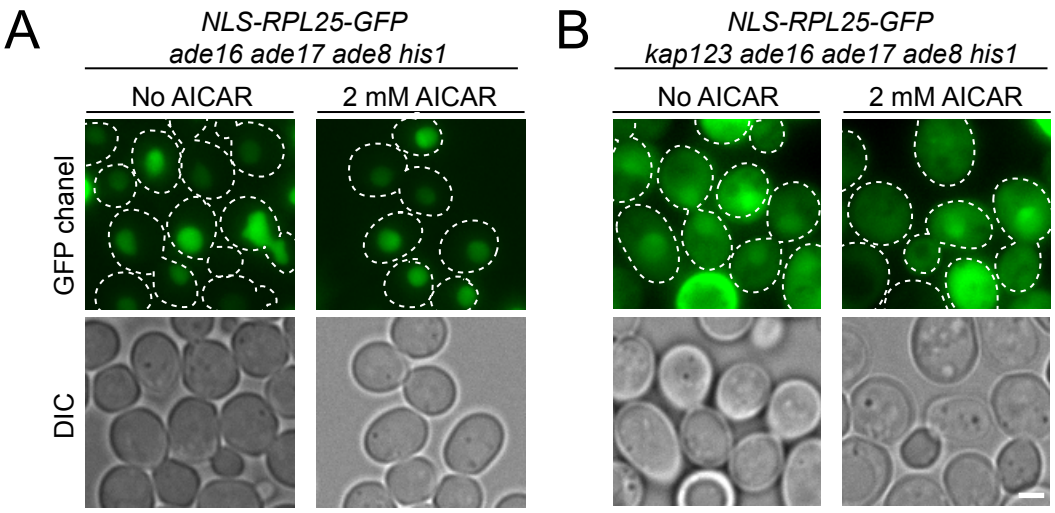

Nucleus only	**80%**	**83%**	8%	10%
Cytoplasmic signal	6%	4%	**79%**	**74%**
signal below threshold	14%	14%	14%	17%
n =	197	199	187	140

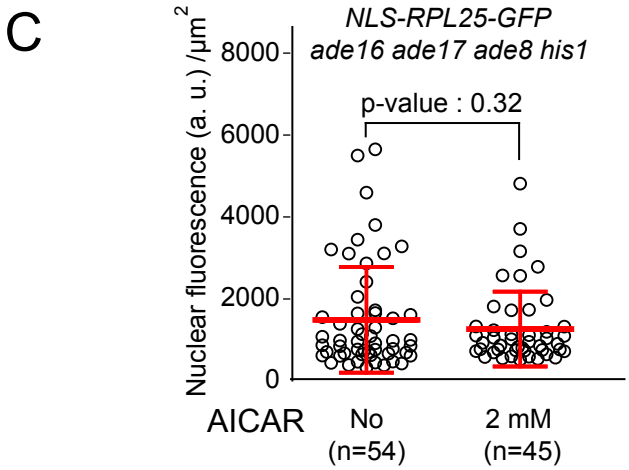

Figure S8. Nuclear localization of NLS-RFPL25-GFP is not affected by AICAR.
A-B, AICAR accumulation does not influence Rpl25 localization. *A*, NLS-Rpl25 mainly localizes in the nucleus, irrespective of AICAR accumulation. Cells (*ade8 ade16 ade17 his1*; Y8480) expressing NLS-Rpl25-GFP were incubated 2 h ± 2 mM AICAR at 30°C and imaged. *B*, NLS-Rpl25 mainly localizes in the cytoplasm in *kap123* deleted cells, irrespective of AICAR accumulation. Cells (*kap123 ade8 ade16 ade17 his1*; Y9623) expressing NLS-Rpl25-GFP were incubated 2 h ± 2 mM AICAR at 30°C and imaged. In *A-B*, a threshold 25% higher than the mean fluorescence field was applied to determine Rpl25 localization (N=3). Representative pictures are shown. White dashed lines: cells. Bar size is 2 µm. *C*, AICAR accumulation does not influence Rpl25 nuclear fluorescence intensity. Analysis was carried out on cells as described in (*A*). Using ImageJ software, 11 slides of a Z-stack were summed and projected. Fluorescence background (i.e field without cells) was measured and subtracted from the pictures. Then, circles containing Rpl25-GFP signal were drawn around the nucleus (Int), and the nuclear fluorescence intensity was calculated as follows: nf = (Int/ circle area). Importantly, nucleus areas do not change with or without AICAR. P-value was determined with a Welch's t-Test and mean and SD are indicated (red lines). Cells were observed in a fully automated Zeiss 200M inverted microscope (Carl Zeiss, Thornwood, NY) equipped with a MS-2000 stage (Applied Scientific Instrumentation, Eugene, OR), a Lambda LS 175 Watt xenon light source (Sutter, Novato, CA), a 100X 1.4NA Plan-Apochromat objective, and a 5 position filter turret. For GFP imaging, we used a FITC filter (Excitation: HQ487/25 – Emission: HQ535/40 – BS: Q505lp).

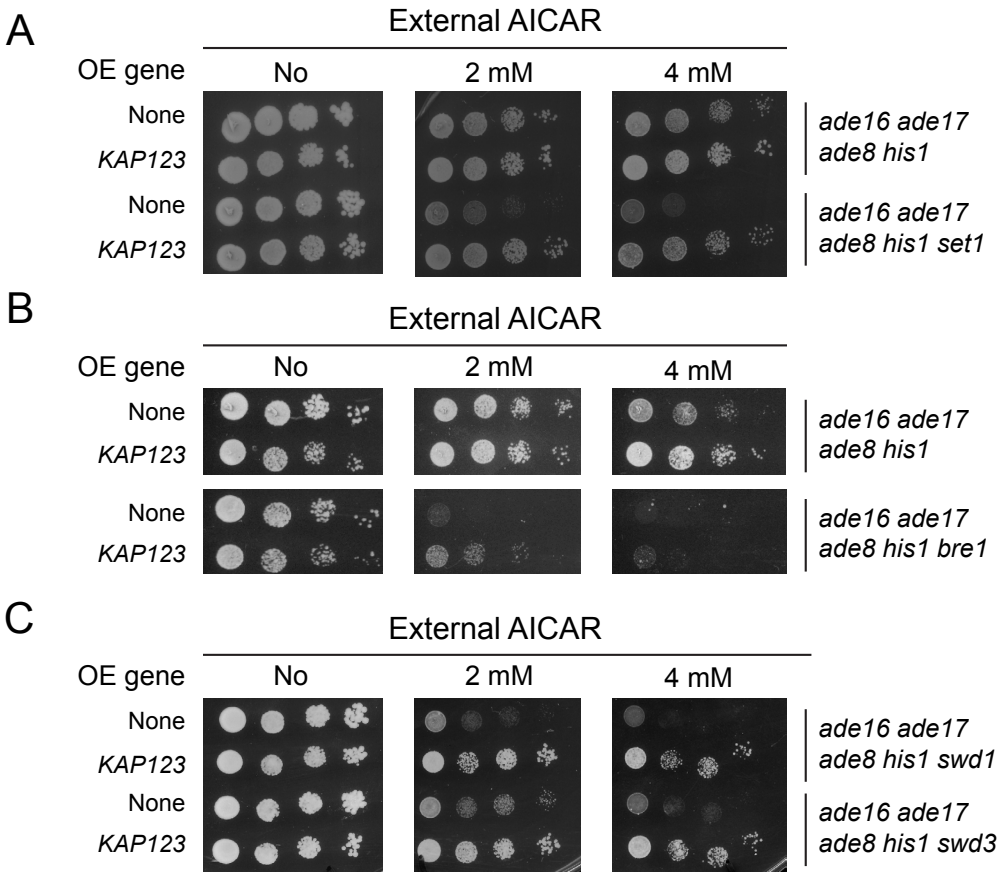

Figure S9. AICAR sensitivity of *bre1*, *swd1* and *swd3* mutants is suppressed by *KAP123* overexpression. Yeast cells (*ade8 ade16 ade17 his1* (Y2950), *ade8 ade16 ade17 his1 set1* (Y9168), *ade8 ade16 ade17 his1 bre1* (Y9082), *ade8 ade16 ade17 his1 swd1* (Y9479) and *ade8 ade16 ade17 his1 swd3* (Y9480)) were transformed by the plasmid allowing overexpression of *KAP123* (p4983) or by the cognate empty vector (YepLac195; None). Transformants were serially diluted and spotted on SDcasaWA medium containing, or lacking, AICAR. Plates were imaged after 2 days at 37°C.

Table S1 part A: List of the 74 proteins bound to ZMP-affinity resin at least four times on 6 independent experiments

ORF name	Protein name	Fold found on ZMP-resin (6 columns)	Protein function
YCR088W	Abp1	6	Actin-binding protein of the cortical actin cytoskeleton, important for activation of the Arp2/3 complex that plays a key role actin in cytoskeleton organization
YOR335C	Ala1	6	Cytoplasmic and mitochondrial alanyl-tRNA synthetase, required for protein synthesis; point mutation (cdc64-1 allele) causes cell cycle arrest at G1; lethality of null mutation is functionally complemented by human homolog
YOR133W	Eft1	6	Elongation factor 2 (EF-2), also encoded by EFT2; catalyzes ribosomal translocation during protein synthesis; contains diphthamide, the unique posttranslationally modified histidine residue specifically ADP-ribosylated by diphtheria toxin
YEL046C	Gly1	6	Threonine aldolase, catalyzes the cleavage of L-allo-threonine and L-threonine to glycine; involved in glycine biosynthesis
YMR186W	Hsc82	6	Cytoplasmic chaperone of the Hsp90 family, redundant in function and nearly identical with Hsp82p, and together they are essential; expressed constitutively at 10-fold higher basal levels than HSP82 and induced 2-3 fold by heat shock
YGR240C	Pfk1	6	Alpha subunit of heterooctameric phosphofructokinase involved in glycolysis, indispensable for anaerobic growth, activated by fructose-2,6-bisphosphate and AMP, mutation inhibits glucose induction of cell cycle-related genes
YMR205C	Pfk2	6	Beta subunit of heterooctameric phosphofructokinase involved in glycolysis, indispensable for anaerobic growth, activated by fructose-2,6-bisphosphate and AMP, mutation inhibits glucose induction of cell cycle-related genes
YGL037C	Pnc1	6	Nicotinamidase that converts nicotinamide to nicotinic acid as part of the NAD(+) salvage pathway, required for life span extension by calorie restriction; PNC1 expression responds to all known stimuli that extend replicative life span
YDR023W	Ses1	6	Cytosolic seryl-tRNA synthetase, class II aminoacyl-tRNA synthetase that aminoacylates tRNA(Ser), displays tRNA-dependent amino acid recognition which enhances discrimination of the serine substrate, interacts with peroxin Pex21p
YAL005C	Ssa1	6	ATPase involved in protein folding and nuclear localization signal (NLS)-directed nuclear transport; member of heat shock protein 70 (HSP70) family; forms a chaperone complex with Ydj1p; localized to the nucleus, cytoplasm, and cell wall
YLL024C	Ssa2	6	ATP binding protein involved in protein folding and vacuolar import of proteins; member of heat shock protein 70 (HSP70) family; associated with the chaperonin-containing T-complex; present in the cytoplasm, vacuolar membrane and cell wall
YPL106C	Sse1	6	ATPase that is a component of the heat shock protein Hsp90 chaperone complex; binds unfolded proteins; member of the heat shock protein 70 (HSP70) family; localized to the cytoplasm
YOR027W	Sti1	6	Hsp90 cochaperone, interacts with the Ssa group of the cytosolic Hsp70 chaperones; activates the ATPase activity of Ssa1p; homolog of mammalian Hop protein
YPR080W	Tef1	6	Translational elongation factor EF-1 alpha; also encoded by TEF2; functions in the binding reaction of aminoacyl-tRNA (AA-tRNA) to ribosomes; may also have a role in tRNA re-export from the nucleus
YKL056C	Tma19	6	Protein that associates with ribosomes; homolog of translationally controlled tumor protein; green fluorescent protein (GFP)-fusion protein localizes to the cytoplasm and relocates to the mitochondrial outer surface upon oxidative stress
YML028W	Tsa1	6	Thioredoxin peroxidase, acts as both a ribosome-associated and free cytoplasmic antioxidant; self-associates to form a high-molecular weight chaperone complex under oxidative stress; deletion results in mutator phenotype
YKL210W	Uba1	6	Ubiquitin activating enzyme (E1), involved in ubiquitin-mediated protein degradation and essential for viability
YBR127C	Vma2	6	Subunit B of the eight-subunit V1 peripheral membrane domain of the vacuolar H+-ATPase (V-ATPase), an electrogenic proton pump found throughout the endomembrane system; contains nucleotide binding sites; also detected in the cytoplasm
YFL039C	Act1	5	Actin, structural protein involved in cell polarization, endocytosis, and other cytoskeletal functions
YLR359W	Ade13	5	Adenylosuccinate lyase, catalyzes two steps in the 'de novo' purine nucleotide biosynthetic pathway; expression is repressed by adenine and activated by Bas1p and Pho2p; mutations in human ortholog ADSL cause adenylosuccinase deficiency
YOL086C	Adh1	5	Alcohol dehydrogenase, fermentative isozyme active as homo- or heterotetramers; required for the reduction of acetaldehyde to ethanol, the last step in the glycolytic pathway
YPL061W	Ald6	5	Cytosolic aldehyde dehydrogenase, activated by Mg2+ and utilizes NADP+ as the preferred coenzyme; required for conversion of acetaldehyde to acetate; constitutively expressed; locates to the mitochondrial outer surface upon oxidative stress
YPR145W	Asn1	5	Asparagine synthetase, isozyme of Asn2p; catalyzes the synthesis of L-asparagine from L-aspartate in the asparagine biosynthetic pathway
YGR124W	Asn2	5	Asparagine synthetase, isozyme of Asn1p; catalyzes the synthesis of L-asparagine from L-aspartate in the asparagine biosynthetic pathway
YDR321W	Asp1	5	Cytosolic L-asparaginase, involved in asparagine catabolism
YER177W	Bmh1	5	14-3-3 protein, major isoform; controls proteome at post-transcriptional level, binds proteins and DNA, involved in regulation of many processes including exocytosis, vesicle transport, Ras/MAPK signaling, and rapamycin-sensitive signaling
YHR068W	Dys1	5	Deoxyhypusine synthase, catalyzes formation of deoxyhypusine, the first step in hypusine biosynthesis; triggers posttranslational hypusination of translation elongation factor eIF-5A and regulates its intracellular levels; tetrameric
YMR208W	Erg12	5	Mevalonate kinase, acts in the biosynthesis of isoprenoids and sterols, including ergosterol, from mevalonate
YKL060C	Fba1	5	Fructose 1,6-bisphosphate aldolase; required for glycolysis and gluconeogenesis; catalyzes conversion of fructose 1,6 bisphosphate to glyceraldehyde-3-P and dihydroxyacetone-P
YOR375C	Gdh1	5	NADP(+)-dependent glutamate dehydrogenase, synthesizes glutamate from ammonia and alpha-ketoglutarate; rate of alpha-ketoglutarate utilization differs from Gdh3p; expression regulated by nitrogen and carbon sources
YPL240C	Hsp82	5	Hsp90 chaperone required for pheromone signaling and negative regulation of Hsf1p; docks with Tom70p for mitochondrial preprotein delivery; promotes telomerase DNA binding and nucleotide addition; interacts with Cns1p, Cpr6p, Cpr7p, Sti1p
YJR070C	Lia1	5	Deoxyhypusine hydroxylase, a HEAT-repeat containing metalloenzyme that catalyzes hypusine formation; binds to and is required for the modification of Hyp2p (eIF5A); complements S. pombe mmd1 mutants defective in mitochondrial positioning
YPR118W	Mri1	5	5'-methylthioribose-1-phosphate isomerase; catalyzes the isomerization of 5-methylthioribose-1-phosphate to 5-methylthioribulose-1-phosphate in the methionine salvage pathway
YER165W	Pab1	5	Poly(A) binding protein, part of the 3'-end RNA-processing complex, mediates interactions between the 5' cap structure and the 3' mRNA poly(A) tail, involved in control of poly(A) tail length, interacts with translation factor eIF-4G
YLR044C	Pdc1	5	Major of three pyruvate decarboxylase isozymes, key enzyme in alcoholic fermentation, decarboxylates pyruvate to acetaldehyde; subject to glucose-, ethanol-, and autoregulation; involved in amino acid catabolism
YBR218C	Pyc2	5	Pyruvate carboxylase isoform, cytoplasmic enzyme that converts pyruvate to oxaloacetate; highly similar to isoform Pyc1p but differentially regulated; mutations in the human homolog are associated with lactic acidosis
YOR184W	Ser1	5	3-phosphoserine aminotransferase, catalyzes the formation of phosphoserine from 3-phosphohydroxypyruvate, required for serine and glycine biosynthesis; regulated by the general control of amino acid biosynthesis mediated by Gcn4p
YJR045C	Ssc1	5	Hsp70 family ATPase, constituent of the import motor component of the Translocase of the Inner Mitochondrial membrane (TIM23 complex); involved in protein translocation and folding; subunit of SceI endonuclease
YNL244C	Sui1	5	Translation initiation factor eIF1; component of a complex involved in recognition of the initiator codon; modulates translation accuracy at the initiation phase
YKR059W	Tif1	5	Translation initiation factor eIF4A, identical to Tif2p; DEA(D/H)-box RNA helicase that couples ATPase activity to RNA binding and unwinding; forms a dumbbell structure of two compact domains connected by a linker; interacts with eIF4G
YPR163C	Tif3	5	Translation initiation factor eIF-4B, has RNA annealing activity; contains an RNA recognition motif and binds to single-stranded RNA
YBR126C	Tps1	5	Synthase subunit of trehalose-6-phosphate synthase/phosphatase complex, which synthesizes the storage carbohydrate trehalose; also found in a monomeric form; expression is induced by the stress response and repressed by the Ras-cAMP pathway
YOR187W	Tuf1	5	Mitochondrial translation elongation factor Tu; comprises both GTPase and guanine nucleotide exchange factor activities, while these activities are found in separate proteins in S. pombe and humans
YGR094W	Vas1	5	Mitochondrial and cytoplasmic valyl-tRNA synthetase
YMR300C	Ade4	4	Phosphoribosylpyrophosphate amidotransferase (PRPPAT; amidophosphoribosyltransferase), catalyzes first step of the 'de novo' purine nucleotide biosynthetic pathway
YJR065C	Arp3	4	Essential component of the Arp2/3 complex; Arp2/3 is a highly conserved actin nucleation center required for the motility and integrity of actin patches; involved in endocytosis and membrane growth and polarity
YGR282C	Bgl2	4	Endo-beta-1,3-glucanase; major protein of the cell wall, involved in cell wall maintenance; involved in incorporation of newly synthesized mannoprotein molecules into the cell wall
YDR099W	Bmh2	4	14-3-3 protein, minor isoform; controls proteome at post-transcriptional level, binds proteins and DNA, involved in regulation of many processes including exocytosis, vesicle transport, Ras/MAPK signaling, and rapamycin-sensitive signaling
YAL038W	Cdc19	4	Pyruvate kinase, functions as a homotetramer in glycolysis to convert phosphoenolpyruvate to pyruvate, the input for aerobic (TCA cycle) or anaerobic (glucose fermentation) respiration
YJR109C	Cpa2	4	Large subunit of carbamoyl phosphate synthetase, which catalyzes a step in the synthesis of citrulline, an arginine precursor
YAL003W	Efb1	4	Translation elongation factor 1 beta; stimulates nucleotide exchange to regenerate EF-1 alpha-GTP for the next elongation cycle; part of the EF-1 complex, which facilitates binding of aminoacyl-tRNA to the ribosomal A site
YHR174W	Eno2	4	Enolase II, a phosphopyruvate hydratase that catalyzes the conversion of 2-phosphoglycerate to phosphoenolpyruvate during glycolysis and the reverse reaction during gluconeogenesis; expression is induced in response to glucose
YDR518W	Eug1	4	Protein disulfide isomerase of the endoplasmic reticulum lumen; EUG1 has a paralog, PDI1, that arose from the whole genome duplication; function overlaps with that of Pdi1p; may interact with nascent polypeptides in the ER
YBR101C	Fes1	4	Hsp70 (Ssa1p) nucleotide exchange factor, cytosolic homolog of Sil1p, which is the nucleotide exchange factor for BiP (Kar2p) in the endoplasmic reticulum
YLR060W	Frs1	4	Beta subunit of cytoplasmic phenylalanyl-tRNA synthetase; forms a tetramer with Frs2p to generate active enzyme; able to hydrolyze mis-aminoacylated tRNA-Phe, which could contribute to translational quality control
YER133W	Glc7	4	Type 1 serine/threonine protein phosphatase catalytic subunit, involved in many processes (eg: glycogen metabolism, sporulation, mitosis); accumulates at mating projections by interaction with Afr1p; interacts with many regulatory subunits
YLL026W	Hsp104	4	Disaggregase; heat shock protein that cooperates with Ydj1p (Hsp40) and Ssa1p (Hsp70) to refold and reactivate previously denatured, aggregated proteins; responsive to stresses including: heat, ethanol, and sodium arsenite
YEL034W	Hyp2	4	Translation elongation factor eIF-5A, previously thought to function in translation initiation; similar to and functionally redundant with Anb1p; structural homolog of bacterial EF-P; undergoes an essential hypusination modification
YPL117C	Idi1	4	Isopentenyl diphosphate:dimethylallyl diphosphate isomerase (IPP isomerase), catalyzes an essential activation step in the isoprenoid biosynthetic pathway; required for viability
YER110C	Kap123	4	Karyopherin beta, mediates nuclear import of ribosomal proteins prior to assembly into ribosomes and import of histones H3 and H4; localizes to the nuclear pore, nucleus, and cytoplasm; exhibits genetic interactions with RAI1
YOR232W	Mge1	4	Mitochondrial matrix cochaperone, acts as a nucleotide release factor for Ssc1p in protein translocation and folding; also acts as cochaperone for Ssq1p in folding of Fe-S cluster proteins; homolog of E. coli GrpE
YJL026W	Rnr2	4	Ribonucleotide-diphosphate reductase (RNR), small subunit; the RNR complex catalyzes the rate-limiting step in dNTP synthesis and is regulated by DNA replication and DNA damage checkpoint pathways via localization of the small subunits
YGR180C	Rnr4	4	Ribonucleotide-diphosphate reductase (RNR) small subunit; the RNR complex catalyzes the rate-limiting step in dNTP synthesis and is regulated by DNA replication and DNA damage checkpoint pathways via localization of the small subunits
YOL039W	Rpp2a	4	Ribosomal protein P2 alpha, a component of the ribosomal stalk, which is involved in the interaction between translational elongation factors and the ribosome; regulates the accumulation of P1 (Rpp1Ap and Rpp1Bp) in the cytoplasm
YDR382W	Rpp2b	4	Ribosomal protein P2 beta, a component of the ribosomal stalk, which is involved in the interaction between translational elongation factors and the ribosome; regulates the accumulation of P1 (Rpp1Ap and Rpp1Bp) in the cytoplasm
YGR214W	Rps0a	4	Protein component of the small (40S) ribosomal subunit, nearly identical to Rps0Bp; required for maturation of 18S rRNA along with Rps0Bp; deletion of either RPS0 gene reduces growth rate, deletion of both genes is lethal
YKR057W	Rps21a	4	Protein component of the small (40S) ribosomal subunit; nearly identical to Rps21Bp and has similarity to rat S21 ribosomal protein
YBL058W	Shp1	4	UBX domain-containing substrate adaptor for Cdc48p; ubiquitin regulatory X domain-containing protein that acts as a substrate recruiting cofactor for Cdc48p; positively regulates Glc7p PPase activity
YNL138W	Srv2	4	CAP (cyclase-associated protein); N-terminus binds adenylate cyclase and facilitates activation by RAS; N-terminus forms novel hexameric star-shaped shuriken structures that directly catalyze cofilin-mediated severing of actin filaments
YNL209W	Ssb2	4	Cytoplasmic ATPase that is a ribosome-associated molecular chaperone, functions with J-protein partner Zuo1p; may be involved in the folding of newly-synthesized polypeptide chains; member of the HSP70 family; homolog of SSB1
YDL084W	Sub2	4	Component of the TREX complex required for nuclear mRNA export; member of the DEAD-box RNA helicase superfamily and is involved in early and late steps of spliceosome assembly; homolog of the human splicing factor hUAP56
YDL185W	Vma1	4	Subunit A of the eight-subunit V1 peripheral membrane domain of the vacuolar H+-ATPase; protein precursor undergoes self-catalyzed splicing to yield the extein Tfp1p and the intein Vde (PI-SceI), which is a site-specific endonuclease
YBL036C	Ybl036c	4	Putative non-specific single-domain racemase; based on structural similarity; binds pyridoxal 5'-phosphate; expression of GFP-fusion protein induced in response to the DNA-damaging agent MMS
YDR002W	Yrb1	4	Ran GTPase binding protein; involved in nuclear protein import and RNA export, ubiquitin-mediated protein degradation during the cell cycle; shuttles between the nucleus and cytoplasm; is essential; homolog of human RanBP1

Table S1 part B : List of the 67 proteins bound to AMP-affinity resin at least twice on 3 independent experiments

OFR name	PROTEIN name	Fold found on AMP-resin (3 columns)	Protein function
YFL039C	**Act1**	**3**	Actin, structural protein involved in cell polarization, endocytosis, and other cytoskeletal functions
YOL086C	**Adh1**	**3**	Alcohol dehydrogenase, fermentative isozyme active as homo- or heterotetramers; required for the reduction of acetaldehyde to ethanol, the last step in the glycolytic pathway
YJR105W	**Ado1**	**3**	Adenosine kinase, required for the utilization of S-adenosylmethionine (AdoMet); may be involved in recycling adenosine produced through the methyl cycle
YML022W	**Apt1**	**3**	Adenine phosphoribosyltransferase, catalyzes the formation of AMP from adenine and 5-phosphoribosylpyrophosphate; involved in the salvage pathway of purine nucleotide biosynthesis
YAL038W	**Cdc19**	**3**	Pyruvate kinase, functions as a homotetramer in glycolysis to convert phosphoenolpyruvate to pyruvate, the input for aerobic (TCA cycle) or anaerobic (glucose fermentation) respiration
YAL003W	**Efb1**	**3**	Translation elongation factor 1 beta; stimulates nucleotide exchange to regenerate EF-1 alpha-GTP for the next elongation cycle; part of the EF-1 complex, which facilitates binding of aminoacyl-tRNA to the ribosomal A site
YOR133W	**Eft1**	**3**	Elongation factor 2 (EF-2), also encoded by EFT2; catalyzes ribosomal translocation during protein synthesis; contains diphthamide, the unique posttranslationally modified histidine residue specifically ADP-ribosylated by diphtheria toxin
YHR174W	**Eno2**	**3**	Enolase II, a phosphopyruvate hydratase that catalyzes the conversion of 2-phosphoglycerate to phosphoenolpyruvate during glycolysis and the reverse reaction during gluconeogenesis; expression is induced in response to glucose
YPR035W	**Gln1**	**3**	Glutamine synthetase (GS), synthesizes glutamine from glutamate and ammonia; with Glt1p, forms the secondary pathway for glutamate biosynthesis from ammonia; expression regulated by nitrogen source and by amino acid limitation
YDL125C	**Hnt1**	**3**	Adenosine 5'-monophosphoramidase; interacts physically and genetically with Kin28p, a CDK and TFIIK subunit, and genetically with CAK1; member of the histidine triad (HIT) superfamily of nucleotide-binding proteins and similar to Hint
YMR186W	**Hsc82**	**3**	Cytoplasmic chaperone of the Hsp90 family, redundant in function and nearly identical with Hsp82p, and together they are essential; expressed constitutively at 10-fold higher basal levels than HSP82 and induced 2-3 fold by heat shock
YLR259C	**Hsp60**	**3**	Tetradecameric mitochondrial chaperonin required for ATP-dependent folding of precursor polypeptides and complex assembly; prevents aggregation and mediates protein refolding after heat shock; role in mtDNA transmission; phosphorylated
YLR432W	**Imd3**	**3**	Inosine monophosphate dehydrogenase, catalyzes the first step of GMP biosynthesis, member of a four-gene family in S. cerevisiae, constitutively expressed
YJL034W	**Kar2**	**3**	ATPase involved in protein import into the ER, also acts as a chaperone to mediate protein folding in the ER and may play a role in ER export of soluble proteins; regulates the unfolded protein response via interaction with Ire1p
YLR044C	**Pdc1**	**3**	Major of three pyruvate decarboxylase isozymes, key enzyme in alcoholic fermentation, decarboxylates pyruvate to acetaldehyde; subject to glucose-, ethanol-, and autoregulation; involved in amino acid catabolism
YCR012W	**Pgk1**	**3**	3-phosphoglycerate kinase, catalyzes transfer of high-energy phosphoryl groups from the acyl phosphate of 1,3-bisphosphoglycerate to ADP to produce ATP; key enzyme in glycolysis and gluconeogenesis
YHR037W	**Put2**	**3**	Delta-1-pyrroline-5-carboxylate dehydrogenase, nuclear-encoded mitochondrial protein involved in utilization of proline as sole nitrogen source; deficiency of the human homolog causes HPII, an autosomal recessive inborn error of metabolism
YMR142C	**Rpl13b**	**3**	Protein component of the large (60S) ribosomal subunit, nearly identical to Rpl13Ap; not essential for viability; has similarity to rat L13 ribosomal protein
YBR031W	**Rpl4a**	**3**	N-terminally acetylated protein component of the large (60S) ribosomal subunit, nearly identical to Rpl4Bp and has similarity to E. coli L4 and rat L4 ribosomal proteins
YER043C	**Sah1**	**3**	S-adenosyl-L-homocysteine hydrolase, catabolizes S-adenosyl-L-homocysteine which is formed after donation of the activated methyl group of S-adenosyl-L-methionine (AdoMet) to an acceptor
YAL005C	**Ssa1**	**3**	ATPase involved in protein folding and nuclear localization signal (NLS)-directed nuclear transport; member of heat shock protein 70 (HSP70) family; forms a chaperone complex with Ydj1p;
YLL024C	**Ssa2**	**3**	ATP binding protein involved in protein folding and vacuolar import of proteins; member of heat shock protein 70 (HSP70) family; associated with the chaperonin-containing T-complex
YDL229W	**Ssb1**	**3**	Cytoplasmic ATPase that is a ribosome-associated molecular chaperone, functions with J-protein partner Zuo1p; may be involved in folding of newly-made polypeptide chains; member of the HSP70 family; interacts with phosphatase subunit Reg1
YNL209W	**Ssb2**	**3**	Cytoplasmic ATPase that is a ribosome-associated molecular chaperone, functions with J-protein partner Zuo1p; may be involved in the folding of newly-synthesized polypeptide chains; member of the HSP70 family; homolog of SSB1
YJR045C	**Ssc1**	**3**	Hsp70 family ATPase, constituent of the import motor component of the Translocase of the Inner Mitochondrial membrane (TIM23 complex); involved in protein translocation and folding; subunit of SceI endonuclease
YJL052W	**Tdh1**	**3**	Glyceraldehyde-3-phosphate dehydrogenase, isozyme 1, involved in glycolysis and gluconeogenesis; tetramer that catalyzes the reaction of glyceraldehyde-3-phosphate to 1,3 bis-phosphoglycerate; detected in the cytoplasm and cell wall
YJR009C	**Tdh2**	**3**	Glyceraldehyde-3-phosphate dehydrogenase, isozyme 2, involved in glycolysis and gluconeogenesis; tetramer that catalyzes the reaction of glyceraldehyde-3-phosphate to 1,3 bis-phosphoglycerate; detected in the cytoplasm and cell wall
YGR192C	**Tdh3**	**3**	Glyceraldehyde-3-phosphate dehydrogenase, isozyme 3, involved in glycolysis and gluconeogenesis; tetramer that catalyzes the reaction of glyceraldehyde-3-phosphate to 1,3 bis-phosphoglycerate; detected in the cytoplasm and cell wall
YPR080W	**Tef1**	**3**	Translational elongation factor EF-1 alpha; also encoded by TEF2; functions in the binding reaction of aminoacyl-tRNA (AA-tRNA) to ribosomes; may also have a role in tRNA re-export from the nucleus
YKL067W	**Ynk1**	**3**	Nucleoside diphosphate kinase, catalyzes the transfer of gamma phosphates from nucleoside triphosphates, usually ATP, to nucleoside diphosphates by a mechanism that involves formation of an autophosphorylated enzyme intermediate
YLR153C	**Acs2**	**2**	Acetyl-coA synthetase isoform which, along with Acs1p, is the nuclear source of acetyl-coA for histone acetylation; mutants affect global transcription; required for growth on glucose; expressed under anaerobic conditions
YLR028C	**Ade16**	**2**	Enzyme of 'de novo' purine biosynthesis containing both 5-aminoimidazole-4-carboxamide ribonucleotide transformylase and inosine monophosphate cyclohydrolase activities, isozyme of Ade17p; ade16 ade17 mutants require adenine and histidine
YLR109W	**Ahp1**	**2**	Thiol-specific peroxiredoxin, reduces hydroperoxides to protect against oxidative damage; function in vivo requires covalent conjugation to Urm1p
YMR116C	**Asc1**	**2**	G-protein beta subunit and guanine nucleotide dissociation inhibitor for Gpa2p; ortholog of RACK1 that inhibits translation; core component of the small (40S) ribosomal subunit; represses Gcn4p in the absence of amino acid starvation
YFL028C	**Caf16**	**2**	Part of evolutionarily-conserved CCR4-NOT regulatory complex; contains single ABC-type ATPase domain but no transmembrane domain; interacts with several subunits of Mediator
YMR173W	**Ddr48**	**2**	DNA damage-responsive protein, expression is increased in response to heat-shock stress or treatments that produce DNA lesions; contains multiple repeats of the amino acid sequence NNNDSYGS
YKL054C	**Def1**	**2**	RNAPII degradation factor, forms a complex with Rad26p in chromatin, enables ubiquitination and proteolysis of RNAPII present in an elongation complex; mutant is deficient in Zip1p loading onto chromosomes during meiosis
YMR124W	**Epo1**	**2**	Protein involved in septin-ER tethering; interacts with ER membrane protein, Scs2p, and Shs1p, a septin ring component, at bud neck to create ER diffusion barrier
YMR029C	**Far8**	**2**	Protein involved in recovery from cell cycle arrest in response to pheromone, in a Far1p-independent pathway; interacts with Far3p, Far7p, Far9p, Far10p, and Far11p
YNL068C	**Fkh2**	**2**	Forkhead family transcription factor with a major role in the expression of G2/M phase genes; positively regulates transcriptional elongation; negative role in chromatin silencing at HML and HMR; substrate of the Cdc28p/Clb5p kinase
YDR236C	**Fmn1**	**2**	Riboflavin kinase, phosphorylates riboflavin to form riboflavin monophosphate (FMN), which is a necessary cofactor for many enzymes; localizes to microsomes and to the mitochondrial inner membrane
YHR176W	**Fmo1**	**2**	Flavin-containing monooxygenase, localized to the cytoplasmic face of the ER membrane; catalyzes oxidation of biological thiols to maintain the ER redox buffer ratio for correct folding of disulfide-bonded proteins
YKL152C	**Gpm1**	**2**	Tetrameric phosphoglycerate mutase, mediates the conversion of 3-phosphoglycerate to 2-phosphoglycerate during glycolysis and the reverse reaction during gluconeogenesis
YOR020C	**Hsp10**	**2**	Mitochondrial matrix co-chaperonin that inhibits the ATPase activity of Hsp60p, a mitochondrial chaperonin; involved in protein folding and sorting in the mitochondria; 10 kD heat shock protein with similarity to E. coli groES
YLR355C	**Ilv5**	**2**	Bifunctional acetohydroxyacid reductoisomerase and mtDNA binding protein; involved in branched-chain amino acid biosynthesis and maintenance of wild-type mitochondrial DNA; found in mitochondrial nucleoids
YML056C	**Imd4**	**2**	Inosine monophosphate dehydrogenase, catalyzes the first step of GMP biosynthesis, member of a four-gene family in S. cerevisiae, constitutively expressed
YOR197W	**Mca1**	**2**	Putative cysteine protease similar to mammalian caspases; involved in regulation of apoptosis upon H2O2 treatment; contributes to clearance of insoluble protein aggregates during normal growth; may be involved in cell cycle progression
YLR203C	**Mss51**	**2**	Specific translational activator for the mitochondrial COX1 mRNA; loosely associated with the matrix face of the mitochondrial inner membrane; influences both COX1 mRNA translation and Cox1p assembly into cytochrome c oxidase
YKR080W	**Mtd1**	**2**	NAD-dependent 5,10-methylenetetrahydrafolate dehydrogenase, plays a catalytic role in oxidation of cytoplasmic one-carbon units; expression is regulated by Bas1p and Bas2p, repressed by adenine, and may be induced by inositol and choline
YDR432W	**Npl3**	**2**	RNA-binding protein that promotes elongation, regulates termination, and carries poly(A) mRNA from nucleus to cytoplasm; required for pre-mRNA splicing; dissociation from mRNAs promoted by Mtr10p; phosphorylated by Sky1p in the cytoplasm
YJL041W	**Nsp1**	**2**	Essential component of the nuclear pore complex, which mediates nuclear import and export, found in both the Nup82 and Nic96 complexes
YLR335W	**Nup2**	**2**	Nucleoporin involved in nucleocytoplasmic transport, binds to either the nucleoplasmic or cytoplasmic faces of the nuclear pore complex depending on Ran-GTP levels; also has a role in chromatin organization
YIR006C	**Pan1**	**2**	Part of actin cytoskeleton-regulatory complex Pan1p-Sla1p-End3p, associates with actin patches on the cell cortex; promotes protein-protein interactions essential for endocytosis; previously thought to be a subunit of poly(A) ribonuclease
YDL055C	**Psa1**	**2**	GDP-mannose pyrophosphorylase (mannose-1-phosphate guanyltransferase), synthesizes GDP-mannose from GTP and mannose-1-phosphate in cell wall biosynthesis; required for normal cell wall structure
YEL054C	**Rpl12a**	**2**	Protein component of the large (60S) ribosomal subunit, nearly identical to Rpl12Bp; rpl12a rpl12b double mutant exhibits slow growth and slow translation; has similarity to E. coli L11 and rat L12 ribosomal proteins
YBR084C-A	**Rpl19a**	**2**	Protein component of the large (60S) ribosomal subunit, nearly identical to Rpl19Bp and has similarity to rat L19 ribosomal protein; rpl19a and rpl19b single null mutations result in slow growth, while the double null mutation is lethal
YLR344W	**Rpl26a**	**2**	Protein component of the large (60S) ribosomal subunit, nearly identical to Rpl26Bp and has similarity to E. coli L24 and rat L26 ribosomal proteins; binds to 5.8S rRNA
YBL092W	**Rpl32**	**2**	Protein component of the large (60S) ribosomal subunit, has similarity to rat L32 ribosomal protein; overexpression disrupts telomeric silencing
YGL076C	**Rpl7a**	**2**	Protein component of the large (60S) ribosomal subunit, nearly identical to Rpl7Bp and has similarity to E. coli L30 and rat L7 ribosomal proteins; contains a conserved C-terminal Nucleic acid Binding Domain (NDB2
YGL147C	**Rpl9a**	**2**	Protein component of the large (60S) ribosomal subunit, nearly identical to Rpl9Bp and has similarity to E. coli L6 and rat L9 ribosomal proteins
YCR031C	**Rps14a**	**2**	Ribosomal protein 59 of the small subunit, required for ribosome assembly and 20S pre-rRNA processing; mutations confer cryptopleurine resistance; nearly identical to Rps14Bp and similar to E. coli S11 and rat S14 ribosomal proteins
YOL121C	**Rps19a**	**2**	Protein component of the small (40S) ribosomal subunit, required for assembly and maturation of pre-40 S particles; mutations in human RPS19 are associated with Diamond Blackfan anemia; nearly identical to Rps19Bp
YNL178W	**Rps3**	**2**	Protein component of the small (40S) ribosomal subunit, has apurinic/apyrimidinic (AP) endonuclease activity; essential for viability; has similarity to E. coli S3 and rat S3 ribosomal proteins
YJR123W	**Rps5**	**2**	Protein component of the small (40S) ribosomal subunit, the least basic of the non-acidic ribosomal proteins; phosphorylated in vivo; essential for viability; has similarity to E. coli S7 and rat S5 ribosomal proteins
YNL096C	**Rps7b**	**2**	Protein component of the small (40S) ribosomal subunit, nearly identical to Rps7Ap; interacts with Kti11p; deletion causes hypersensitivity to zymocin; has similarity to rat S7 and Xenopus S8 ribosomal proteins
YER081W	**Ser3**	**2**	3-phosphoglycerate dehydrogenase, catalyzes the first step in serine and glycine biosynthesis; isozyme of Ser33p
YIL074C	**Ser33**	**2**	3-phosphoglycerate dehydrogenase, catalyzes the first step in serine and glycine biosynthesis; isozyme of Ser3p

Table S1 part B (continued)

OFR name	PROTEIN name	Fold found on AMP-resin (3 columns)	Protein function
YNL167C	**Sko1**	**2**	Basic leucine zipper transcription factor of the ATF/CREB family; forms a complex with Tup1p and Cyc8p to both activate and repress transcription; cytosolic and nuclear protein involved in osmotic and oxidative stress responses
YBL007C	**Sla1**	**2**	Cytoskeletal protein binding protein required for assembly of the cortical actin cytoskeleton; interacts with proteins regulating actin dynamics and proteins required for endocytosis; found in the nucleus and cell cortex; has 3 SH3 domains
YBL075C	**Ssa3**	**2**	ATPase involved in protein folding and the response to stress; plays a role in SRP-dependent cotranslational protein-membrane targeting and translocation; member of the heat shock protein 70 (HSP70) family; localized to the cytoplasm
YER103W	**Ssa4**	**2**	Heat shock protein that is highly induced upon stress; plays a role in SRP-dependent cotranslational protein-membrane targeting and translocation; member of the HSP70 family; cytoplasmic protein that concentrates in nuclei upon starvation
YPL106C	**Sse1**	**2**	ATPase that is a component of the heat shock protein Hsp90 chaperone complex; binds unfolded proteins; member of the heat shock protein 70 (HSP70) family; localized to the cytoplasm
YLR369W	**Ssq1**	**2**	Mitochondrial hsp70-type molecular chaperone, required for assembly of iron/sulfur clusters into proteins at a step after cluster synthesis, and for maturation of Yfh1p, which is a homolog of human frataxin implicated in Friedreich's ataxia
YOR027W	**Sti1**	**2**	Hsp90 cochaperone, interacts with the Ssa group of the cytosolic Hsp70 chaperones and activates Ssa1p ATPase activity; interacts with Hsp90 chaperones and inhibits their ATPase activity; homolog of mammalian Hop
YLR150W	**Stm1**	**2**	Protein required for optimal translation under nutrient stress; perturbs association of Yef3p with ribosomes; involved in TOR signaling; binds G4 quadruplex and purine motif triplex nucleic acid; helps maintain telomere structure
YDL084W	**Sub2**	**2**	Component of the TREX complex required for nuclear mRNA export; member of the DEAD-box RNA helicase superfamily and is involved in early and late steps of spliceosome assembly; homolog of the human splicing factor hUAP56
YKR059W	**Tif1**	**2**	Translation initiation factor eIF4A, identical to Tif2p; DEA(D/H)-box RNA helicase that couples ATPase activity to RNA binding and unwinding; forms a dumbbell structure of two compact domains connected by a linker; interacts with eIF4G
YPR163C	**Tif3**	**2**	Translation initiation factor eIF-4B, has RNA annealing activity; contains an RNA recognition motif and binds to single-stranded RNA
YML028W	**Tsa1**	**2**	Thioredoxin peroxidase, acts as both a ribosome-associated and free cytoplasmic antioxidant; self-associates to form a high-molecular weight chaperone complex under oxidative stress; deletion results in mutator phenotype
YCR084C	**Tup1**	**2**	General repressor of transcription, forms complex with Cyc8p, involved in the establishment of repressive chromatin structure through interactions with histones H3 and H4, appears to enhance expression of some genes
YDL185W	**Vma1**	**2**	Subunit A of the eight-subunit V1 peripheral membrane domain of the vacuolar H+-ATPase; protein precursor undergoes self-catalyzed splicing to yield the extein Tfp1p and the intein Vde (PI-SceI), which is a site-specific endonuclease

Table S1 part C : List of proteins bound to SZMP-affinity resin at least three times on 4 independent experiments

ORF name	Protein name	Fold found on SZMP-resin (4 columns)	Protein function
YOR198C	Bfr1	4	Component of mRNP complexes associated with polyribosomes; implicated in secretion and nuclear segregation; multicopy suppressor of BFA (Brefeldin A) sensitivity
YAL038W	Cdc19	4	Pyruvate kinase, functions as a homotetramer in glycolysis to convert phosphoenolpyruvate to pyruvate, the input for aerobic (TCA cycle) or anaerobic (glucose fermentation) respiration
YHR019C	Ded81	4	Cytosolic asparaginyl-tRNA synthetase, required for protein synthesis, catalyzes the specific attachment of asparagine to its cognate tRNA
YOR133W	Eft1	4	Elongation factor 2 (EF-2), also encoded by EFT2; catalyzes ribosomal translocation during protein synthesis; contains diphthamide, the unique posttranslationally modified histidine residue specifically ADP-ribosylated by diphtheria toxin
YDR385W	Eft2	4	Elongation factor 2 (EF-2), also encoded by EFT1; catalyzes ribosomal translocation during protein synthesis; contains diphthamide, the unique posttranslationally modified histidine residue specifically ADP-ribosylated by diphtheria toxin
YHR193C	Egd2	4	Alpha subunit of the heteromeric nascent polypeptide-associated complex (NAC) involved in protein sorting and translocation, associated with cytoplasmic ribosomes
YER025W	Gcd11	4	Gamma subunit of the translation initiation factor eIF2, involved in the identification of the start codon; binds GTP when forming the ternary complex with GTP and tRNAi-Met
YDR091C	Rli1	4	Essential iron-sulfur protein required for ribosome biogenesis and translation initiation and termination; facilitates binding of a multifactor complex (MFC) of initiation factors to the small ribosomal subunit; predicted ABC family ATPase
YPR102C	Rpl11a	4	Protein of the large 60S ribosomal subunit, nearly identical to Rpl11Bp but expressed at twice the level; involved in ribosomal assembly; depletion causes degradation of 60S proteins and RNA; similar to E. coli L5 and rat L11
YGR085C	Rpl11b	4	Protein component of the large (60S) ribosomal subunit, nearly identical to Rpl11Ap; involved in ribosomal assembly; depletion causes degradation of proteins and RNA of the 60S subunit; has similarity to E. coli L5 and rat L11
YMR142C	Rpl13b	4	Protein component of the large (60S) ribosomal subunit, nearly identical to Rpl13Ap; not essential for viability; has similarity to rat L13 ribosomal protein
YNL069C	Rpl16b	4	N-terminally acetylated protein component of the large (60S) ribosomal subunit, binds to 5.8 S rRNA; has similarity to Rpl16Ap, E. coli L13 and rat L13a ribosomal proteins; transcriptionally regulated by Rap1p
YKL180W	Rpl17a	4	Protein component of the large (60S) ribosomal subunit, nearly identical to Rpl17Bp and has similarity to E. coli L22 and rat L17 ribosomal proteins; copurifies with the Dam1 complex (aka DASH complex)
YBR084C-A	Rpl19a	4	Protein component of the large (60S) ribosomal subunit, nearly identical to Rpl19Bp and has similarity to rat L19 ribosomal protein; rpl19a and rpl19b single null mutations result in slow growth, while the double null mutation is lethal
YBL027W	Rpl19b	4	Protein component of the large (60S) ribosomal subunit, nearly identical to Rpl19Ap and has similarity to rat L19 ribosomal protein; rpl19a and rpl19b single null mutations result in slow growth, while the double null mutation is lethal
YPL220W	Rpl1a	4	N-terminally acetylated protein component of the large (60S) ribosomal subunit, nearly identical to Rpl1Bp and has similarity to E. coli L1 and rat L10a ribosomal proteins; rpl1a rpl1b double null mutation is lethal
YGL135W	Rpl1b	4	N-terminally acetylated protein component of the large (60S) ribosomal subunit, nearly identical to Rpl1Ap and has similarity to E. coli L1 and rat L10a ribosomal proteins; rpl1a rpl1b double null mutation is lethal
YMR242C	Rpl20a	4	Protein component of the large (60S) ribosomal subunit, nearly identical to Rpl20Bp and has similarity to rat L18a ribosomal protein
YOR312C	Rpl20b	4	Protein component of the large (60S) ribosomal subunit, nearly identical to Rpl20Ap and has similarity to rat L18a ribosomal protein
YGR034W	Rpl26b	4	Protein component of the large (60S) ribosomal subunit, nearly identical to Rpl26Ap and has similarity to E. coli L24 and rat L26 ribosomal proteins; binds to 5.8S rRNA
YHR010W	Rpl27a	4	Protein component of the large (60S) ribosomal subunit, nearly identical to Rpl27Bp and has similarity to rat L27 ribosomal protein
YDR471W	Rpl27b	4	Protein component of the large (60S) ribosomal subunit, nearly identical to Rpl27Ap and has similarity to rat L27 ribosomal protein
YOR063W	Rpl3	4	Protein component of the large (60S) ribosomal subunit, has similarity to E. coli L3 and rat L3 ribosomal proteins; involved in the replication and maintenance of killer double stranded RNA virus
YDL075W	Rpl31a	4	Protein component of the large (60S) ribosomal subunit, nearly identical to Rpl31Bp and has similarity to rat L31 ribosomal protein; associates with the karyopherin Sxm1p; loss of both Rpl31p and Rpl39p confers lethality
YPL143W	Rpl33a	4	N-terminally acetylated ribosomal protein L37 of the large (60S) ribosomal subunit, nearly identical to Rpl33Bp and has similarity to rat L35a; rpl33a null mutant exhibits slow growth while rpl33a rpl33b double null mutant is inviable
YPL249C-A	Rpl36b	4	Protein component of the large (60S) ribosomal subunit, nearly identical to Rpl36Ap and has similarity to rat L36 ribosomal protein; binds to 5.8 S rRNA
YBR031W	Rpl4a	4	N-terminally acetylated protein component of the large (60S) ribosomal subunit, nearly identical to Rpl4Bp and has similarity to E. coli L4 and rat L4 ribosomal proteins
YPL131W	Rpl5	4	Protein component of the large (60S) ribosomal subunit with similarity to E. coli L18 and rat L5 ribosomal proteins; binds 5S rRNA and is required for 60S subunit assembly
YML073C	Rpl6a	4	N-terminally acetylated protein component of the large (60S) ribosomal subunit, has similarity to Rpl6Bp and to rat L6 ribosomal protein; binds to 5.8S rRNA
YGL076C	Rpl7a	4	Protein component of the large (60S) ribosomal subunit, nearly identical to Rpl7Bp and has similarity to E. coli L30 and rat L7 ribosomal proteins; contains a conserved C-terminal Nucleic acid Binding Domain (NDB2)
YLR340W	Rpp0	4	Conserved ribosomal protein P0 of the ribosomal stalk, which is involved in interaction between translational elongation factors and the ribosome; similar to rat P0, human P0, and E. coli L10e; phosphorylated on serine 302
YOR369C	Rps12	4	Protein component of the small (40S) ribosomal subunit; has similarity to rat ribosomal protein S12
YCR031C	Rps14a	4	Ribosomal protein 59 of the small subunit, required for ribosome assembly and 20S pre-rRNA processing; mutations confer cryptopleurine resistance; nearly identical to Rps14Bp and similar to E. coli S11 and rat S14 ribosomal proteins
YJL191W	Rps14b	4	Ribosomal protein 59 of the small subunit, required for ribosome assembly and 20S pre-rRNA processing; mutations confer cryptopleurine resistance; nearly identical to Rps14Ap and similar to E. coli S11 and rat S14 ribosomal proteins
YOL040C	Rps15	4	Protein component of the small (40S) ribosomal subunit; has similarity to E. coli S19 and rat S15 ribosomal proteins
YMR143W	Rps16a	4	Protein component of the small (40S) ribosomal subunit; identical to Rps16Bp and has similarity to E. coli S9 and rat S16 ribosomal proteins
YDL083C	Rps16b	4	Protein component of the small (40S) ribosomal subunit; identical to Rps16Ap and has similarity to E. coli S9 and rat S16 ribosomal proteins
YML024W	Rps17a	4	Ribosomal protein 51 (rp51) of the small (40s) subunit; nearly identical to Rps17Bp and has similarity to rat S17 ribosomal protei
YDR447C	Rps17b	4	Ribosomal protein 51 (rp51) of the small (40s) subunit; nearly identical to Rps17Ap and has similarity to rat S17 ribosomal protein
YDR450W	Rps18a	4	Protein component of the small (40S) ribosomal subunit; nearly identical to Rps18Bp and has similarity to E. coli S13 and rat S18 ribosomal proteins
YML026C	Rps18b	4	Protein component of the small (40S) ribosomal subunit; nearly identical to Rps18Ap and has similarity to E. coli S13 and rat S18 ribosomal proteins
YOL121C	Rps19a	4	Protein component of the small (40S) ribosomal subunit, required for assembly and maturation of pre-40 S particles; mutations in human RPS19 are associated with Diamond Blackfan anemia; nearly identical to Rps19Bp
YNL302C	Rps19b	4	Protein component of the small (40S) ribosomal subunit, required for assembly and maturation of pre-40 S particles; mutations in human RPS19 are associated with Diamond Blackfan anemia; nearly identical to Rps19Ap
YLR441C	Rps1a	4	Ribosomal protein 10 (rp10) of the small (40S) subunit; nearly identical to Rps1Bp and has similarity to rat S3a ribosomal protein
YML063W	Rps1b	4	Ribosomal protein 10 (rp10) of the small (40S) subunit; nearly identical to Rps1Ap and has similarity to rat S3a ribosomal protein
YGL123W	Rps2	4	Protein component of the small (40S) subunit, essential for control of translational accuracy; phosphorylation by C-terminal domain kinase I (CTDK-I) enhances translational accuracy; methylated on one or more arginine residues by Hmt1p
YHL015W	Rps20	4	Protein component of the small (40S) ribosomal subunit; overproduction suppresses mutations affecting RNA polymerase III-dependent transcription; has similarity to E. coli S10 and rat S20 ribosomal proteins
YNL178W	Rps3	4	Protein component of the small (40S) ribosomal subunit, has apurinic/apyrimidinic (AP) endonuclease activity; essential for viability; has similarity to E. coli S3 and rat S3 ribosomal proteins
YJR145C	Rps4a	4	Protein component of the small (40S) ribosomal subunit; mutation affects 20S pre-rRNA processing; identical to Rps4Bp and has similarity to rat S4 ribosomal protei
YHR203C	Rps4b	4	Protein component of the small (40S) ribosomal subunit; identical to Rps4Ap and has similarity to rat S4 ribosomal protein
YJR123W	Rps5	4	Protein component of the small (40S) ribosomal subunit, the least basic of the non-acidic ribosomal proteins; phosphorylated in vivo; essential for viability; has similarity to E. coli S7 and rat S5 ribosomal proteins
YBL072C	Rps8a	4	Protein component of the small (40S) ribosomal subunit; identical to Rps8Bp and has similarity to rat S8 ribosomal protein
YER102W	Rps8b	4	Protein component of the small (40S) ribosomal subunit; identical to Rps8Ap and has similarity to rat S8 ribosomal protein
YPL081W	Rps9a	4	Protein component of the small (40S) ribosomal subunit; nearly identical to Rps9Bp and has similarity to E. coli S4 and rat S9 ribosomal proteins
YBR189W	Rps9b	4	Protein component of the small (40S) ribosomal subunit; nearly identical to Rps9Ap and has similarity to E. coli S4 and rat S9 ribosomal proteins
YLR058C	Shm2	4	Cytosolic serine hydroxymethyltransferase, converts serine to glycine plus 5,10 methylenetetrahydrofolate; major isoform involved in generating precursors for purine, pyrimidine, amino acid, and lipid biosynthesis
YLL024C	Ssa2	4	ATP binding protein involved in protein folding and vacuolar import of proteins; member of heat shock protein 70 (HSP70) family; associated with the chaperonin-containing T-complex;
YNL209W	Ssb2	4	Cytoplasmic ATPase that is a ribosome-associated molecular chaperone, functions with J-protein partner Zuo1p; may be involved in the folding of newly-synthesized polypeptide chains; member of the HSP70 family; homolog of SSB1
YLR150W	Stm1	4	Protein required for optimal translation under nutrient stress; perturbs association of Yef3p with ribosomes; involved in TOR signaling; binds G4 quadruplex and purine motif triplex nucleic acid; helps maintain telomere structure
YPR080W	Tef1	4	Translational elongation factor EF-1 alpha; also encoded by TEF2; functions in the binding reaction of aminoacyl-tRNA (AA-tRNA) to ribosomes; may also have a role in tRNA re-export from the nucleus
YBR118W	Tef2	4	Translational elongation factor EF-1 alpha; also encoded by TEF1; functions in the binding reaction of aminoacyl-tRNA (AA-tRNA) to ribosomes; may also have a role in tRNA re-export from the nucleus
YLR249W	Yef3	4	Gamma subunit of translational elongation factor eEF1B, stimulates the binding of aminoacyl-tRNA (AA-tRNA) to ribosomes by releasing eEF1A (Tef1p/Tef2p) from the ribosomal complex; contains two ABC cassettes; binds and hydrolyzes ATP
YFL039C	Act1	3	Actin, structural protein involved in cell polarization, endocytosis, and other cytoskeletal functions
YOL139C	Cdc33	3	Cytoplasmic mRNA cap binding protein and translation initiation factor eIF4E; the eIF4E-cap complex is responsible for mediating cap-dependent mRNA translation via interactions with translation initiation factor eIF4G (Tif4631p or Tif4632p
YNR001C	Cit1	3	Citrate synthase, catalyzes the condensation of acetyl coenzyme A and oxaloacetate to form citrate; the rate-limiting enzyme of the TCA cycle; nuclear encoded mitochondrial protein
YOR204W	Ded1	3	ATP-dependent DEAD (Asp-Glu-Ala-Asp)-box RNA helicase, required for translation initiation of all yeast mRNAs; mutations in human DEAD-box DBY are a frequent cause of male infertility
YLL018C	Dps1	3	Aspartyl-tRNA synthetase, primarily cytoplasmic; homodimeric enzyme that catalyzes the specific aspartylation of tRNA(Asp); class II aminoacyl tRNA synthetase; binding to its own mRNA may confer autoregulation
YPL037C	Egd1	3	Subunit beta1 of the nascent polypeptide-associated complex (NAC) involved in protein targeting, associated with cytoplasmic ribosomes; enhances DNA binding of the Gal4p activator; homolog of human BTF3b
YLR300W	Exg1	3	Major exo-1,3-beta-glucanase of the cell wall, involved in cell wall beta-glucan assembly; exists as three differentially glycosylated isoenzymes
YBR009C	Hhf1	3	Histone H4, core histone protein required for chromatin assembly and chromosome function; one of two identical histone proteins (see also HHF2); contributes to telomeric silencing; N-terminal domain involved in maintaining genomic integrity
YNL030W	Hhf2	3	Histone H4, core histone protein required for chromatin assembly and chromosome function; one of two identical histone proteins (see also HHF1); contributes to telomeric silencing; N-terminal domain involved in maintaining genomic integrity
YMR186W	Hsc82	3	Cytoplasmic chaperone of the Hsp90 family, redundant in function and nearly identical with Hsp82p, and together they are essential; expressed constitutively at 10-fold higher basal levels than HSP82 and induced 2-3 fold by heat shock
YLR259C	Hsp60	3	Tetradecameric mitochondrial chaperonin required for ATP-dependent folding of precursor polypeptides and complex assembly; prevents aggregation and mediates protein refolding after heat shock; role in mtDNA transmission; phosphorylated

Table S1 part C (continued)

ORF name	Protein name	Fold found on SZMP-resin (4 columns)	Protein function
YPR033C	**Hts1**	**3**	Cytoplasmic and mitochondrial histidine tRNA synthetase; efficient mitochondrial localization requires both a presequence and an amino-terminal sequence
YEL034W	**Hyp2**	**3**	Translation elongation factor eIF-5A that may function in translation initiation; similar to and functionally redundant with Anb1p; structural homolog of bacterial EF-P; undergoes an essential hypusination modification
YLR432W	**Imd3**	**3**	Inosine monophosphate dehydrogenase, catalyzes the first step of GMP biosynthesis, member of a four-gene family in S. cerevisiae, constitutively expressed
YML056C	**Imd4**	**3**	Inosine monophosphate dehydrogenase, catalyzes the first step of GMP biosynthesis, member of a four-gene family in S. cerevisiae, constitutively expressed
YDR037W	**Krs1**	**3**	Protein component of the large (60S) ribosomal subunit, nearly identical to Rpl12Ap; rpl12a rpl12b double mutant exhibits slow growth and slow translation; has similarity to E. coli L11 and rat L12 ribosomal proteins
YDL051W	**Lhp1**	**3**	RNA binding protein required for maturation of tRNA and U6 snRNA precursors; acts as a molecular chaperone for RNAs transcribed by polymerase III
YPL004C	**Lsp1**	**3**	Primary component of eisosomes, which are large immobile patch structures at the cell cortex associated with endocytosis, along with Pil1p and Sur7p; null mutants show activation of Pkc1p/Ypk1p stress resistance pathways; member of the BAR domain family
YKL009W	**Mrt4**	**3**	Protein involved in mRNA turnover and ribosome assembly, localizes to the nucleolus
YDL014W	**Nop1**	**3**	Nucleolar protein, component of the small subunit processome complex, which is required for processing of pre-18S rRNA; has similarity to mammalian fibrillarin
YGR159C	**Nsr1**	**3**	Nucleolar protein that binds nuclear localization sequences, required for pre-rRNA processing and ribosome biogenesis
YER165W	**Pab1**	**3**	Poly(A) binding protein, part of the 3'-end RNA-processing complex, mediates interactions between the 5' cap structure and the 3' mRNA poly(A) tail, involved in control of poly(A) tail length, interacts with translation factor eIF-4G
YGR086C	**Pil1**	**3**	Primary component of eisosomes, which are large immobile cell cortex structures associated with endocytosis; null mutants show activation of Pkc1p/Ypk1p stress resistance pathways
YGL008C	**Pma1**	**3**	Plasma membrane H+-ATPase, pumps protons out of the cell; major regulator of cytoplasmic pH and plasma membrane potential; P2-type ATPase; Hsp30p plays a role in Pma1p regulation; interactions with Std1p appear to propagate [GAR+]
YLR196W	**Pwp1**	**3**	Protein with WD-40 repeats involved in rRNA processing; associates with trans-acting ribosome biogenesis factors; similar to beta-transducin superfamily
YEL054C	**Rpl12a**	**3**	Protein component of the large (60S) ribosomal subunit, nearly identical to Rpl12Bp; rpl12a rpl12b double mutant exhibits slow growth and slow translation; has similarity to E. coli L11 and rat L12 ribosomal proteins
YDR418W	**Rpl12b**	**3**	Protein component of the large (60S) ribosomal subunit, nearly identical to Rpl12Ap; rpl12a rpl12b double mutant exhibits slow growth and slow translation; has similarity to E. coli L11 and rat L12 ribosomal proteins
YDL082W	**Rpl13a**	**3**	Protein component of the large (60S) ribosomal subunit, nearly identical to Rpl13Bp; not essential for viability; has similarity to rat L13 ribosomal protein
YLR029C	**Rpl15a**	**3**	Protein component of the large (60S) ribosomal subunit, nearly identical to Rpl15Bp and has similarity to rat L15 ribosomal protein; binds to 5.8 S rRNA
YJL177W	**Rpl17b**	**3**	Protein component of the large (60S) ribosomal subunit, nearly identical to Rpl17Ap and has similarity to E. coli L22 and rat L17 ribosomal proteins
YOL120C	**Rpl18a**	**3**	Protein component of the large (60S) ribosomal subunit, identical to Rpl18Bp and has similarity to rat L18 ribosomal protein; intron of RPL18A pre-mRNA forms stem-loop structures that are a target for Rnt1p cleavage leading to degradation
YNL301C	**Rpl18b**	**3**	Protein component of the large (60S) ribosomal subunit, identical to Rpl18Ap and has similarity to rat L18 ribosomal protein
YBR191W	**Rpl21a**	**3**	Protein component of the large (60S) ribosomal subunit, nearly identical to Rpl21Bp and has similarity to rat L21 ribosomal protein
YPL079W	**Rpl21b**	**3**	Protein component of the large (60S) ribosomal subunit, nearly identical to Rpl21Ap and has similarity to rat L21 ribosomal protein
YGL031C	**Rpl24a**	**3**	Ribosomal protein L30 of the large (60S) ribosomal subunit, nearly identical to Rpl24Bp and has similarity to rat L24 ribosomal protein; not essential for translation but may be required for normal translation rate
YGR148C	**Rpl24b**	**3**	Ribosomal protein L30 of the large (60S) ribosomal subunit, nearly identical to Rpl24Ap and has similarity to rat L24 ribosomal protein; not essential for translation but may be required for normal translation rate
YOL127W	**Rpl25**	**3**	Primary rRNA-binding ribosomal protein component of the large (60S) ribosomal subunit, has similarity to E. coli L23 and rat L23a ribosomal proteins; binds to 25S rRNA via a conserved C-terminal motif
YLR344W	**Rpl26a**	**3**	Protein component of the large (60S) ribosomal subunit, nearly identical to Rpl26Bp and has similarity to E. coli L24 and rat L26 ribosomal proteins; binds to 5.8S rRNA
YFR031C-A	**Rpl2a**	**3**	Protein component of the large (60S) ribosomal subunit, identical to Rpl2Bp and has similarity to E. coli L2 and rat L8 ribosomal proteins
YIL018W	**Rpl2b**	**3**	Protein component of the large (60S) ribosomal subunit, identical to Rpl2Ap and has similarity to E. coli L2 and rat L8 ribosomal proteins; expression is upregulated at low temperatures
YBL092W	**Rpl32**	**3**	Protein component of the large (60S) ribosomal subunit, has similarity to rat L32 ribosomal protein; overexpression disrupts telomeric silencing
YOR234C	**Rpl33b**	**3**	Ribosomal protein L37 of the large (60S) ribosomal subunit, nearly identical to Rpl33Ap and has similarity to rat L35a; rpl33b null mutant exhibits normal growth while rpl33a rpl33b double null mutant is inviable
YMR194W	**Rpl36a**	**3**	N-terminally acetylated protein component of the large (60S) ribosomal subunit, nearly identical to Rpl36Bp and has similarity to rat L36 ribosomal protein; binds to 5.8 S rRNA
YDR012W	**Rpl4b**	**3**	Protein component of the large (60S) ribosomal subunit, nearly identical to Rpl4Ap and has similarity to E. coli L4 and rat L4 ribosomal proteins
YHL033C	**Rpl8a**	**3**	Ribosomal protein L4 of the large (60S) ribosomal subunit, nearly identical to Rpl8Bp and has similarity to rat L7a ribosomal protein; mutation results in decreased amounts of free 60S subunits
YLL045C	**Rpl8b**	**3**	Ribosomal protein L4 of the large (60S) ribosomal subunit, nearly identical to Rpl8Ap and has similarity to rat L7a ribosomal protein; mutation results in decreased amounts of free 60S subunits
YER074W	**Rps24a**	**3**	Protein component of the small (40S) ribosomal subunit; identical to Rps24Bp and has similarity to rat S24 ribosomal protein
YIL069C	**Rps24b**	**3**	Protein component of the small (40S) ribosomal subunit; identical to Rps24Ap and has similarity to rat S24 ribosomal protein
YGR027C	**Rps25a**	**3**	Protein component of the small (40S) ribosomal subunit; nearly identical to Rps25Bp and has similarity to rat S25 ribosomal protein
YLR333C	**Rps25b**	**3**	Protein component of the small (40S) ribosomal subunit; nearly identical to Rps25Ap and has similarity to rat S25 ribosomal protein
YOR167C	**Rps28a**	**3**	Protein component of the small (40S) ribosomal subunit; nearly identical to Rps28Bp and has similarity to rat S28 ribosomal protein
YLR264W	**Rps28b**	**3**	Protein component of the small (40S) ribosomal subunit; nearly identical to Rps28Ap and has similarity to rat S28 ribosomal protein
YPL090C	**Rps6a**	**3**	Protein component of the small (40S) ribosomal subunit; identical to Rps6Bp and has similarity to rat S6 ribosomal protein
YBR181C	**Rps6b**	**3**	Protein component of the small (40S) ribosomal subunit; identical to Rps6Ap and has similarity to rat S6 ribosomal protein
YNL096C	**Rps7b**	**3**	Protein component of the small (40S) ribosomal subunit, nearly identical to Rps7Ap; interacts with Kti11p; deletion causes hypersensitivity to zymocin; has similarity to rat S7 and Xenopus S8 ribosomal proteins
YHL034C	**Sbp1**	**3**	Putative RNA binding protein; involved in translational repression and found in cytoplasmic P bodies; found associated with small nucleolar RNAs snR10 and snR11
YDR023W	**Ses1**	**3**	Cytosolic seryl-tRNA synthetase, class II aminoacyl-tRNA synthetase that aminoacylates tRNA(Ser), displays tRNA-dependent amino acid recognition which enhances discrimination of the serine substrate, interacts with peroxin Pex21p
YDL229W	**Ssb1**	**3**	Cytoplasmic ATPase that is a ribosome-associated molecular chaperone, functions with J-protein partner Zuo1p; may be involved in folding of newly-made polypeptide chains
YHR064C	**Ssz1**	**3**	Hsp70 protein that interacts with Zuo1p (a DnaJ homolog) to form a ribosome-associated complex that binds the ribosome via the Zuo1p subunit; also involved in pleiotropic drug resistance via sequential activation of PDR1 and PDR5; binds ATP
YPL237W	**Sui3**	**3**	Beta subunit of the translation initiation factor eIF2, involved in the identification of the start codon; proposed to be involved in mRNA binding
YIL078W	**Ths1**	**3**	Threonyl-tRNA synthetase, essential cytoplasmic protein
YMR260C	**Tif11**	**3**	Translation initiation factor eIF1A, essential protein that forms a complex with Sui1p (eIF1) and the 40S ribosomal subunit and scans for the start codon; C-terminus associates with Fun12p (eIF5B); N terminus interacts with eIF2 and eIF3
YKL035W	**Ugp1**	**3**	UDP-glucose pyrophosphorylase (UGPase), catalyses the reversible formation of UDP-Glc from glucose 1-phosphate and UTP, involved in a wide variety of metabolic pathways, expression modulated by Pho85p through Pho4p
YDL185W	**Vma1**	**3**	Subunit A of the eight-subunit V1 peripheral membrane domain of the vacuolar H+-ATPase; protein precursor undergoes self-catalyzed splicing to yield the extein Tfp1p and the intein Vde (PI-SceI), which is a site-specific endonuclease
YBR127C	**Vma2**	**3**	Subunit B of the eight-subunit V1 peripheral membrane domain of the vacuolar H+-ATPase (V-ATPase), an electrogenic proton pump found throughout the endomembrane system; contains nucleotide binding sites
YGR285C	**Zuo1**	**3**	Ribosome-associated chaperone, functions in ribosome biogenesis and, in partnership with Ssz1p and SSb1/2, as a chaperone for nascent polypeptide chains

Table S1 part D : List of proteins bound to AICAR-affinity resin at least three times on 5 independent experiments

ORF name	Protein name	Fold found on AICAR-resin (5 columns)	Protein function
YAL003W	**Efb1**	**5**	Translation elongation factor 1 beta; stimulates nucleotide exchange to regenerate EF-1 alpha-GTP for the next elongation cycle; part of the EF-1 complex, which facilitates binding of aminoacyl-tRNA to the ribosomal A site
YLR300W	**Exg1**	**5**	Major exo-1,3-beta-glucanase of the cell wall, involved in cell wall beta-glucan assembly; exists as three differentially glycosylated isoenzymes
YEL034W	**Hyp2**	**5**	Translation elongation factor eIF-5A that may function in translation initiation; similar to and functionally redundant with Anb1p; structural homolog of bacterial EF-P; undergoes an essential hypusination modification
YLR432W	**Imd3**	**5**	Inosine monophosphate dehydrogenase, catalyzes the first step of GMP biosynthesis, member of a four-gene family in S. cerevisiae, constitutively expressed
YML056C	**Imd4**	**5**	Inosine monophosphate dehydrogenase, catalyzes the first step of GMP biosynthesis, member of a four-gene family in S. cerevisiae, constitutively expressed
YER165W	**Pab1**	**5**	Poly(A) binding protein, part of the 3'-end RNA-processing complex, mediates interactions between the 5' cap structure and the 3' mRNA poly(A) tail, involved in control of poly(A) tail length, interacts with translation factor eIF-4G
YGL037C	**Pnc1**	**5**	Nicotinamidase that converts nicotinamide to nicotinic acid as part of the NAD(+) salvage pathway, required for life span extension by calorie restriction; PNC1 expression responds to all known stimuli that extend replicative life span
YOR369C	**Rps12**	**5**	Protein component of the small (40S) ribosomal subunit; has similarity to rat ribosomal protein S12
YHL015W	**Rps20**	**5**	Protein component of the small (40S) ribosomal subunit; overproduction suppresses mutations affecting RNA polymerase III-dependent transcription; has similarity to E. coli S10 and rat S20 ribosomal proteins
YHL034C	**Sbp1**	**5**	Putative RNA binding protein; involved in translational repression and found in cytoplasmic P bodies; found associated with small nucleolar RNAs snR10 and snR11
YDR023W	**Ses1**	**5**	Cytosolic seryl-tRNA synthetase, class II aminoacyl-tRNA synthetase that aminoacylates tRNA(Ser), displays tRNA-dependent amino acid recognition which enhances discrimination of the serine substrate, interacts with peroxin Pex21p
YDL229W	**Ssb1**	**5**	Cytoplasmic ATPase that is a ribosome-associated molecular chaperone, functions with J-protein partner Zuo1p; may be involved in folding of newly-made polypeptide chains; member of the HSP70 family; interacts with phosphatase subunit Reg1p
YNL209W	**Ssb2**	**5**	Cytoplasmic ATPase that is a ribosome-associated molecular chaperone, functions with J-protein partner Zuo1p; may be involved in the folding of newly-synthesized polypeptide chains; member of the HSP70 family; homolog of SSB1
YLR150W	**Stm1**	**5**	Protein required for optimal translation under nutrient stress; perturbs association of Yef3p with ribosomes; involved in TOR signaling; binds G4 quadruplex and purine motif triplex nucleic acid; helps maintain telomere structure
YHR019C	**Ded81**	**4**	Cytosolic asparaginyl-tRNA synthetase, required for protein synthesis, catalyzes the specific attachment of asparagine to its cognate tRNA
YOR133W	**Eft1**	**4**	Elongation factor 2 (EF-2), also encoded by EFT2; catalyzes ribosomal translocation during protein synthesis; contains diphthamide, the unique posttranslationally modified histidine residue specifically ADP-ribosylated by diphtheria toxin
YDR385W	**Eft2**	**4**	Elongation factor 2 (EF-2), also encoded by EFT1; catalyzes ribosomal translocation during protein synthesis; contains diphthamide, the unique posttranslationally modified histidine residue specifically ADP-ribosylated by diphtheria toxin
YPL037C	**Egd1**	**4**	Subunit beta1 of the nascent polypeptide-associated complex (NAC) involved in protein targeting, associated with cytoplasmic ribosomes; enhances DNA binding of the Gal4p activator; homolog of human BTF3b
YOL123W	**Hrp1**	**4**	Subunit of cleavage factor I, a five-subunit complex required for the cleavage and polyadenylation of pre-mRNA 3' ends; RRM-containing heteronuclear RNA binding protein and hnRNPA/B family member that binds to poly (A) signal sequences
YLR259C	**Hsp60**	**4**	Tetradecameric mitochondrial chaperonin required for ATP-dependent folding of precursor polypeptides and complex assembly; prevents aggregation and mediates protein refolding after heat shock; role in mtDNA transmission; phosphorylated
YDL051W	**Lhp1**	**4**	RNA binding protein required for maturation of tRNA and U6 snRNA precursors; acts as a molecular chaperone for RNAs transcribed by polymerase III; homologous to human La (SS-B) autoantigen
YDR432W	**Npl3**	**4**	RNA binding protein required for maturation of tRNA and U6 snRNA precursors; acts as a molecular chaperone for RNAs transcribed by polymerase III; homologous to human La (SS-B) autoantigen
YPR102C	**Rpl11a**	**4**	Protein of the large 60S ribosomal subunit, nearly identical to Rpl11Bp but expressed at twice the level; involved in ribosomal assembly; depletion causes degradation of 60S proteins and RNA; similar to E. coli L5 and rat L11
YGR085C	**Rpl11b**	**4**	Protein component of the large (60S) ribosomal subunit, nearly identical to Rpl11Ap; involved in ribosomal assembly; depletion causes degradation of proteins and RNA of the 60S subunit; has similarity to E. coli L5 and rat L11
YGR034W	**Rpl26b**	**4**	Protein component of the large (60S) ribosomal subunit, nearly identical to Rpl26Ap and has similarity to E. coli L24 and rat L26 ribosomal proteins; binds to 5.8S rRNA
YDL075W	**Rpl31a**	**4**	Protein component of the large (60S) ribosomal subunit, nearly identical to Rpl31Bp and has similarity to rat L31 ribosomal protein; associates with the karyopherin Sxm1p; loss of both Rpl31p and Rpl39p confers lethality
YPL131W	**Rpl5**	**4**	Protein component of the large (60S) ribosomal subunit with similarity to E. coli L18 and rat L5 ribosomal proteins; binds 5S rRNA and is required for 60S subunit assembly
YML024W	**Rps17a**	**4**	Ribosomal protein 51 (rp51) of the small (40s) subunit; nearly identical to Rps17Bp and has similarity to rat S17 ribosomal prote
YDR447C	**Rps17b**	**4**	Ribosomal protein 51 (rp51) of the small (40s) subunit; nearly identical to Rps17Ap and has similarity to rat S17 ribosomal protein
YOL121C	**Rps19a**	**4**	Protein component of the small (40S) ribosomal subunit, required for assembly and maturation of pre-40 S particles; mutations in human RPS19 are associated with Diamond Blackfan anemia; nearly identical to Rps19Bp
YNL302C	**Rps19b**	**4**	Protein component of the small (40S) ribosomal subunit, required for assembly and maturation of pre-40 S particles; mutations in human RPS19 are associated with Diamond Blackfan anemia; nearly identical to Rps19Ap
YNL178W	**Rps3**	**4**	Protein component of the small (40S) ribosomal subunit, has apurinic/apyrimidinic (AP) endonuclease activity; essential for viability; has similarity to E. coli S3 and rat S3 ribosomal proteins
YJR123W	**Rps5**	**4**	Protein component of the small (40S) ribosomal subunit, the least basic of the non-acidic ribosomal proteins; phosphorylated in vivo; essential for viability; has similarity to E. coli S7 and rat S5 ribosomal proteins
YBR118W	**Tef2**	**4**	Translational elongation factor EF-1 alpha; also encoded by TEF1; functions in the binding reaction of aminoacyl-tRNA (AA-tRNA) to ribosomes; may also have a role in tRNA re-export from the nucleu
YIL078W	**Ths1**	**4**	Threonyl-tRNA synthetase, essential cytoplasmic protein
YPR163C	**Tif3**	**4**	Translation initiation factor eIF-4B, has RNA annealing activity; contains an RNA recognition motif and binds to single-stranded RNA
YFL039C	**Act1**	**3**	Actin, structural protein involved in cell polarization, endocytosis, and other cytoskeletal functions
YMR116C	**Asc1**	**3**	G-protein beta subunit and guanine nucleotide dissociation inhibitor for Gpa2p; ortholog of RACK1 that inhibits translation; core component of the small (40S) ribosomal subunit; represses Gcn4p in the absence of amino acid starvation
YAL038W	**Cdc19**	**3**	Pyruvate kinase, functions as a homotetramer in glycolysis to convert phosphoenolpyruvate to pyruvate, the input for aerobic (TCA cycle) or anaerobic (glucose fermentation) respiration
YLL018C	**Dps1**	**3**	Aspartyl-tRNA synthetase, primarily cytoplasmic; homodimeric enzyme that catalyzes the specific aspartylation of tRNA(Asp); class II aminoacyl tRNA synthetase; binding to its own mRNA may confer autoregulation
YHR193C	**Egd2**	**3**	Alpha subunit of the heteromeric nascent polypeptide-associated complex (NAC) involved in protein sorting and translocation, associated with cytoplasmic ribosomes
YGR200C	**Elp2**	**3**	Subunit of Elongator complex, which is required for modification of wobble nucleosides in tRNA; target of Kluyveromyces lactis zymocin
YER025W	**Gcd11**	**3**	Gamma subunit of the translation initiation factor eIF2, involved in the identification of the start codon; binds GTP when forming the ternary complex with GTP and tRNAi-Met
YER133W	**Glc7**	**3**	Type 1 serine/threonine protein phosphatase catalytic subunit, involved in many processes (eg: glycogen metabolism, sporulation, mitosis); accumulates at mating projections by interaction with Afr1p; interacts with many regulatory subunits
YMR186W	**Hsc82**	**3**	Cytoplasmic chaperone of the Hsp90 family, redundant in function and nearly identical with Hsp82p, and together they are essential; expressed constitutively at 10-fold higher basal levels than HSP82 and induced 2-3 fold by heat shock
YPL240C	**Hsp82**	**3**	Hsp90 chaperone required for pheromone signaling and negative regulation of Hsf1p; docks with Tom70p for mitochondrial preprotein delivery; promotes telomerase DNA binding and nucleotide addition; interacts with Cns1p, Cpr6p, Cpr7p, Sti1p
YDR037W	**Krs1**	**3**	Lysyl-tRNA synthetase
YPL004C	**Lsp1**	**3**	Primary component of eisosomes, which are large immobile patch structures at the cell cortex associated with endocytosis, along with Pil1p and Sur7p
YLR044C	**Pdc1**	**3**	Major of three pyruvate decarboxylase isozymes, key enzyme in alcoholic fermentation, decarboxylates pyruvate to acetaldehyde; subject to glucose-, ethanol-, and autoregulation; involved in amino acid catabolism
YLR406C	**Rpl31b**	**3**	Protein component of the large (60S) ribosomal subunit, nearly identical to Rpl31Ap and has similarity to rat L31 ribosomal protein; associates with the karyopherin Sxm1p; loss of both Rpl31p and Rpl39p confers lethality
YLR448W	**Rpl6b**	**3**	Protein component of the large (60S) ribosomal subunit, has similarity to Rpl6Ap and to rat L6 ribosomal protein; binds to 5.8S rRNA
YOL039W	**Rpp2a**	**3**	Ribosomal protein P2 alpha, a component of the ribosomal stalk, which is involved in the interaction between translational elongation factors and the ribosome; regulates the accumulation of P1 (Rpp1Ap and Rpp1Bp) in the cytoplasm
YDR382W	**Rpp2b**	**3**	Ribosomal protein P2 beta, a component of the ribosomal stalk, which is involved in the interaction between translational elongation factors and the ribosome; regulates the accumulation of P1 (Rpp1Ap and Rpp1Bp) in the cytoplasm
YGR214W	**Rps0a**	**3**	Protein component of the small (40S) ribosomal subunit, nearly identical to Rps0Bp; required for maturation of 18S rRNA along with Rps0Bp; deletion of either RPS0 gene reduces growth rate, deletion of both genes is lethal
YLR048W	**Rps0b**	**3**	Protein component of the small (40S) ribosomal subunit, nearly identical to Rps0Ap; required for maturation of 18S rRNA along with Rps0Ap; deletion of either RPS0 gene reduces growth rate, deletion of both genes is lethal
YOR167C	**Rps28a**	**3**	Protein component of the small (40S) ribosomal subunit; nearly identical to Rps28Bp and has similarity to rat S28 ribosomal protein
YLR264W	**Rps28b**	**3**	Protein component of the small (40S) ribosomal subunit; nearly identical to Rps28Ap and has similarity to rat S28 ribosomal protein
YPR181C	**Sec23**	**3**	GTPase-activating protein, stimulates the GTPase activity of Sar1p; component of the Sec23p-Sec24p heterodimer of the COPII vesicle coat, involved in ER to Golgi transport
YLL024C	**Ssa2**	**3**	ATP binding protein involved in protein folding and vacuolar import of proteins; member of heat shock protein 70 (HSP70) family
YJR007W	**Sui2**	**3**	Alpha subunit of the translation initiation factor eIF2, involved in the identification of the start codon; phosphorylation of Ser51 is required for regulation of translation by inhibiting the exchange of GDP for GTP
YJR009C	**Tdh2**	**3**	Glyceraldehyde-3-phosphate dehydrogenase, isozyme 2, involved in glycolysis and gluconeogenesis; tetramer that catalyzes the reaction of glyceraldehyde-3-phosphate to 1,3 bis-phosphoglycerate; detected in the cytoplasm and cell wall
YGR192C	**Tdh3**	**3**	Glyceraldehyde-3-phosphate dehydrogenase, isozyme 3, involved in glycolysis and gluconeogenesis; tetramer that catalyzes the reaction of glyceraldehyde-3-phosphate to 1,3 bis-phosphoglycerate; detected in the cytoplasm and cell wall
YPR080W	**Tef1**	**3**	Translational elongation factor EF-1 alpha; also encoded by TEF2; functions in the binding reaction of aminoacyl-tRNA (AA-tRNA) to ribosomes; may also have a role in tRNA re-export from the nucleus
YKR059W	**Tif1**	**3**	Translation initiation factor eIF4A, identical to Tif2p; DEA(D/H)-box RNA helicase that couples ATPase activity to RNA binding and unwinding; forms a dumbbell structure of two compact domains connected by a linker; interacts with eIF4G
YJL138C	**Tif2**	**3**	Translation initiation factor eIF4A, identical to Tif1p; DEA(D/H)-box RNA helicase that couples ATPase activity to RNA binding and unwinding; forms a dumbbell structure of two compact domains connected by a linker; interacts with eIF4G
YLR262C-A	**Tma7**	**3**	Protein of unknown that associates with ribosomes; null mutant exhibits translation defects, altered polyribosome profiles, and resistance to the translation inhibitor anisomcyin
YDL185W	**Vma1**	**3**	Subunit A of the eight-subunit V1 peripheral membrane domain of the vacuolar H+-ATPase; protein precursor undergoes self-catalyzed splicing to yield the extein Tfp1p and the intein Vde (PI-SceI), which is a site-specific endonuclease
YLR249W	**Yef3**	**3**	Gamma subunit of translational elongation factor eEF1B, stimulates the binding of aminoacyl-tRNA (AA-tRNA) to ribosomes by releasing eEF1A (Tef1p/Tef2p) from the ribosomal complex; contains two ABC cassettes; binds and hydrolyzes ATP
YHR020W	**Yhr020w**	**3**	Protein of unknown function that may interact with ribosomes, based on co-purification experiments; has similarity to proline-tRNA ligase; YHR020W is an essential gene

Table S2: List of the 57 proteins less abundant in the presence of AICAR

Protein Name	Protein Function	Mean abundance + AICAR	Mean abundance - AICAR	Ratio + vs - AICAR	T-test p-value + vs - AICAR
Btn2	v-SNARE binding protein	5.5E+05	2.7E+06	0.20	0.010
Crz1	Transcription factor	8.3E+05	3.3E+06	0.25	0.043
Snu13	RNA binding protein; part of U3 snoRNP	2.8E+06	1.1E+07	0.25	0.022
Hhf1	Histone H4	5.2E+07	2.0E+08	0.26	0.041
Srp40	Role in preribosome assembly or transport	4.5E+06	1.7E+07	0.26	0.029
Htb2	Histone H2B	2.0E+06	7.8E+06	0.26	0.004
Dep1	Component of the Rpd3L histone deacetylase complex	4.3E+05	1.6E+06	0.28	0.002
Isw1	ATPase subunit of imitation-switch chromatin remodelers	2.5E+06	8.2E+06	0.31	0.012
Htz1	Histone variant H2AZ	9.8E+06	3.1E+07	0.31	0.022
Rpo31	RNA polymerase III largest subunit C160	1.1E+05	3.6E+05	0.32	0.035
Abf1	DNA binding protein with possible chromatin-reorganizing activity	6.0E+06	1.9E+07	0.32	0.034
Spc110	Inner plaque spindle pole body (SPB) component	3.2E+06	9.9E+06	0.32	0.046
Hta1	Histone H2A	2.2E+08	6.6E+08	0.33	0.006
Pho2	Homeobox transcription factor	7.7E+05	2.3E+06	0.33	0.012
Imp2'	Transcriptional activator	5.4E+04	1.6E+05	0.34	0.013
Hht1	Histone H3	1.5E+07	4.4E+07	0.34	0.031
Tub4	Gamma-tubulin	3.4E+05	9.9E+05	0.34	0.035
Mcr1	NADH-cytochrome b5 reductase	2.1E+06	6.0E+06	0.35	0.040
Srm1	Nucleotide exchange factor for Gsp1p	1.3E+07	3.8E+07	0.35	0.018
Nit2	Nit protein	2.9E+05	8.1E+05	0.35	0.031
Tfa1	TFIIE large subunit	2.4E+06	6.9E+06	0.35	0.037
Hho1	Histone H1	7.5E+06	2.0E+07	0.37	0.046
Pxr1	Essential protein involved in rRNA and snoRNA maturation	7.4E+06	2.0E+07	0.37	0.009
Mot1	Essential protein involved in regulation of transcription	9.7E+07	2.5E+08	0.39	0.023
Taf7	TFIID subunit involved in RNA polymerase II transcription	3.8E+06	9.7E+06	0.39	0.010
Raf1	Anti-repressor that increases 2 micron plasmid copy number	3.1E+06	8.0E+06	0.39	0.010
Ylr455w	Component of the NuA3b histone acetyltransferase complex	2.9E+06	7.4E+06	0.40	0.008
Nop8	Nucleolar protein required for 60S ribosomal subunit biogenesis	3.0E+05	7.4E+05	0.40	0.049
Mpp10	Component of the SSU processome and 90S preribosome	9.3E+05	2.3E+06	0.40	0.004
Rpb4	RNA polymerase II subunit B32	1.3E+06	3.3E+06	0.41	0.007
Rep2	Master regulator that regulates transcript levels of the FLP1 gene	8.0E+06	1.9E+07	0.41	0.009
Rpc34	RNA polymerase III subunit C34	2.0E+06	4.9E+06	0.42	0.040
Gcg1	Gamma-glutamyl cyclotransferase	3.4E+06	8.0E+06	0.42	0.005
Arp5	Nuclear actin-related protein involved in chromatin remodeling	2.7E+06	6.4E+06	0.43	0.016
Rap1	DNA-binding protein involved in regulation of transcription	6.9E+06	1.6E+07	0.43	0.020
Nop56	Essential nucleolar protein	1.2E+08	2.9E+08	0.43	0.014
Scp1	Component of yeast cortical actin cytoskeleton	7.1E+05	1.6E+06	0.43	0.024
Fpr3	Nucleolar peptidyl-prolyl cis-trans isomerase (PPIase)	5.2E+07	1.2E+08	0.44	0.009
Rpc82	RNA polymerase III subunit C82	3.9E+06	8.8E+06	0.44	0.011
Tfc3	Subunit of the RNA polymerase III transcription initiation factor complex	2.6E+06	5.8E+06	0.45	0.007
Tfg2	TFIIF (Transcription Factor II) middle subunit	1.0E+06	2.3E+06	0.46	0.017
Nop7	Nucleolar protein involved in rRNA processing	3.3E+06	7.3E+06	0.46	0.012
Esf2	Essential nucleolar protein involved in pre-18S rRNA processing	5.0E+05	1.1E+06	0.46	0.046
Nop6	rRNA-binding protein required for 40S ribosomal subunit biogenesis	4.4E+06	9.5E+06	0.46	0.008
Itc1	Subunit of the ATP-dependent Isw2p-Itc1p chromatin remodeling complex	3.3E+06	7.2E+06	0.46	0.021
Rpc25	RNA polymerase III subunit C25	1.6E+06	3.4E+06	0.47	0.010
Bdf1	Protein involved in transcription initiation at TATA-containing promoters	3.6E+06	7.8E+06	0.47	0.033
Rcm1	rRNA m5C methyltransferase	5.9E+05	1.2E+06	0.47	0.028
Rxt3	Subunit of the RPD3L complex	1.1E+06	2.3E+06	0.47	0.012
Mip1	Catalytic subunit of the mitochondrial DNA polymerase	6.2E+05	1.3E+06	0.47	0.013
Cyc2	Mitochondrial peripheral inner membrane protein	5.3E+05	1.1E+06	0.48	0.032
Sen1	Helicase required for RNA polymerase II transcription	2.1E+06	4.3E+06	0.49	0.015
Arp4	Nuclear actin-related protein involved in chromatin remodeling	9.0E+06	1.8E+07	0.49	0.011
Rpa49	RNA polymerase I subunit A49	9.9E+06	2.0E+07	0.49	0.038
Noc2	Protein that forms a nucleolar complex with Mak21p	4.4E+06	9.1E+06	0.49	0.010
Rgd1	GTPase-activating protein for Rho3p and Rho4p,	1.9E+06	3.9E+06	0.50	0.006
Swc4	Component of the Swr1p complex	1.1E+06	2.2E+06	0.50	0.002

Table S3: GO term analyses for the 57 proteins less abundant in the presence of AICAR

Biological process	Fold Enrichment	p-Value
Chromatin assembly	16.07	8.15E-05
Chromatin organization	7.04	2.05E-07
rRNA metabolic process	5.91	1.22E-04
Transcription, DNA-templated	5.67	5.73E-10
Regulation of biosynthetic process	3.6	7.75E-06

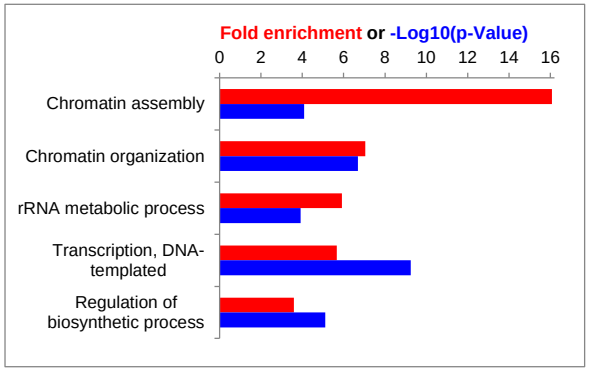

Cellular component	Fold Enrichment	p-Value
Nuclear nucleosome	100	5.03E-10
Nuclear chromatin	13.73	9.31E-11
Nuclear chromosome	6.97	7.16E-08
Nuclear lumen	5.9	1.98E-20
Nucleolus	5.55	7.70E-04

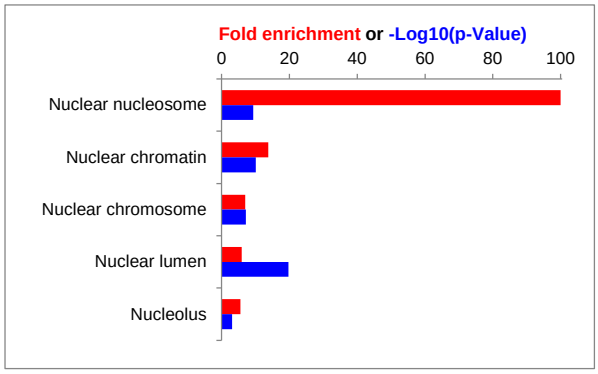

Table S4: List of the 92 proteins more abundant when Kap123 is overexpressed

Protein Name	Protein Function	Mean abundance + AICAR	Mean abundance - AICAR	Ratio + vs - AICAR	T-test p-value + vs - AICAR
Tkl2	Transketolase	2.40E+06	4.57E+05	5.25	0.024
Mcm2	Protein involved in DNA replication	1.89E+06	4.16E+05	4.53	0.044
Vps72	Htz1p-binding component of the SWR1 complex	7.31E+05	1.65E+05	4.42	0.048
Tfc6	Subunit of RNA polymerase III transcription initiation factor complex	2.29E+06	5.43E+05	4.21	0.025
Lam1	Putative sterol transfer protein	4.00E+05	1.03E+05	3.87	0.026
Vps1	Dynamin-like GTPase	1.80E+08	4.67E+07	3.86	0.034
Orc2	Subunit of the origin recognition complex,	6.97E+05	1.91E+05	3.65	0.039
Htz1	Histone variant H2AZ	3.52E+07	9.79E+06	3.59	0.049
Rtg3	Basic helix-loop-helix-leucine zipper transcription factor	5.45E+06	1.53E+06	3.56	0.044
Urb2	Protein required for metabolism of the rRNA primary transcript	5.01E+05	1.42E+05	3.53	0.047
Elc1	Elongin C	1.33E+06	3.79E+05	3.51	0.027
Htb2	Histone H2B	4.69E+06	1.36E+06	3.45	0.032
Pop1	Subunit of both RNase MRP and nuclear RNase P	3.34E+06	9.86E+05	3.39	0.039
Hos3	Trichostatin A-insensitive homodimeric histone deacetylase	9.85E+06	2.92E+06	3.37	0.022
Ams1	Vacuolar alpha mannosidase	1.16E+06	3.53E+05	3.27	0.047
Rod1	Alpha-arrestin involved in ubiquitin-dependent endocytosis	1.00E+06	3.14E+05	3.20	0.014
Isw1	ATPase subunit of imitation-switch chromatin remodelers	9.98E+06	3.13E+06	3.19	0.050
Hsp30	Negative regulator of the H(+)-ATPase Pma1p	2.50E+07	8.15E+06	3.06	0.017
Yaf9	Subunit of NuA4 histone H4 acetyltransferase and SWR1 complexes	1.53E+06	5.01E+05	3.05	0.019
Noc3	Subunit of the nuclear Noc2p complex and pre-replicative complexes	7.98E+06	2.62E+06	3.04	0.014
Uls1	Swi2/Snf2-related translocase, SUMO-Targeted Ubiquitin Ligase	3.50E+05	1.18E+05	2.96	0.001
Epl1	Subunit of NuA4, histone H4/H2A acetyltransferase complex	2.62E+06	8.89E+05	2.95	0.033
Hfi1	Adaptor protein required for structural integrity of the SAGA complex	1.55E+06	5.28E+05	2.94	0.002
Tfc4	Subunit of RNA polymerase III transcription initiation factor complex	1.22E+06	4.17E+05	2.92	0.013
Ask10	Component of RNA polymerase II holoenzyme	4.23E+06	1.52E+06	2.78	0.017
Lsp1	Primary component of eisosomes	4.70E+08	1.70E+08	2.76	0.015
Swc4	Component of the Swr1p complex	3.82E+06	1.40E+06	2.72	0.000
Pde1	Low-affinity cyclic AMP phosphodiesterase	1.24E+06	4.57E+05	2.72	0.016
Rap1	DNA-binding protein involved in regulation of transcription	1.52E+07	5.66E+06	2.69	0.011
Pdc2	Transcription factor required for synthesis of pyruvate decarboxylase	1.44E+06	5.39E+05	2.67	0.022
Pma1	Plasma membrane H+-ATPase	3.14E+07	1.18E+07	2.66	0.046
Sds3	Component of the Rpd3p/Sin3p deacetylase complex	1.19E+06	4.50E+05	2.64	0.023
Nde1	Mitochondrial external NADH dehydrogenase,	2.27E+06	8.64E+05	2.63	0.026
Dbp10	Putative ATP-dependent RNA helicase	3.39E+06	1.30E+06	2.61	0.047
Rad7	Nucleotide excision repair (NER) protein	2.69E+06	1.05E+06	2.56	0.042
Mec1	Genome integrity checkpoint protein, PI kinase superfamily member	4.21E+05	1.66E+05	2.53	0.024
Eaf1	Component of the NuA4 histone acetyltransferase complex	2.24E+06	8.96E+05	2.50	0.026
Fpr4	Peptidyl-prolyl cis-trans isomerase	7.31E+07	2.93E+07	2.49	0.008
Gph1	Non-essential glycogen phosphorylase	8.88E+06	3.58E+06	2.48	0.008
Arp5	Nuclear actin-related protein involved in chromatin remodeling	9.55E+06	3.87E+06	2.47	0.014
Spc110	Inner plaque spindle pole body (SPB) component	3.80E+06	1.54E+06	2.46	0.019
Suv3	ATP-dependent RNA helicase	1.57E+06	6.38E+05	2.46	0.009
Hxk1	Hexokinase isoenzyme 1	7.55E+05	3.09E+05	2.45	0.008
Mot1	Essential abundant protein involved in regulation of transcription	6.78E+06	2.79E+06	2.43	0.009
Ctt1	Cytosolic catalase T	9.20E+06	3.79E+06	2.43	0.001
Ykl023w	Putative protein of unknown function	5.93E+06	2.47E+06	2.40	0.030
Mak5	Essential nucleolar protein; putative DEAD-box RNA helicase	1.28E+06	5.34E+05	2.39	0.005
Ald3	Cytoplasmic aldehyde dehydrogenase	2.38E+07	9.98E+06	2.38	0.045
Top1	Topoisomerase I	1.95E+07	8.24E+06	2.36	0.040
Arp4	Nuclear actin-related protein involved in chromatin remodeling	2.22E+07	9.41E+06	2.36	0.016
Fpr3	Nucleolar peptidyl-prolyl cis-trans isomerase	3.10E+08	1.32E+08	2.35	0.038
Ppn1	Dual endo- and exopolyphosphatase	1.06E+07	4.54E+06	2.35	0.017
Sen1	ATP-dependent 5' to 3' RNA/DNA and DNA helicase	6.88E+06	3.00E+06	2.29	0.021
Rgc1	Putative regulator of the Fps1p glycerol channel	1.17E+07	5.12E+06	2.28	0.034
Chs1	Chitin synthase I	6.31E+05	2.77E+05	2.28	0.045
Chd1	Nucleosome remodeling factor	1.66E+07	7.28E+06	2.27	0.005
Pil1	Primary component of eisosomes	7.23E+08	3.19E+08	2.27	0.006
Sin3	Component of the Sin3p-Rpd3p histone deacetylase complex	5.13E+06	2.27E+06	2.26	0.004
Pet127	Protein with a role in 5'-end processing of mitochondrial RNAs	4.60E+06	2.05E+06	2.24	0.030
Nqm1	Transaldolase of unknown function	1.92E+06	8.61E+05	2.23	0.001
Ssa4	Heat shock protein	3.06E+06	1.38E+06	2.22	0.020
Reb1	RNA polymerase I enhancer binding protein	8.98E+06	4.05E+06	2.22	0.015
Mss116	Mitochondrial transcription elongation factor	1.80E+07	8.11E+06	2.22	0.020
Mpd1	Member of the protein disulfide isomerase (PDI) family	3.95E+07	1.79E+07	2.21	0.023
Ino80	ATPase and nucleosome spacing factor	1.91E+07	8.65E+06	2.21	0.007
Mpp10	Component of the SSU processome and 90S preribosome	1.81E+06	8.24E+05	2.20	0.013
Spt5	Regulator of Pol I and Pol II transcription and pre-mRNA processing	1.08E+07	4.92E+06	2.19	0.048
Nop1	Nucleolar component of the small subunit processome complex	2.78E+08	1.27E+08	2.18	0.015
Noc2	Protein involved in ribosome biogenesis	3.50E+07	1.60E+07	2.18	0.011
Dss1	3'-5' exoribonuclease	2.58E+06	1.19E+06	2.17	0.001
Slh1	Putative RNA helicase related to Ski2p	1.08E+06	5.02E+05	2.16	0.032
Pmt1	Protein O-mannosyltransferase	1.11E+06	5.24E+05	2.11	0.005
Enp1	Protein associated with U3 and U14 snoRNAs	4.15E+06	1.96E+06	2.11	0.018
Set2	Histone methyltransferase with a role in transcriptional elongation	6.86E+05	3.25E+05	2.11	0.036
Hsp31	Methylglyoxalase that converts methylglyoxal to D-lactate	5.74E+06	2.72E+06	2.11	0.006
Itc1	Subunit of the Isw2p-Itc1p chromatin remodeling complex	1.03E+07	4.88E+06	2.11	0.027
Tfc7	Subunit of RNA polymerase III transcription initiation factor complex	8.07E+06	3.85E+06	2.09	0.001
Nhp2	Nuclear protein essential for function of H/ACA-type snoRNPs	7.79E+07	3.73E+07	2.09	0.011

Table S4 (continued)

Protein Name	Protein Function	Mean abundance + AICAR	Mean abundance - AICAR	Ratio + vs - AICAR	T-test p-value + vs - AICAR
Rqc2	Component of RQC, which mediates nascent chain degradation	1.67E+07	8.01E+06	2.09	0.018
Mdj1	Co-chaperone stimulating the ATPase activity of Ssc1p	3.60E+06	1.73E+06	2.08	0.028
Nop58	Protein involved in pre-rRNA processing	1.20E+08	5.78E+07	2.08	0.050
Nop8	Nucleolar protein required for 60S ribosomal subunit biogenesis	9.76E+05	4.74E+05	2.06	0.013
Rpb2	RNA polymerase II second largest subunit B150	7.68E+06	3.73E+06	2.06	0.008
Kog1	Subunit of TORC1	1.45E+06	7.09E+05	2.05	0.007
Yfr006w	Putative X-Pro aminopeptidase	8.73E+06	4.26E+06	2.05	0.048
Gcy1	Putative NADP(+) coupled glycerol dehydrogenase	1.61E+06	7.89E+05	2.04	0.021
Top2	Topoisomerase II	4.73E+07	2.33E+07	2.03	0.012
Rvb1	ATP-dependent DNA helicase	7.53E+07	3.72E+07	2.03	0.015
Kre33	Protein required for biogenesis of the small ribosomal subunit	1.61E+07	7.96E+06	2.02	0.008
Tdh1	Glyceraldehyde-3-phosphate dehydrogenase	1.28E+08	6.36E+07	2.02	0.012
Ssf1	Constituent of 66S pre-ribosomal particles	5.36E+06	2.66E+06	2.01	0.047
Tra1	Subunit of SAGA and NuA4 histone acetyltransferase complexes	3.72E+06	1.86E+06	2.00	0.013

Table S5: GO term analyses for the 92 proteins more abundant when Kap123 is overexpressed

Biological process	Fold Enrichment	p-Value
Histone exchange	25.27	4.38E-03
Regulation of chromatin organization	14.15	1.73E-03
Chromatin assembly	9.8	9.26E-04
Histone modification	9.13	5.63E-08
Chromatin organization	6.57	1.37E-13
Transcription, DNA-templated	4.1	1.74E-09
Regulation of gene expression	3.02	2.07E-08

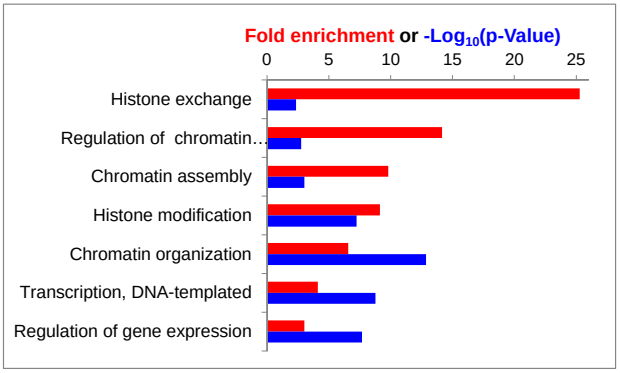

Cellular component	Fold Enrichment	p-Value
NuA4 histone acetyltransferase complex	26.06	8.86E-06
INO80-type complex	19.05	7.35E-05
Swi-SNF-type complex	10.79	1.27E-04
Nuclear chromatin	6.87	2.97E-07
Nuclear chromosome	4.77	5.49E-07
Nucleolus	4.62	1.61E-05
Nuclear lumen	3.87	1.13E-14

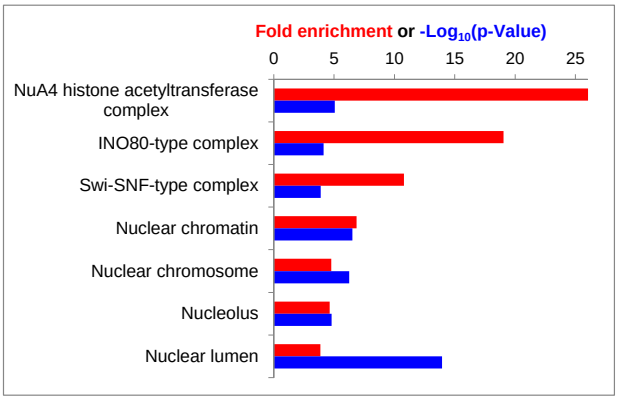

Table S6 : Yeast strains used in this study

Strain Name	Genotype
BY4741	*MAT**a** his3Δ1 leu2Δ0 ura3Δ0 lys2Δ0*
BY4742	*MATalpha his3Δ1 leu2Δ0 ura3Δ0 lys2Δ0*
Y1162	*MATalpha ade16::KanMX4 ade17::KanMX4 his3Δ1 leu2Δ0 ura3Δ0 lys2Δ0*
Y2950	*MAT*alpha *ade16::KanMX4 ade17::KanMX4 ade8::KanMX4 his1::KanMX4 his3Δ1 leu2Δ0 ura3Δ0*
Y3655	*MAT**a** fum1::LEU2 ade16::KanMX4 ade17::KanMX4 ade8::KanMX4 his1::KanMX4 his3Δ1 leu2Δ0 ura3Δ0*
Y6986	*MAT*alpha *ade16::KanMX4 ade17::KanMX4 ade8::KanMX4 his1::KanMX4 his3Δ1::HIS3-LEU2 leu2Δ0 ura3Δ0*
Y7321	*MATalpha thi3 (S402F) ade16::kanMX4 ade17::kanMX4 ade8::kanMX4 his1::kanMX4 his3 Δ 1::HIS3-LEU2 leu2Δ0 ura3 Δ 0*
Y8480	*MAT**a** ade16::KanMX4 ade17::KanMX4 ade8::KanMX4 his1::KanMX4 his3Δ1 leu2Δ0 ura3Δ0*
Y8908	*MAT**a** ade3::KanMX4 ade16::KanMX4 ade17::KanMX4 ade8::KanMX4 his1::KanMX4 his3Δ1 leu2Δ0 ura3Δ0*
Y9082	*MAT**a** bre1:: KanMX4 ade16::KanMX4 ade17::KanMX4 ade8::KanMX4 his1::KanMX4 his3Δ1 leu2Δ0 ura3Δ0*
Y9168	*MAT*alpha *set1::KanMX4 ade16::KanMX4 ade17::KanMX4 ade8::KanMX4 his1::KanMX4 his3Δ1 leu2Δ0 ura3Δ0 met15Δ0*
Y9479	*MAT*alpha *swd1::KanMX4 ade16::KanMX4 ade17::KanMX4 ade8::KanMX4 his1::KanMX4 his3Δ1 leu2Δ0 ura3Δ0 lys2Δ0*
Y9480	*MAT*alpha *swd3::KanMX4 ade16::KanMX4 ade17::KanMX4 ade8::KanMX4 his1::KanMX4 his3Δ1 leu2Δ0 ura3Δ0 lys2Δ0*
Y9623	*MATalpha kap123::KanMX4 ade16::KanMX4 ade17::KanMX4 his3Δ1 leu2Δ0 ura3Δ0*
Y9715	*MATalpha ynk1::KanMX4 ade16::KanMX4 ade17::KanMX4 his3Δ1 leu2Δ0 ura3Δ0*
Y10846	*MAT**a** ade16::KanMX4 ade17::KanMX4 aah1::KanMX4 his3Δ1 leu2Δ0 ura3Δ0*
Y10867	*MAT**a** snf4::KanMX4 ade16::KanMX4 ade17::KanMX4 ade8::KanMX4 his1::KanMX4 his3Δ1 leu2Δ0 ura3Δ0*
Y10422	*MAT*alpha *ade13::URA3 ade16::KanMX4 ade17::KanMX4 ade8::KanMX4 his1::KanMX4 his3Δ1 leu2Δ0 ura3Δ0*

Table S7: Plasmids used in this study

Plasmid Name	Relevant criteria	Source
pCM189	*$tetO_7$ promoter CEN ARS URA3 Amp^R*	(1)
pET15b	His6-Tag *Amp^R*	#69661-3 Merck
pGFP-C-Fus	*pMET25-GFP URA3 CEN*	(2)
pRRLSin-PGK-IRES-ZsGreen-WPRE	*pPGK-EGFP URA3 Amp^R*	#12252 Addgene
pFL44L	*2 µ URA3 Amp^R*	F. Lacroute
YepLac195	*2 µ URA3 Amp^R*	(3)
P4919	*URA6* in YepLac195	This study
P4979	*PAN3 URA6* in pFL44L	This study
P4983	*KAP123* in YepLac195	This study
P5055	*Myc-KAP123* in pCM189	This study
P5486	*URA6* in pRRLSin-PGK-IRES-ZsGreen-WPRE	This study
P5653	*RPL25-NSL* in pGFP-C-Fus	This study

References cited:

(1) Garí E, Piedrafita L, Aldea M, Herrero E. (1997) A set of vectors with a tetracycline-regulatable promoter system for modulated gene expression in *Saccharomyces cerevisiae*. *Yeast.* **13**: 837–848.

(2) Niedenthal RK, Riles L, Johnston M, Hegemann JH. (1996) Green fluorescent protein as a marker for gene expression and subcellular localization in budding yeast. *Yeast*. **12**(8):773-86.

(3) Gietz RD, Sugino A. (1988) New yeast-*Escherichia coli* shuttle vectors constructed with *in vitro* mutagenized yeast genes lacking six-base pair restriction sites. *Gene*. **74**(2):527-34.

Table S8: Mass spectrometry acquisition parameters

	LTQ	LTQ-Orbitrap XL	Q-Exactive
MS mass range	300-1700	300-1700	300-2000
MS resolution	-	70000	70000
AGC target	3.10^4 in 10 ms	5.10^5 in 500 ms	10^6 in 100 ms
MS/MS strategy	TOP 3	TOP 6	TOP 15
MS/MS mode	CID	CID	HCD
MS/MS resolution	-	-	35000
MS^2 AGC target	10^4 in 100 ms	10^4 in 50 ms	10^5 in 120 ms
Ion isolation window	2 m/z	3 m/z	3 m/z
Normalized collision energy	35	35	25
Charge state selection	2-4+	2-3	2-3
Dynamix exclusion duration	20 s	30 s	30 s
Sequest MS mass tolerance	1.4 Da	10 ppm	10 ppm
Sequest MS^2 mass tolerance	0.6 Da	0.6 Da	0.02 Da